

Astroparticle Physics

2021/22

1. **Historical introduction - basic properties of cosmic rays**
2. **Hadronic interactions and accelerator data**
3. **Cascade equations**
4. **Electromagnetic cascades**
5. **Extensive air showers**
6. **Detectors for extensive air showers**
7. **High-energy cosmic rays and the knee in the energy spectrum of cosmic rays**
8. **Radio detection of extensive air showers**
9. **Acceleration, Astrophysical accelerators and beam dumps**
10. **Extragalactic propagation of cosmic rays**
11. **Ultra-high-energy energy cosmic rays**
12. **Astrophysical gamma rays and neutrinos**
13. **Neutrino astronomy**
14. **Gamma-ray astronomy**

lecture 8

Radio detection of extensive air showers

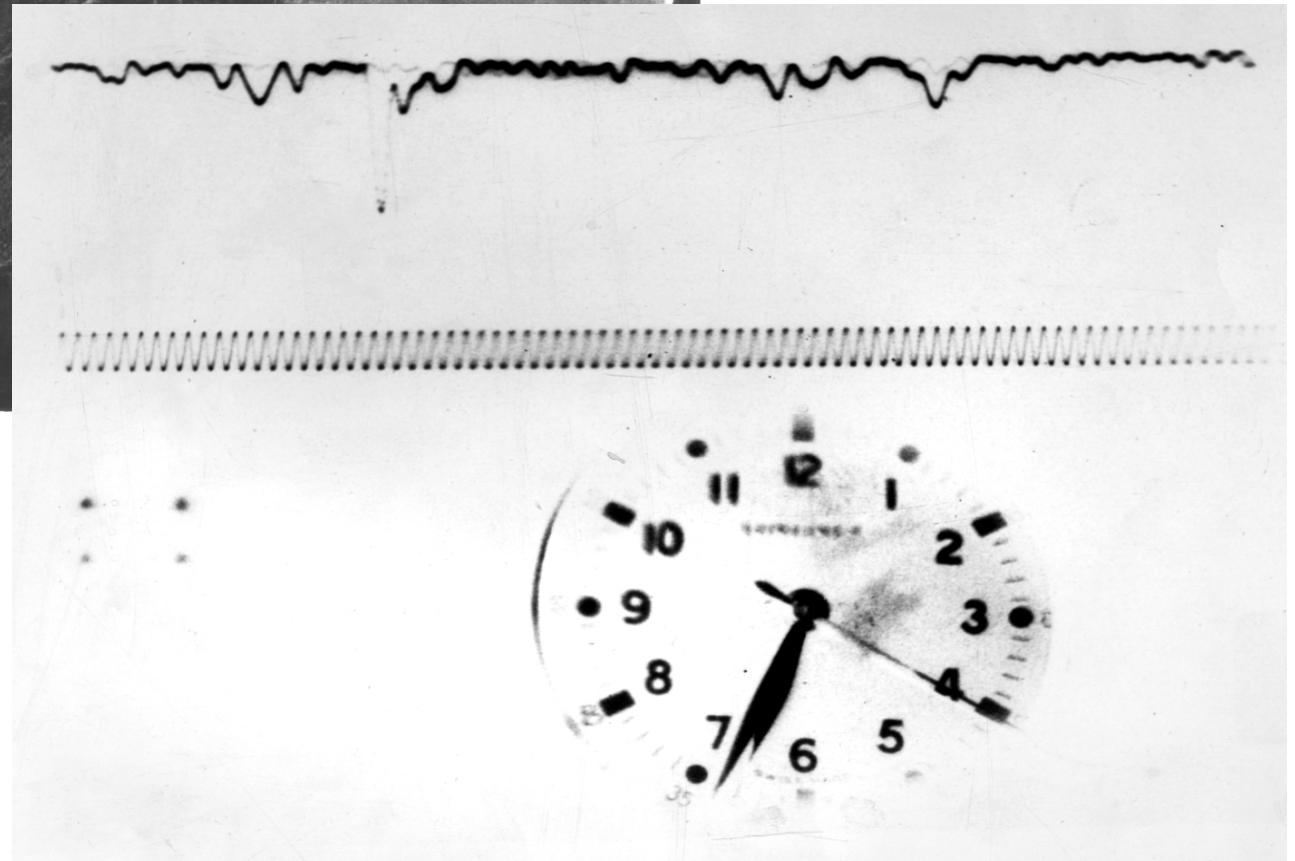
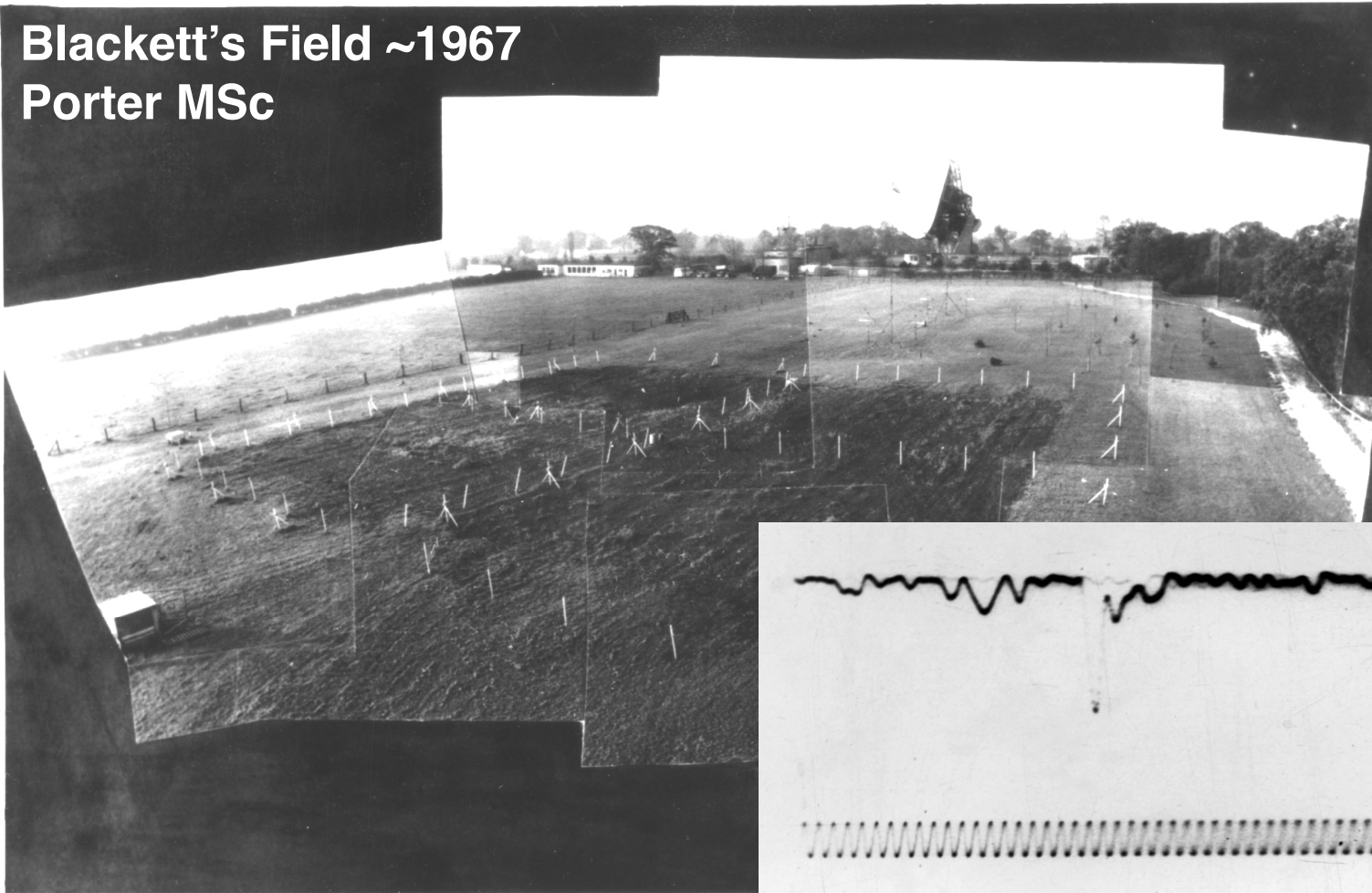
Gaisser chapter 16

16 Extensive air showers

- 16.1 Basic features of air showers
- 16.2 The Heitler–Matthews splitting model
- 16.3 Muons in air showers
- 16.4 Nuclei and the superposition model
- 16.5 Elongation rate theorem
- 16.6 Shower universality and cross section measurement
- 16.7 Particle detector arrays
- 16.8 Atmospheric Cherenkov light detectors
- 16.9 Fluorescence telescopes
- 16.10 Radio signal detection

First radio detection of air showers 1965

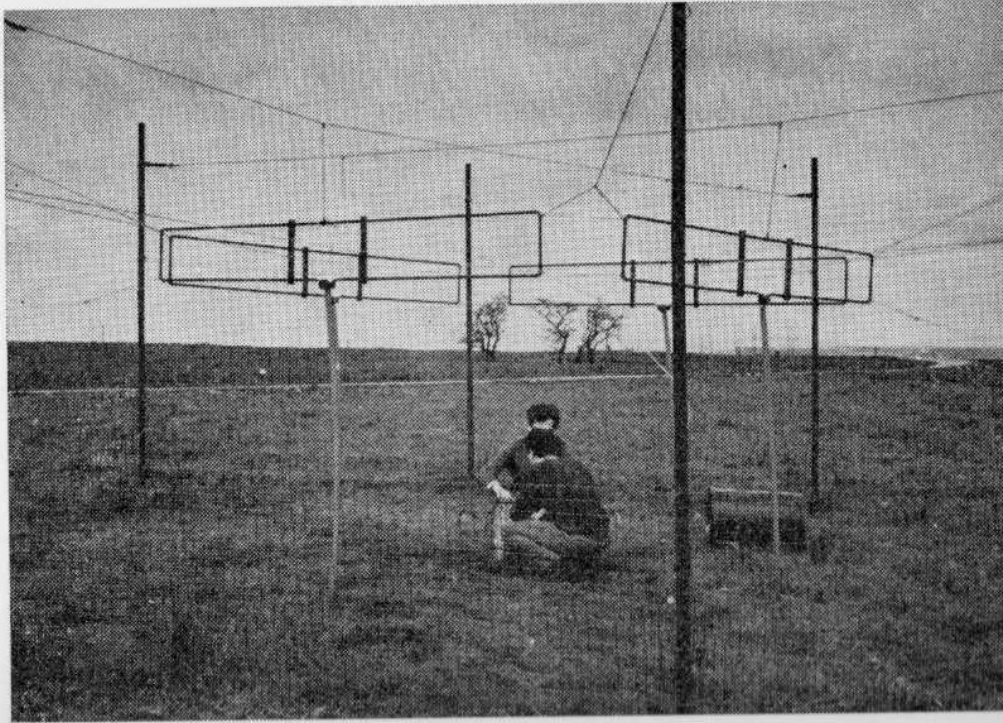
Blackett's Field ~1967
Porter MSc



Jelley et al Nature 1965
R. A. Porter MSc Thesis 1967

Haverah Park (Leeds)

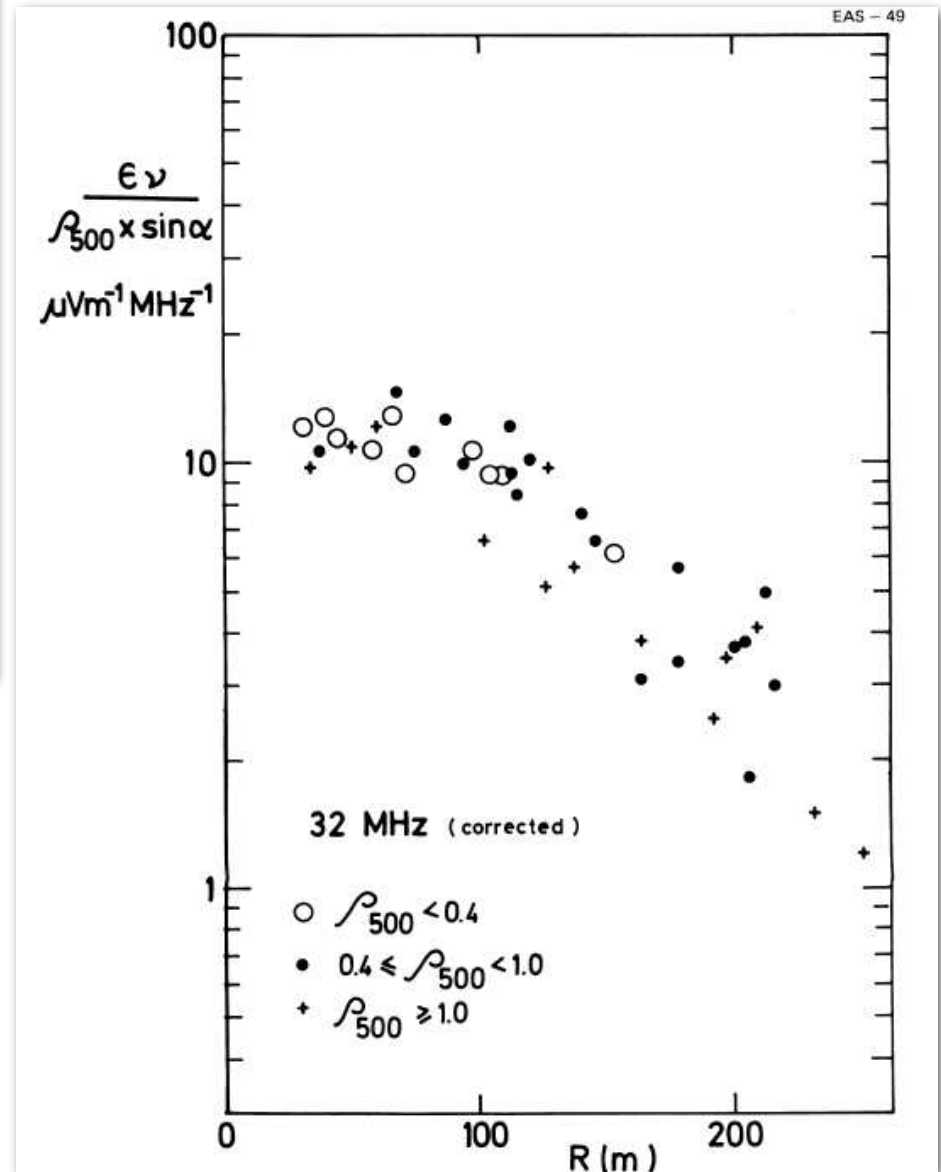
Allan 1971

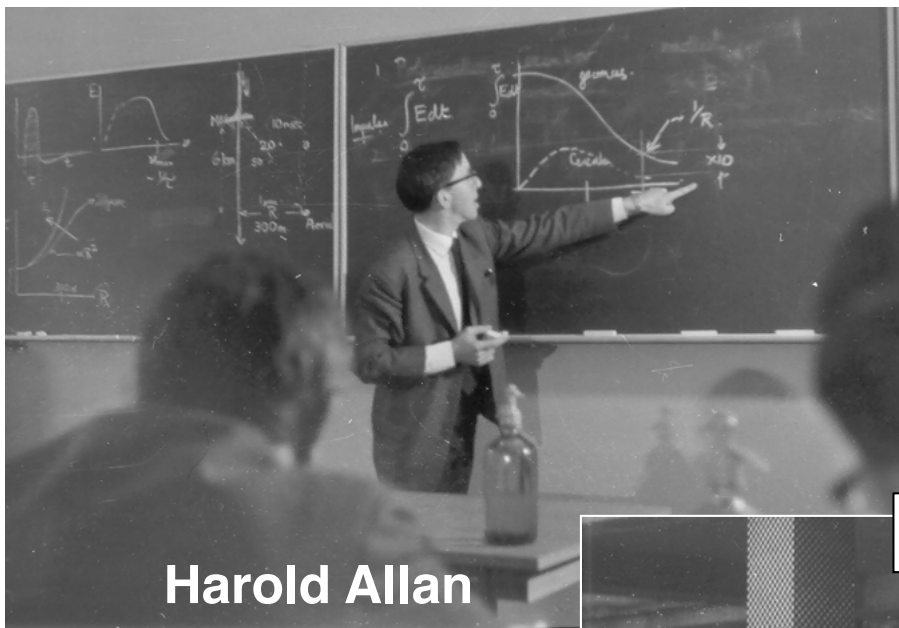


Recent receiving antennas (44 MHz) forming part of the Haverah Park Extensive Air Shower Array.

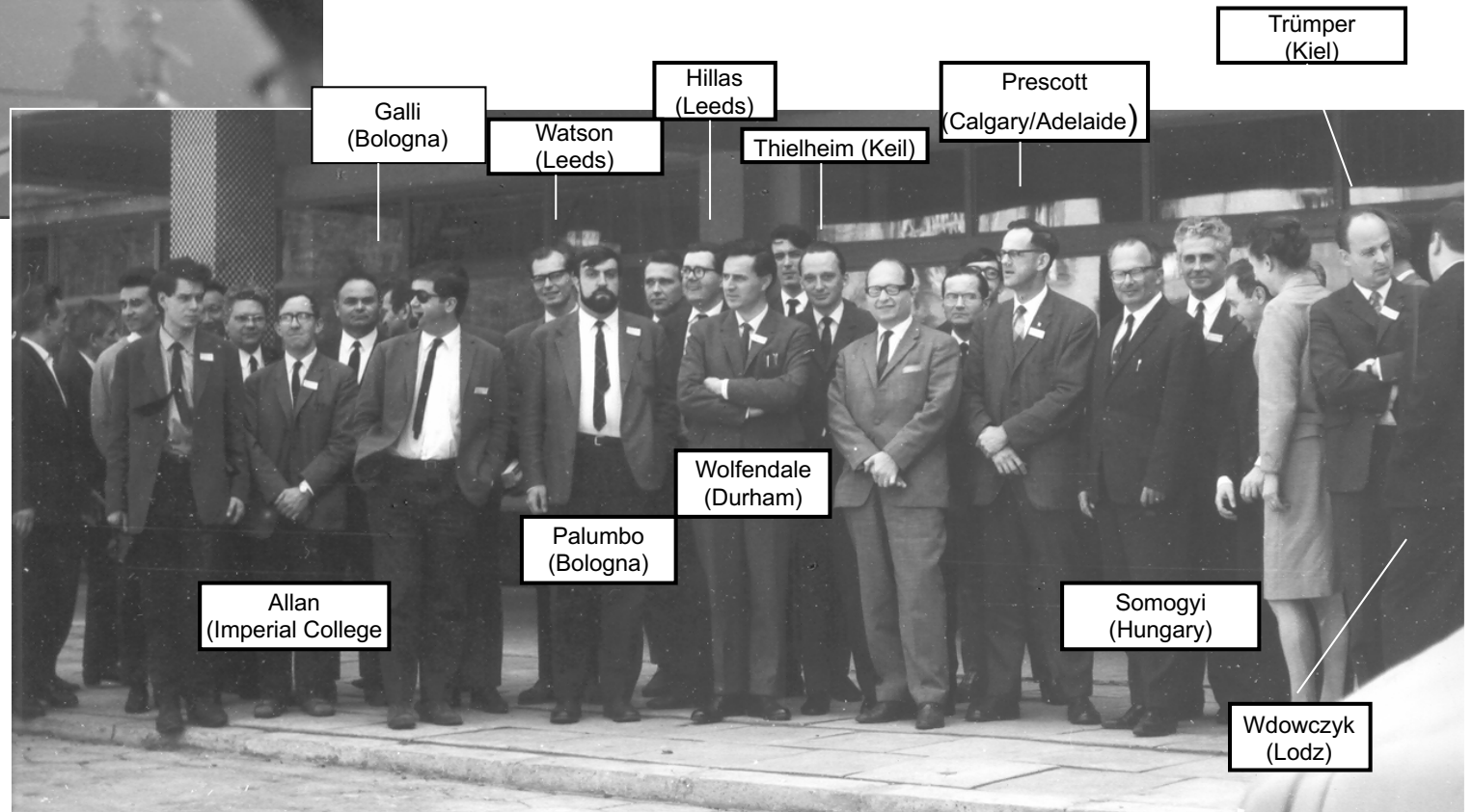
$$\varepsilon_\nu = 2 \left(\frac{E_p}{10^{17}} \right) \left(\frac{\sin \alpha \cos \theta}{\sin 45 \cos 30} \right) \exp \left(\frac{-r}{r_0} \right) \left(\frac{\nu}{50} \right)^{-1} \mu\text{V/m/MHz}$$

$r_0 = 110$ m at $\nu = 55$ MHz. $\alpha =$ angle to B, $\theta =$ Zenith angle





Harold Allan



First European Symposium on High Energy Interactions and Extensive Air Shower: Lodz, Poland April 1968

The renaissance of radio detection of cosmic rays

TIM HUEGE¹

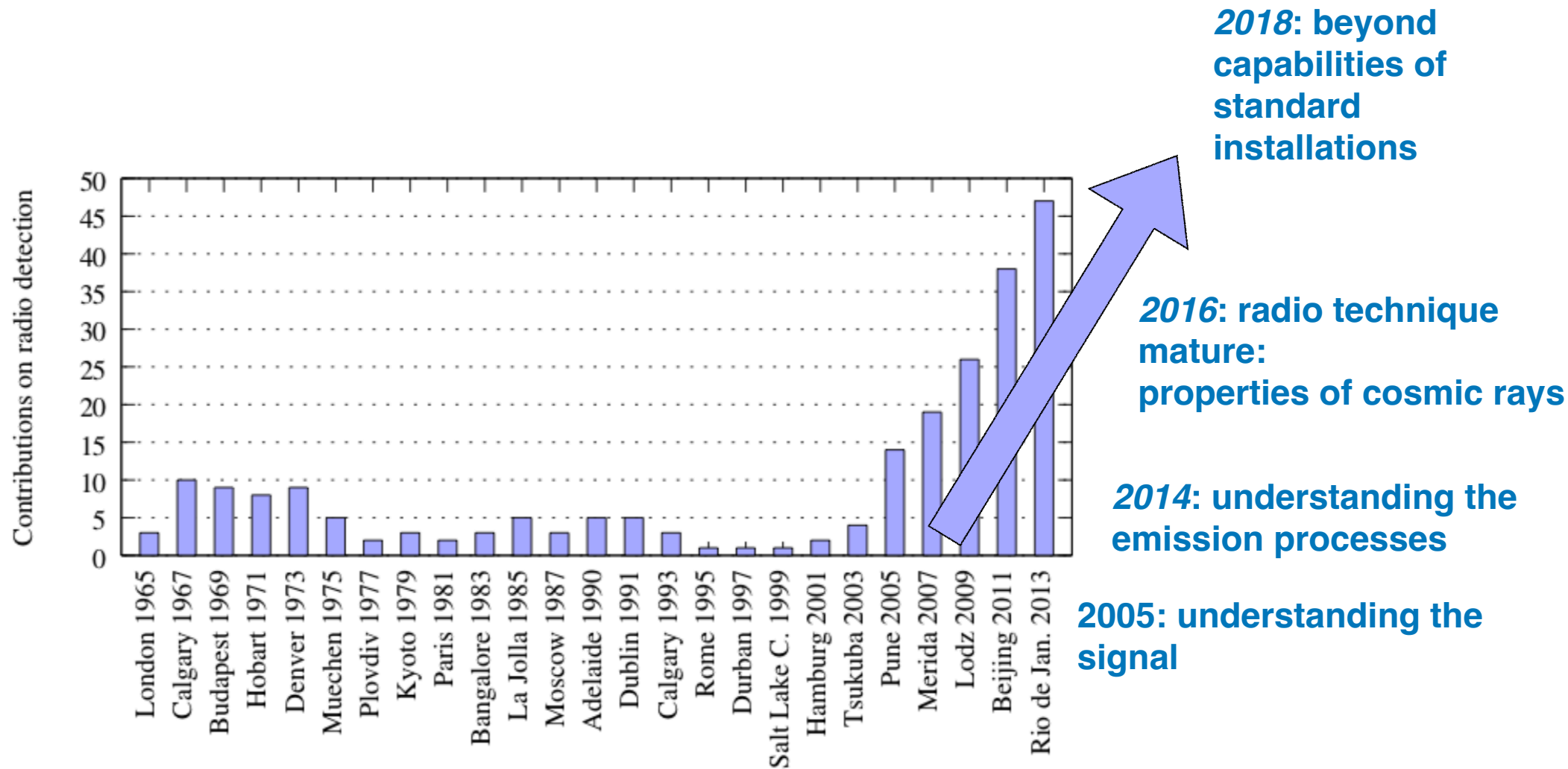
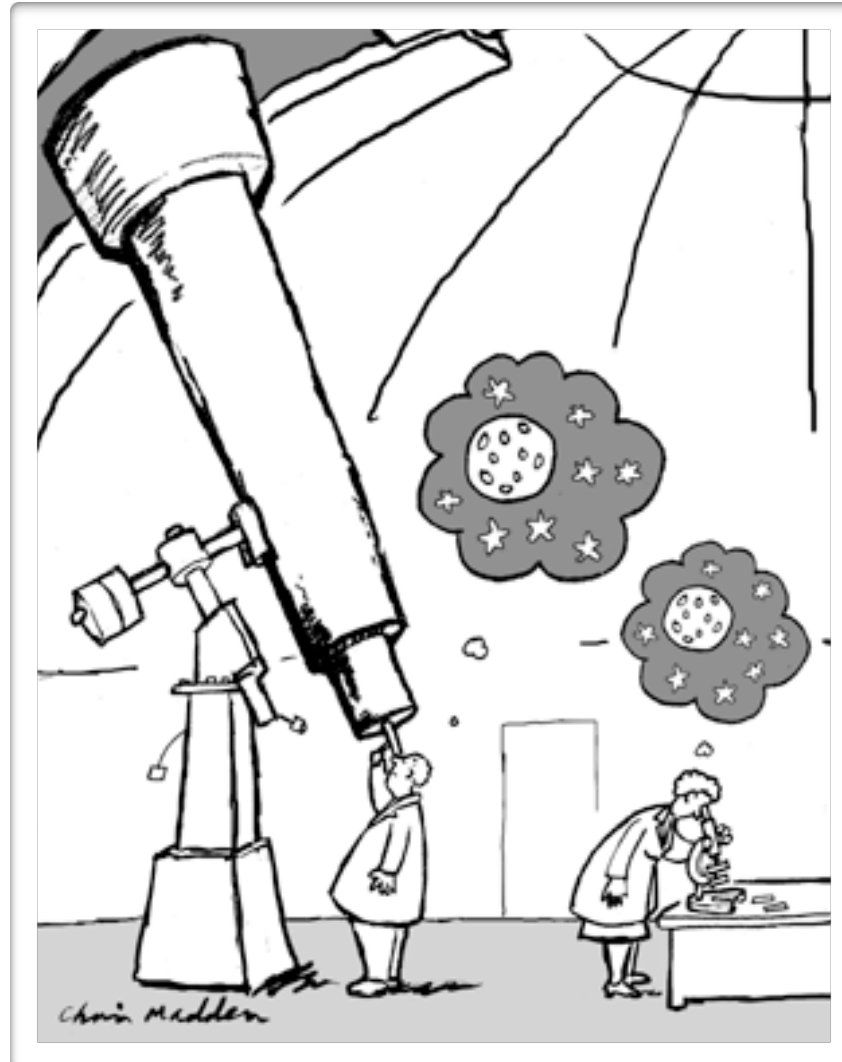


Figure 1: Number of contributions related to radio detection of cosmic rays or neutrinos to the ICRCs since 1965. The field has grown very impressively since the modern activities started around 2003. Data up to 2007 were taken from [11].

Radio Detectors



Radio detection of extensive air showers around the world

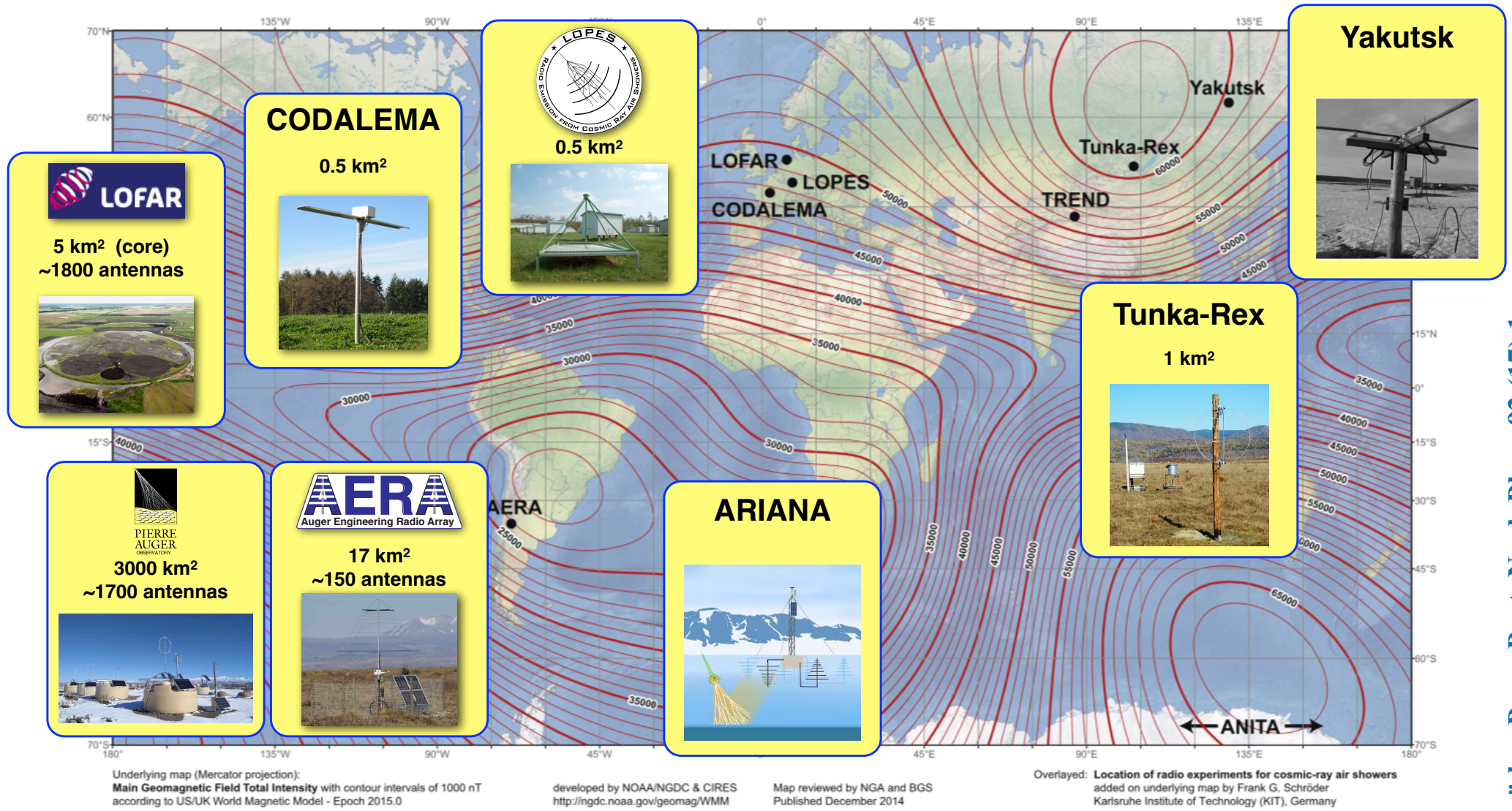
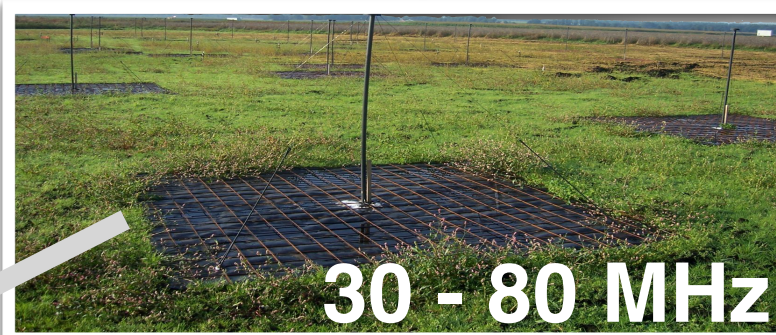


Fig. 21. Map of the total geomagnetic field strengths (world magnetic model [207]) and the location of various radio experiments detecting cosmic-ray air showers.

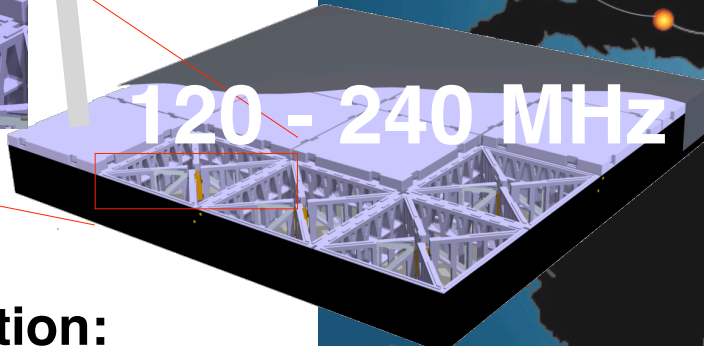
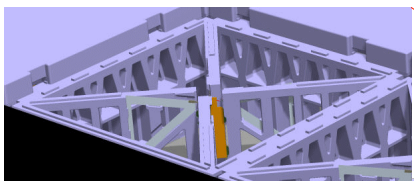
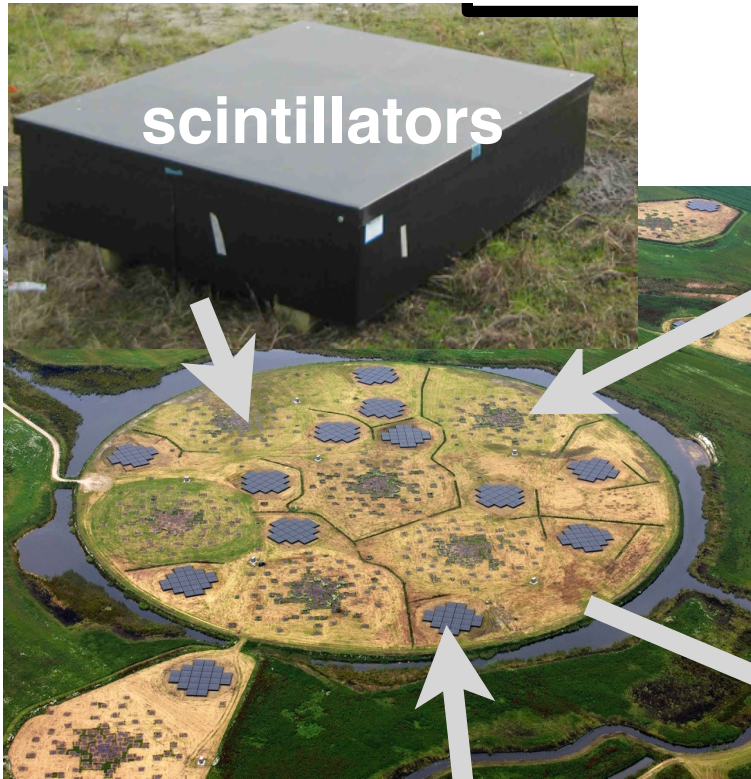
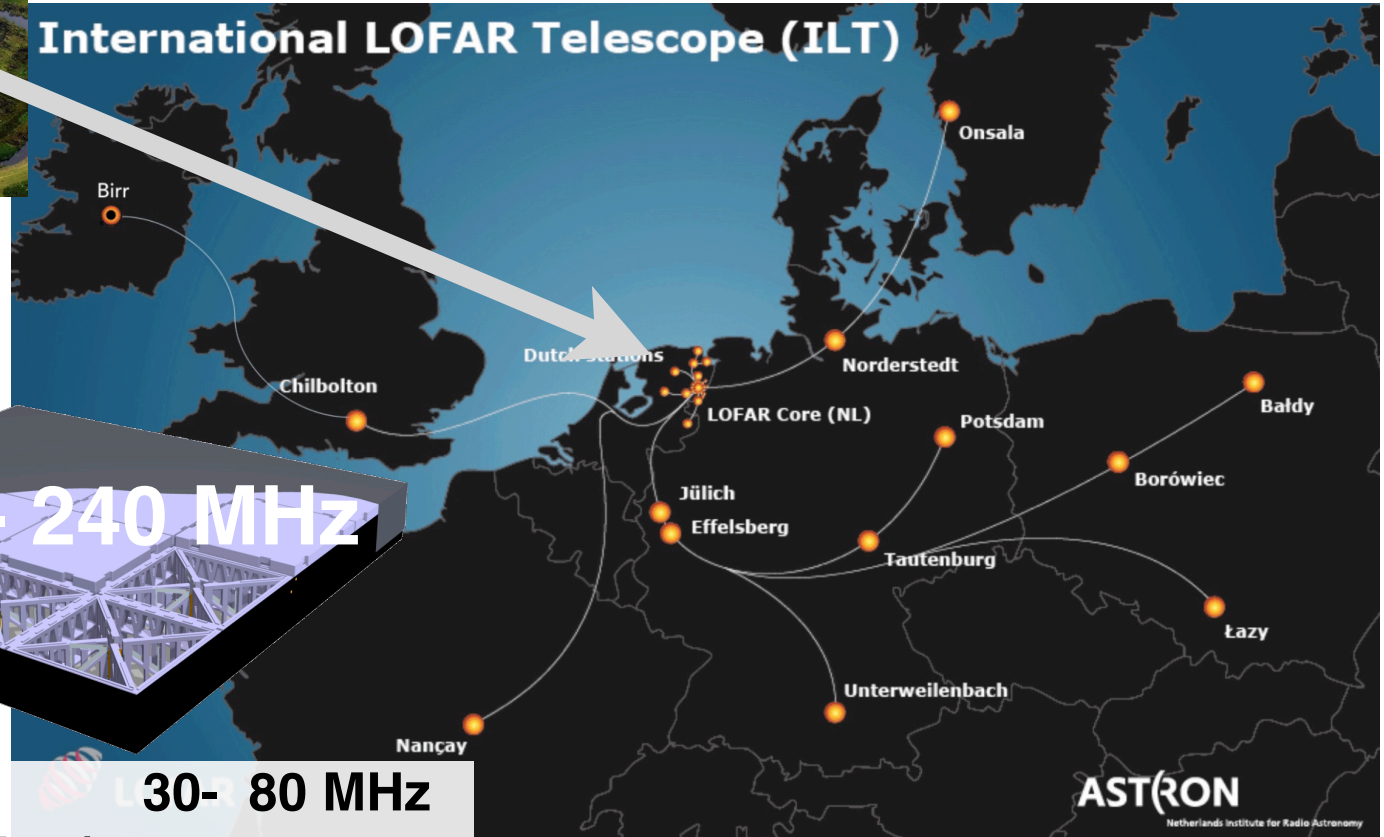


LOFAR



core
23 stations ~5 km²

International LOFAR Telescope (ILT)



each (dutch) station:
96 low-band antennas
high-band antennas (2x24 tiles) 120-240 MHz

M. van Haarlem et al., A&A 556 (2013) A2

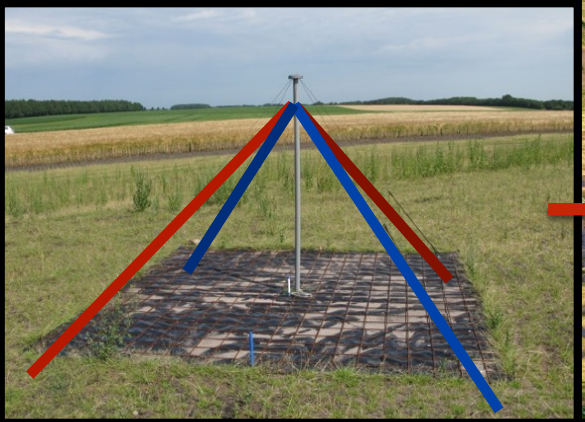
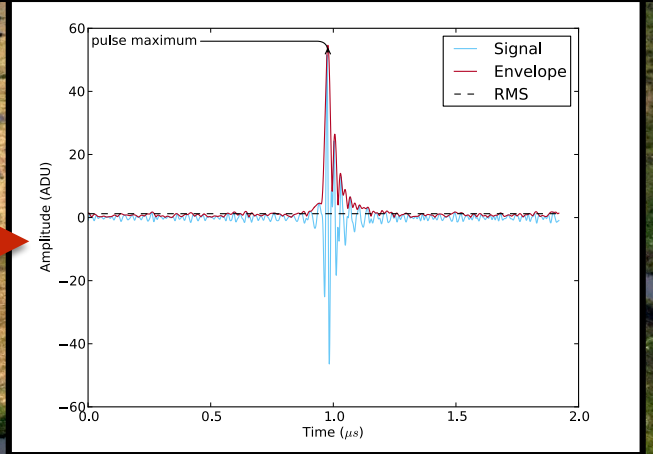
LORA
LOFAR Radboud Array
scintillator detectors



Superterp:
* diameter ~ 300 m
* 20 LORA detectors
* 6 LBA stations
(= 6 x 48 antennas)
* more LBA stations
around superterp

trigger: 13 of 20
detectors

offline analysis
P. Schellart et al., A&A 560, 98 (2013)



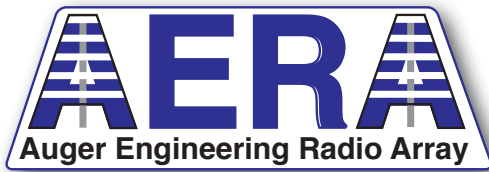
Low Band Antennas (LBA)
30 - 80 MHz

buffer
2 ms read-out

Selection this analysis:
4+ LBA stations



PIERRE
AUGER
OBSERVATORY

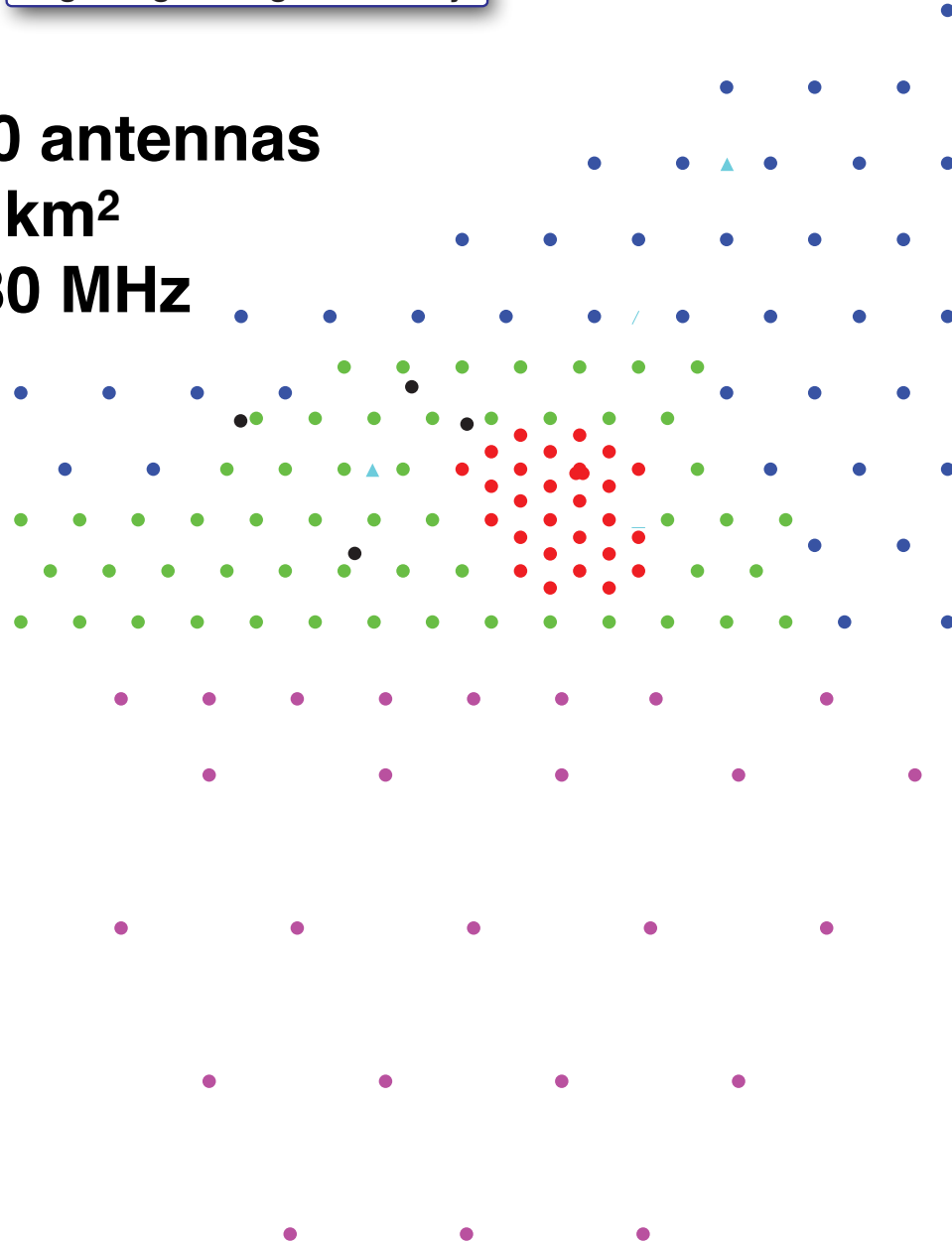


AERA
Auger Engineering Radio Array

~150 antennas

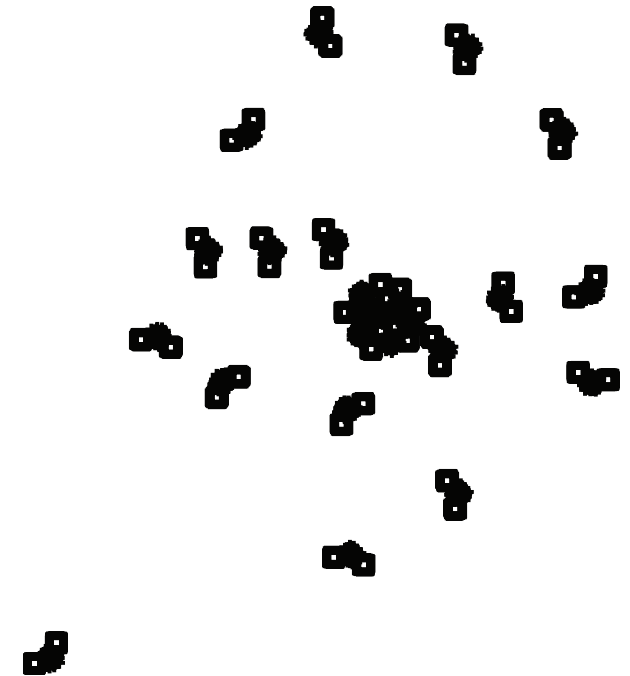
~17 km²

30-80 MHz



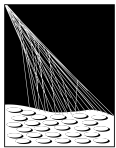
LOFAR core

23 stations ~5 km²

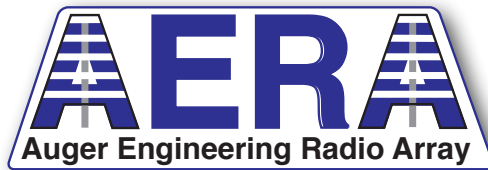


>2000 antennas

1 km



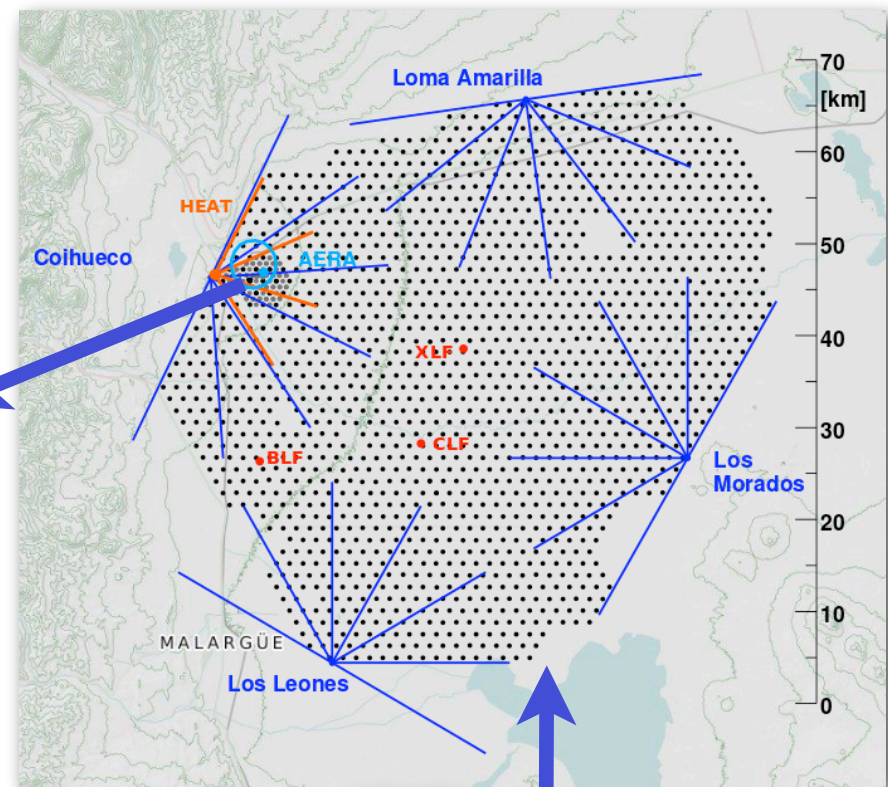
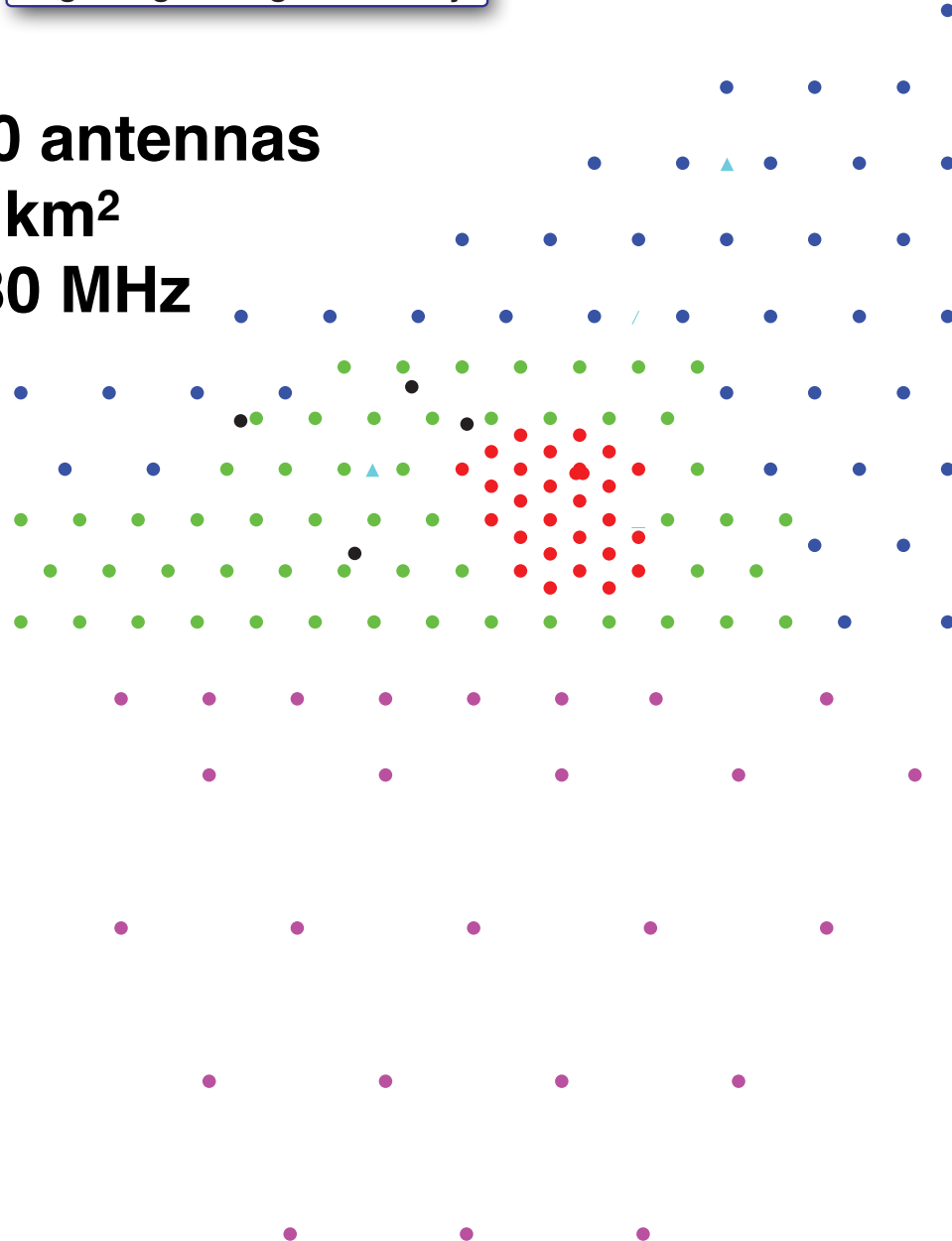
PIERRE
AUGER
OBSERVATORY



~150 antennas

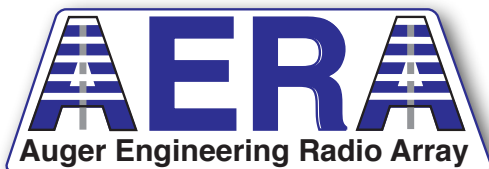
~17 km²

30-80 MHz





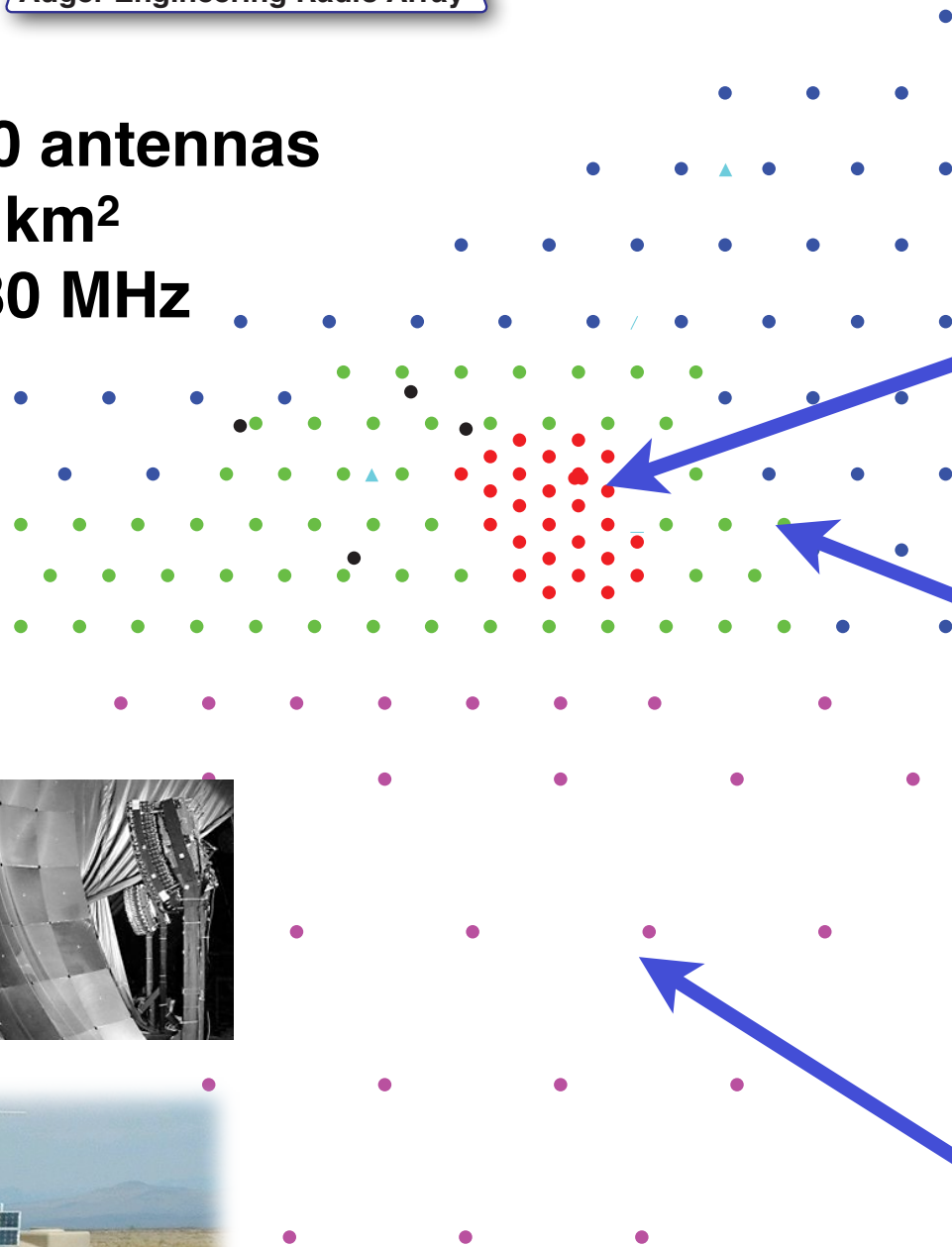
PIERRE
AUGER
OBSERVATORY



~150 antennas

~17 km²

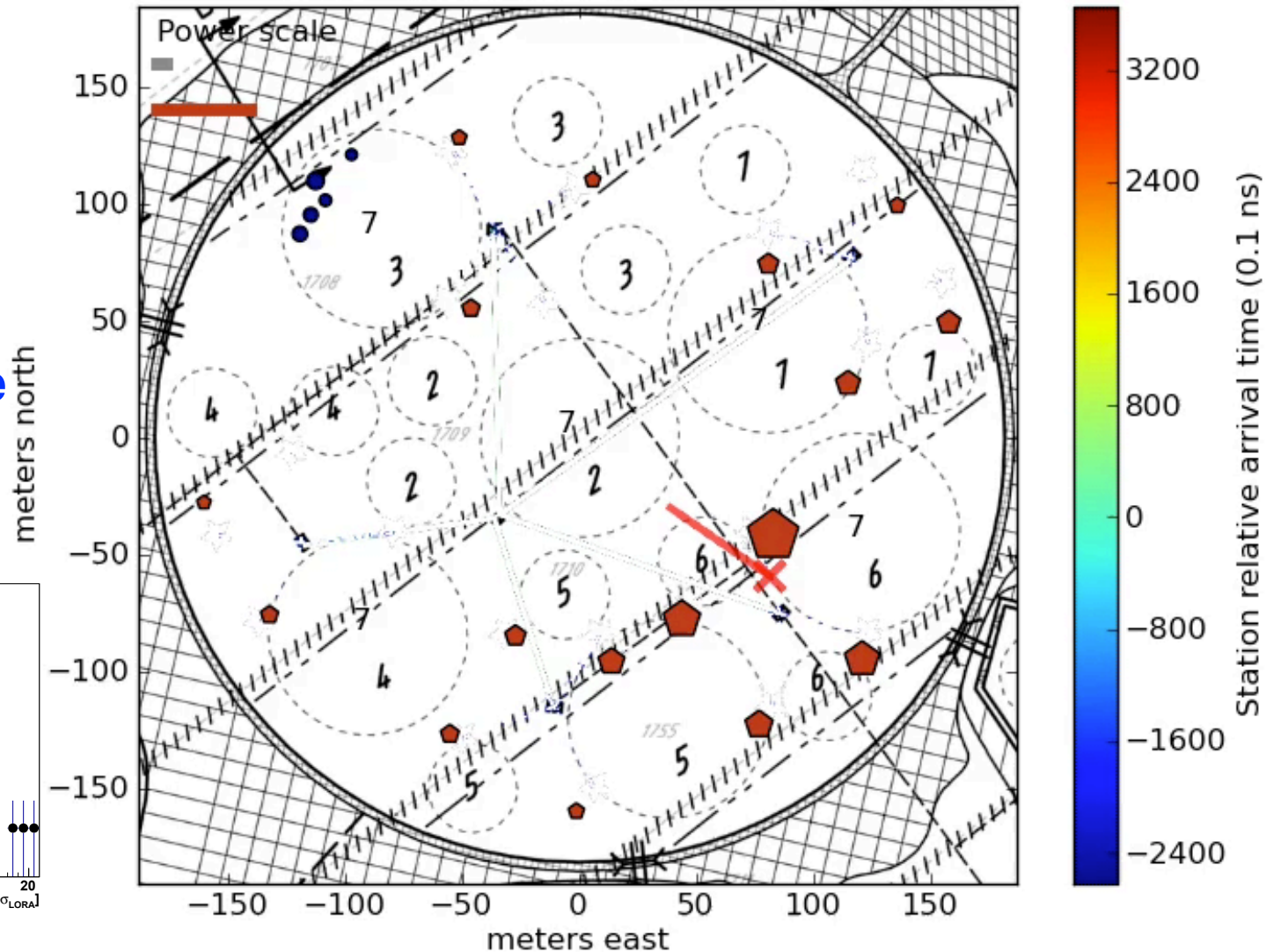
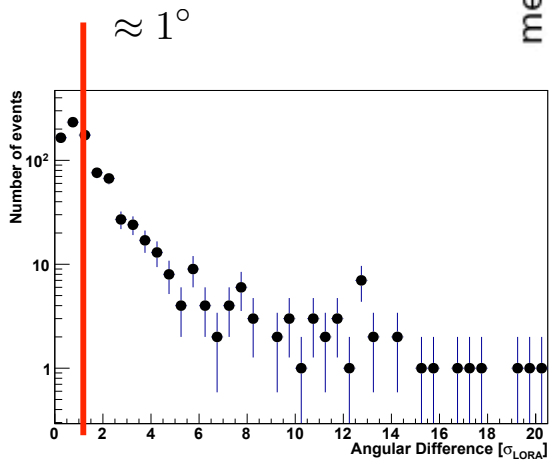
30-80 MHz



A measured air shower

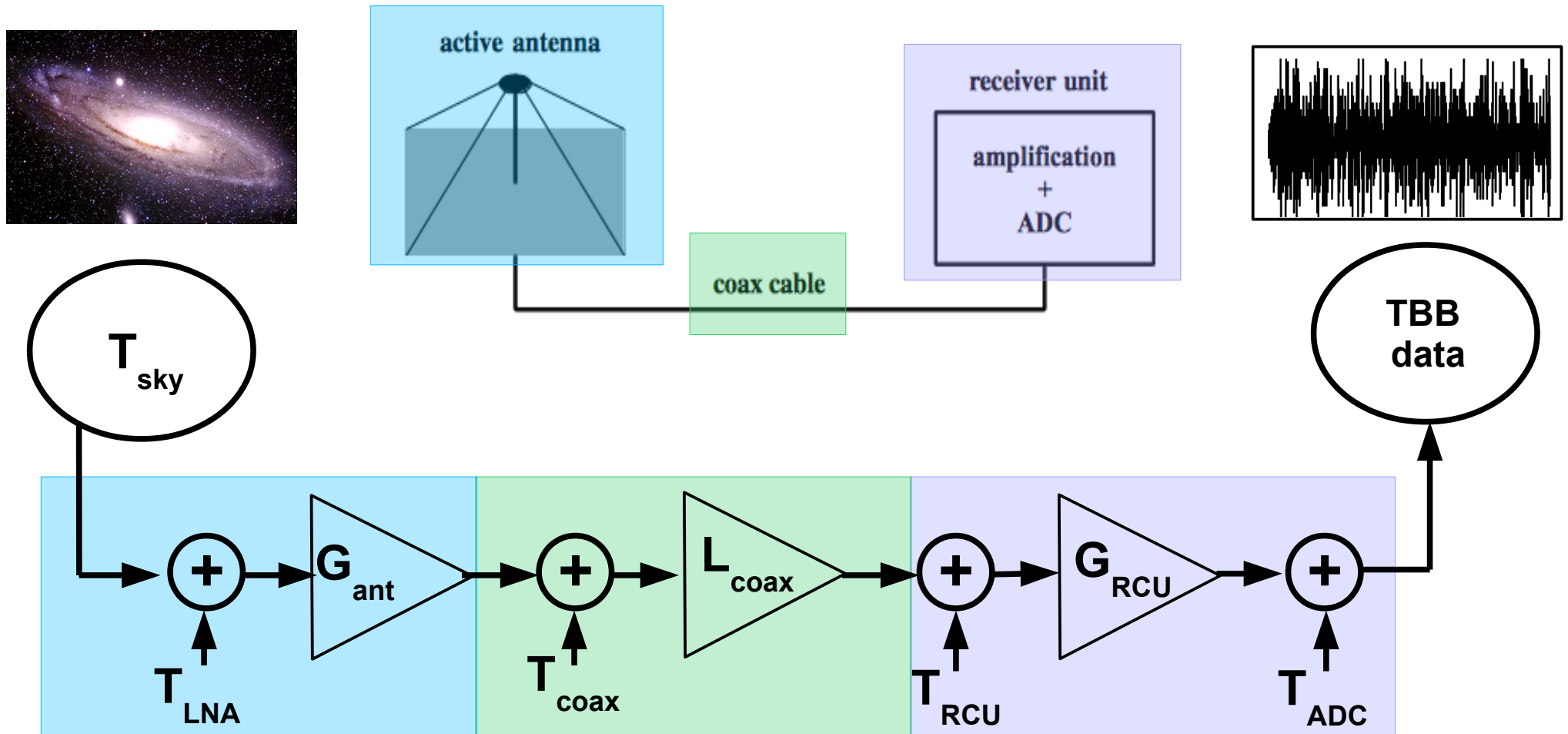
CR event 1307923194.21 -252.2 ns

angular difference
particles - radio



Circles: LOFAR antennas, Pentagons: LORA particle detectors, size denotes signal strength

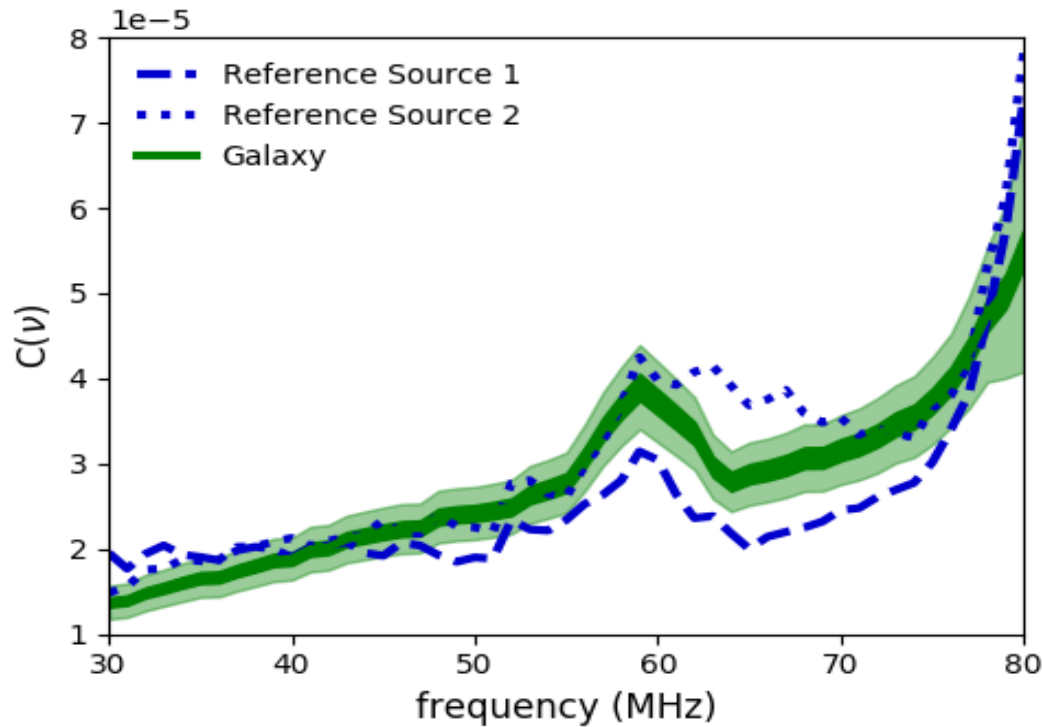
LOFAR Signal Chain



$G_{\text{ant}}, L_{\text{coax}}, G_{\text{RCU}} \longrightarrow$ Freq. Dependent losses and gains
 $T_{\text{LNA}}, T_{\text{coax}}, T_{\text{RCU}}, T_{\text{ADC}} \longrightarrow$ Constant noise values

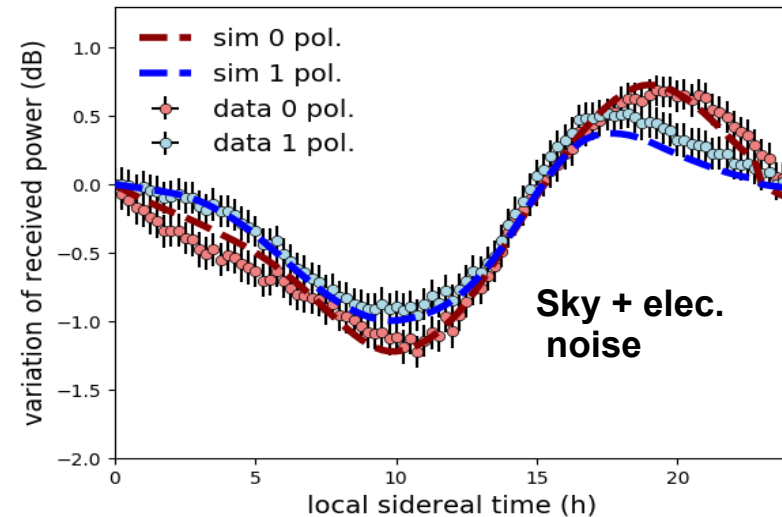
Calibration Results

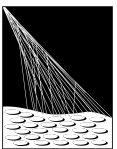
$$C^2(\nu) = A(\nu)L_{\text{coax}}(\nu)G_{\text{RCU}}(\nu)S$$



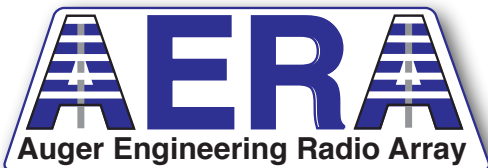
- Galaxy model now limits systematic uncertainties
- Uncertainties from electronic noise are found by comparing resulting calibration constants for different antennas

Uncertainty	Percentage
event-to-event fluctuation	4
galaxy model	12
electronic noise < 77 MHz	5-6
electronic noise > 77 MHz	10-20
total < 77 MHz	14



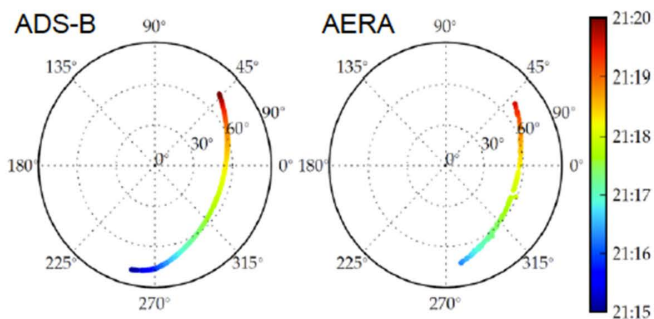
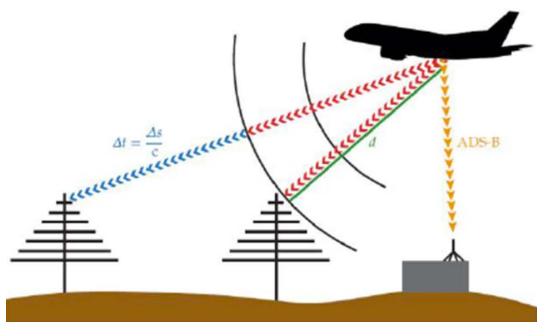
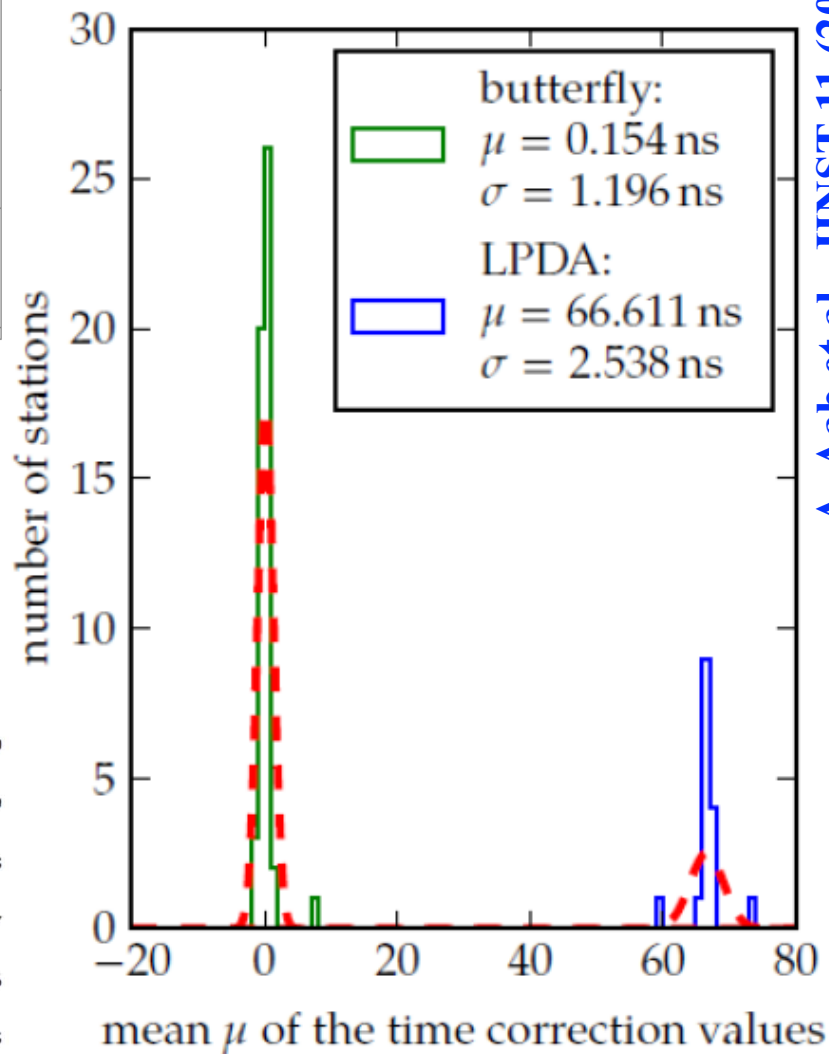
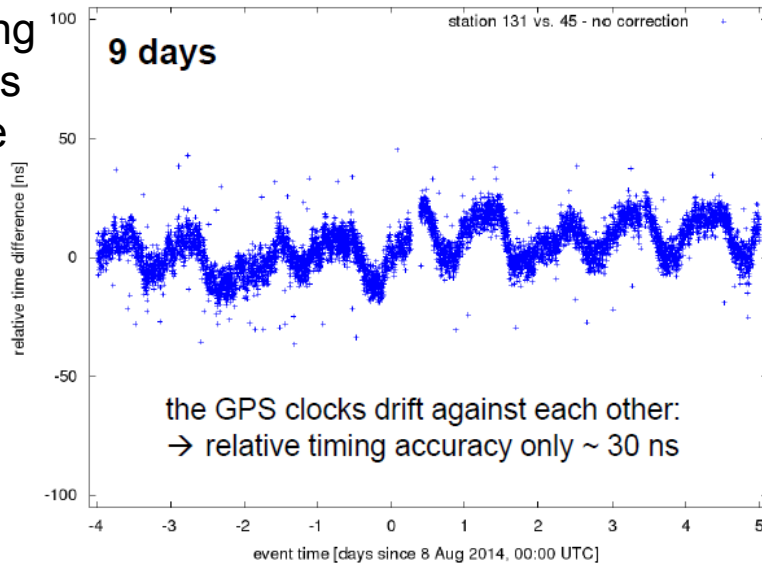


PIERRE
AUGER
OBSERVATORY

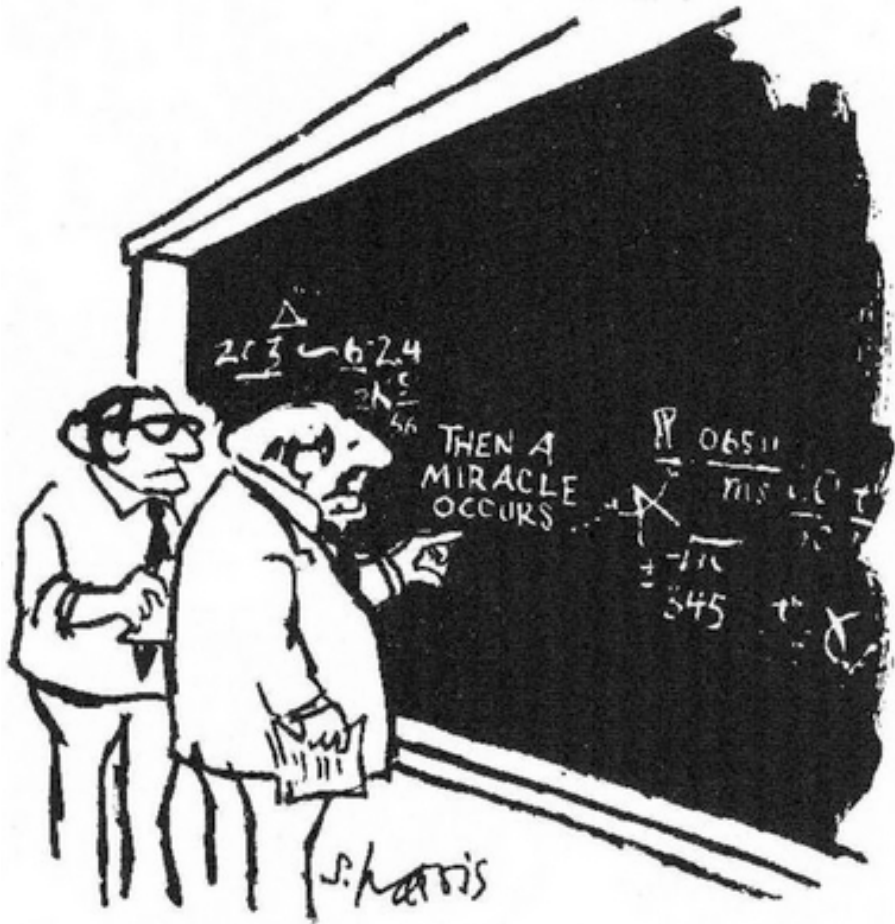


Timing calibration

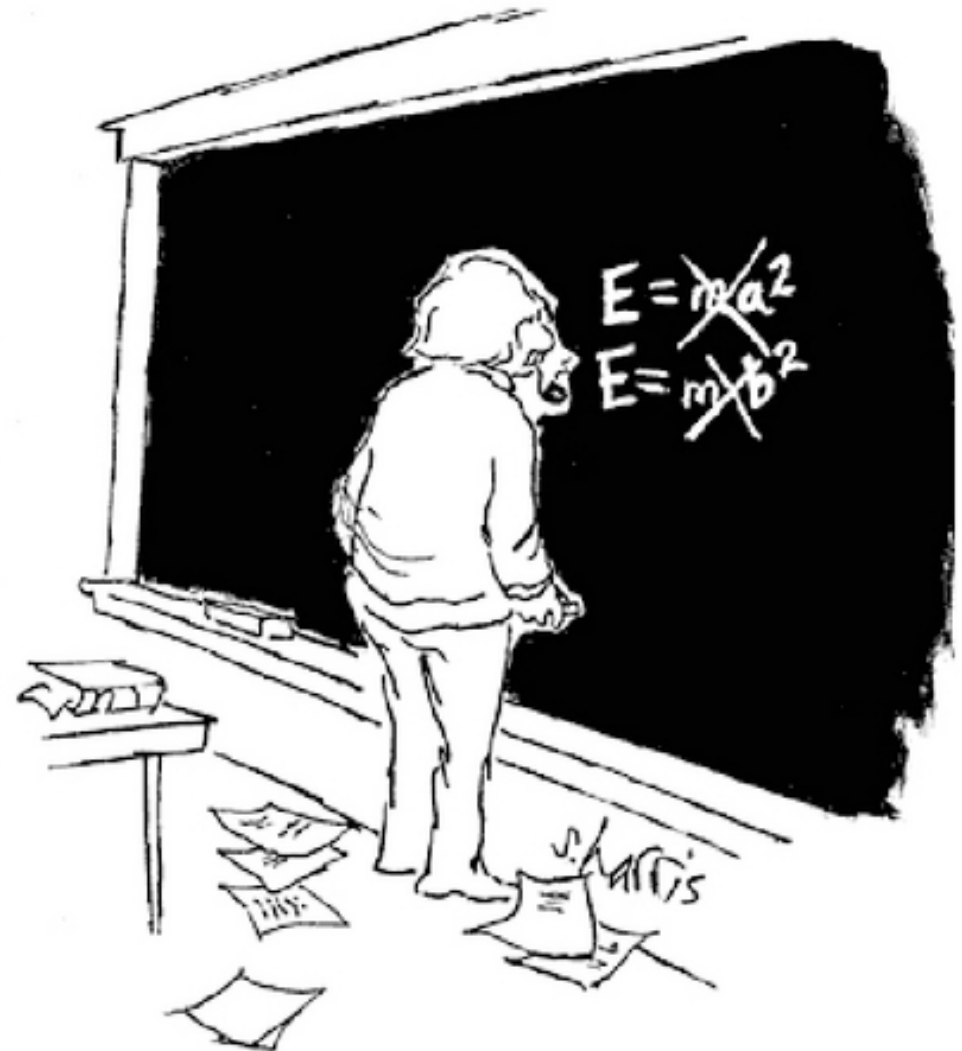
Use beacon broadcasting at 4 different frequencies to measure relative time shifts



Radiation Processes



"I think you should be more explicit here in step two."

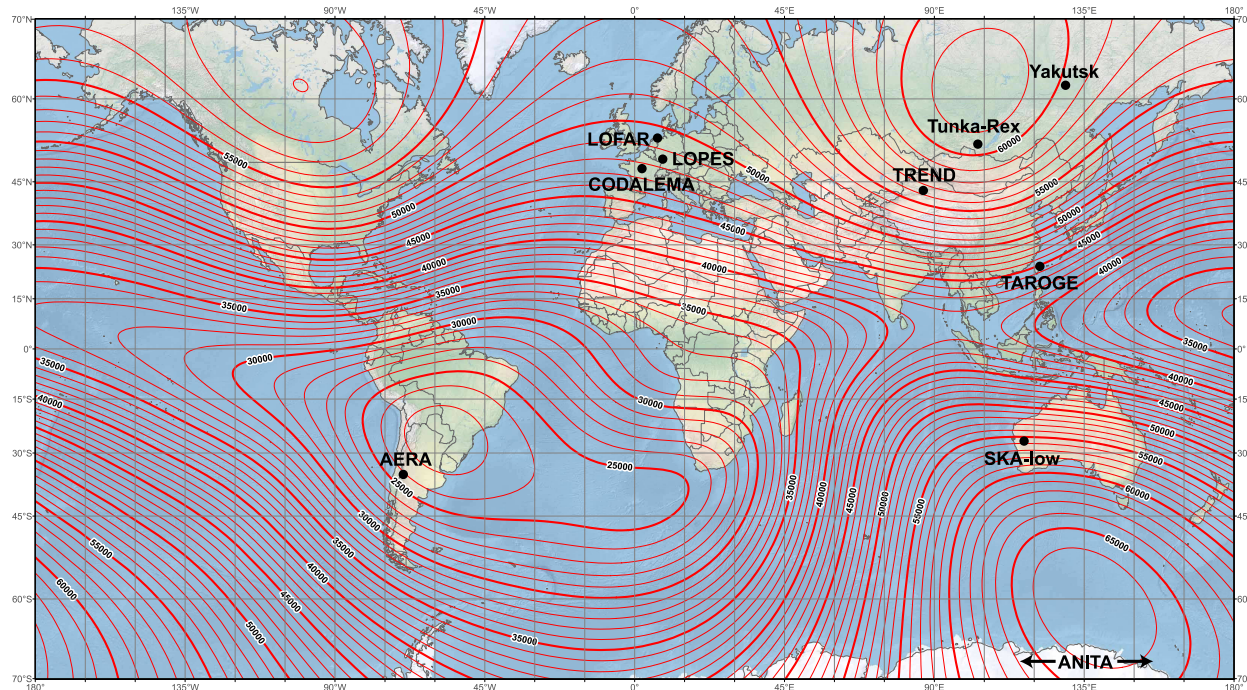


Radio Emission in Air Showers



Mainly: Charge separation in geomagnetic field

$$\vec{E} \propto \vec{v} \times \vec{B}$$



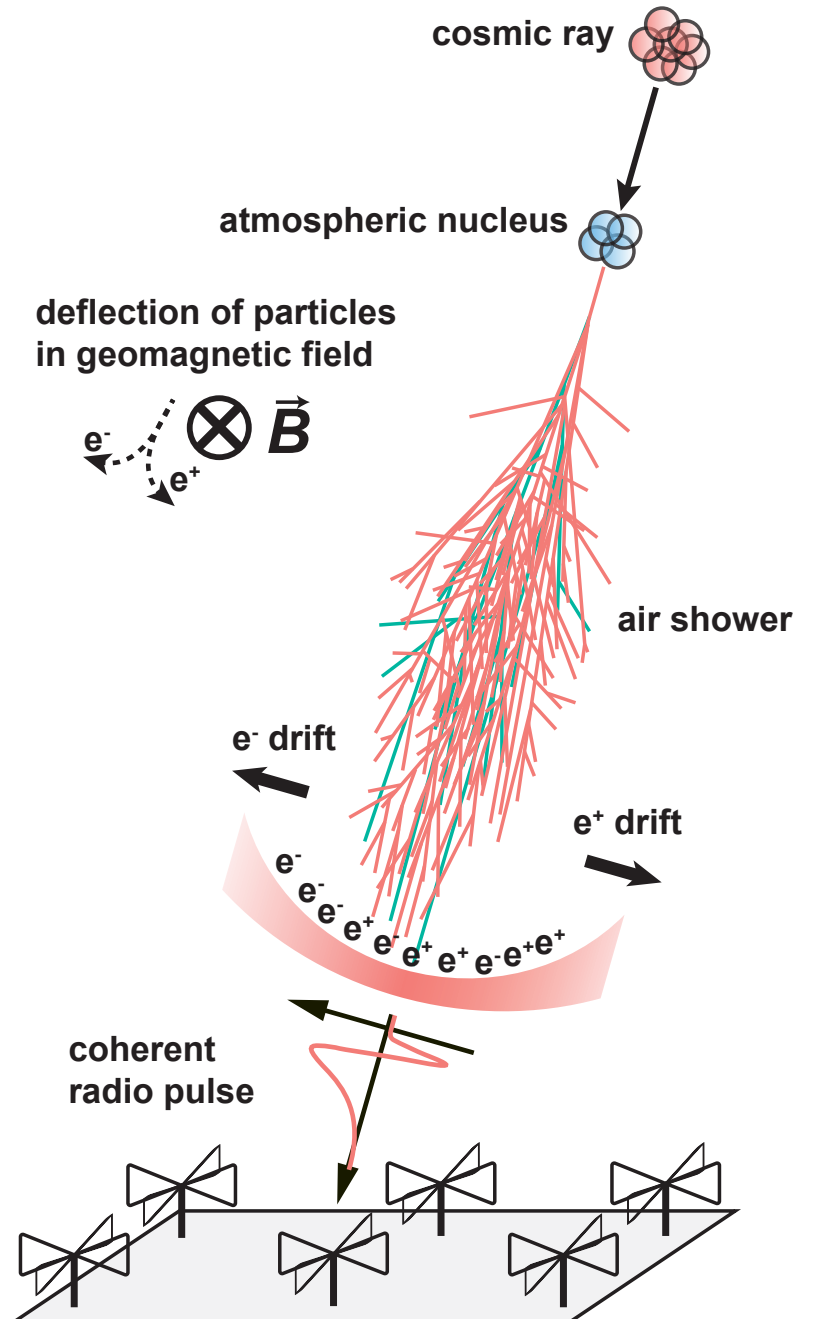
Underlying map (Mercator projection):
Main Geomagnetic Field Total Intensity with contour intervals of 1000 nT
according to US/UK World Magnetic Model - Epoch 2015.0

developed by NOAA/NGDC & CIRES
<http://ngdc.noaa.gov/geomag/WMM>

Map reviewed by NGA and BGS
Published December 2014

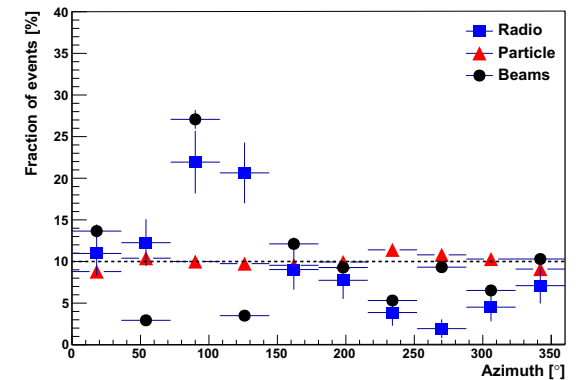
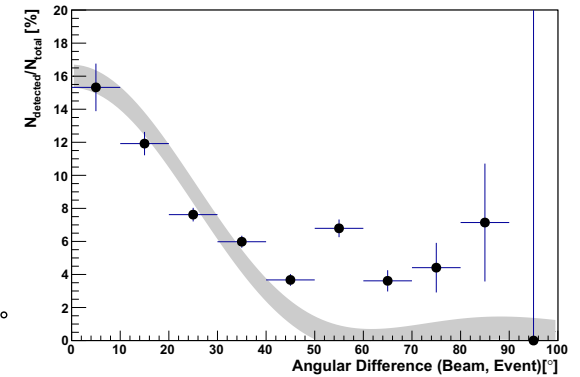
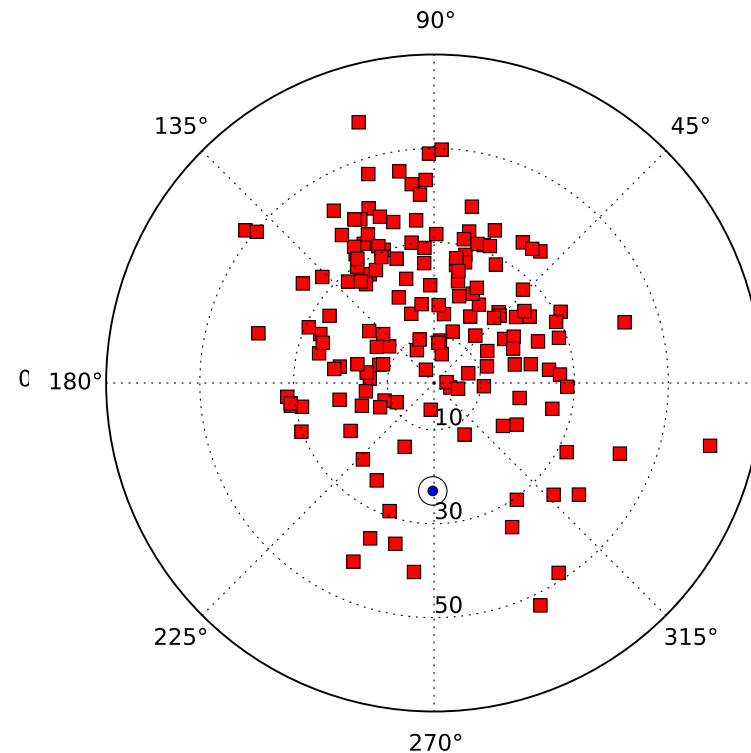
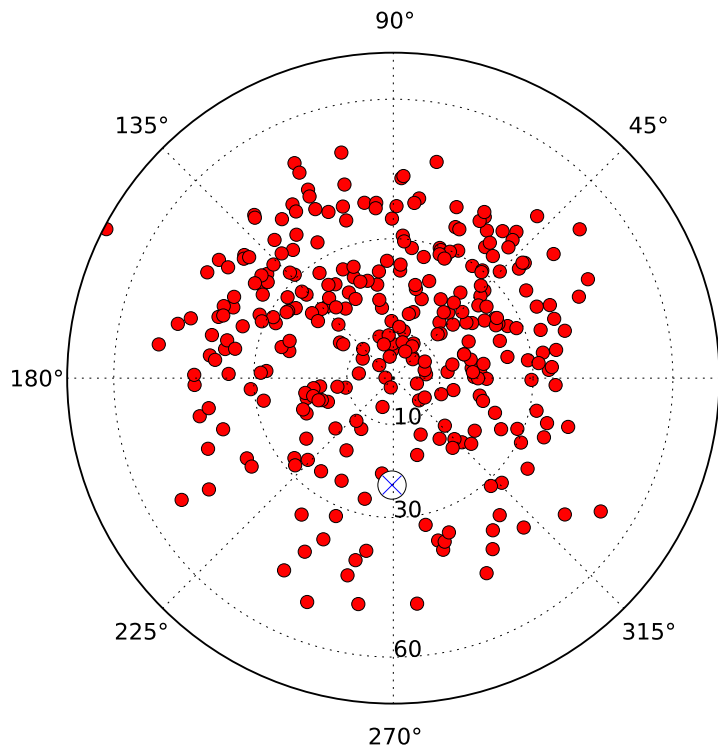
Overlaid: Location of radio experiments for cosmic-ray air showers
added on underlying map by Frank G. Schröder
Karlsruhe Institute of Technology (KIT), Germany

F. Schröder, Prog. Part. Nucl. Phys. 93 (2017) 1



Arrival direction of showers with strong radio signals

north-south asymmetry
 $v \times B$ effect



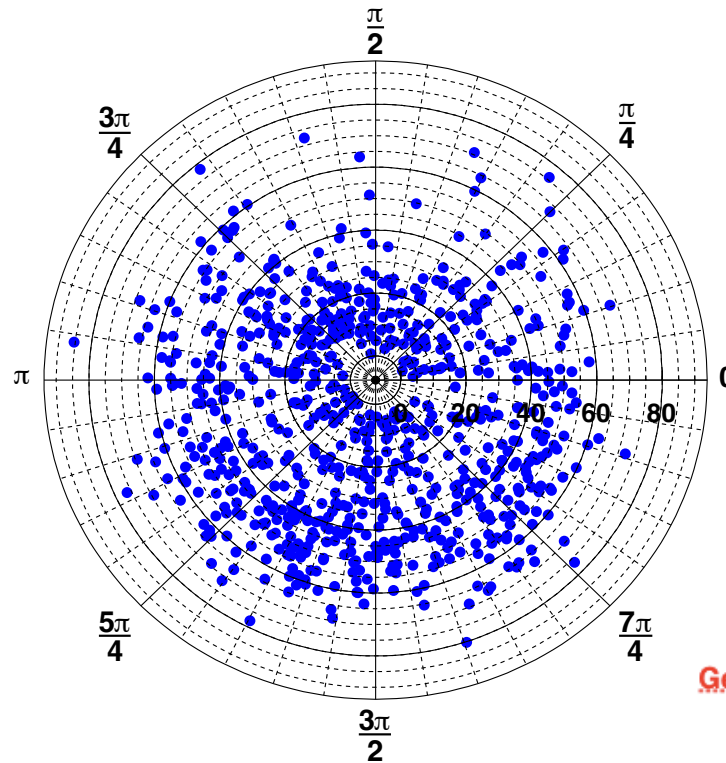
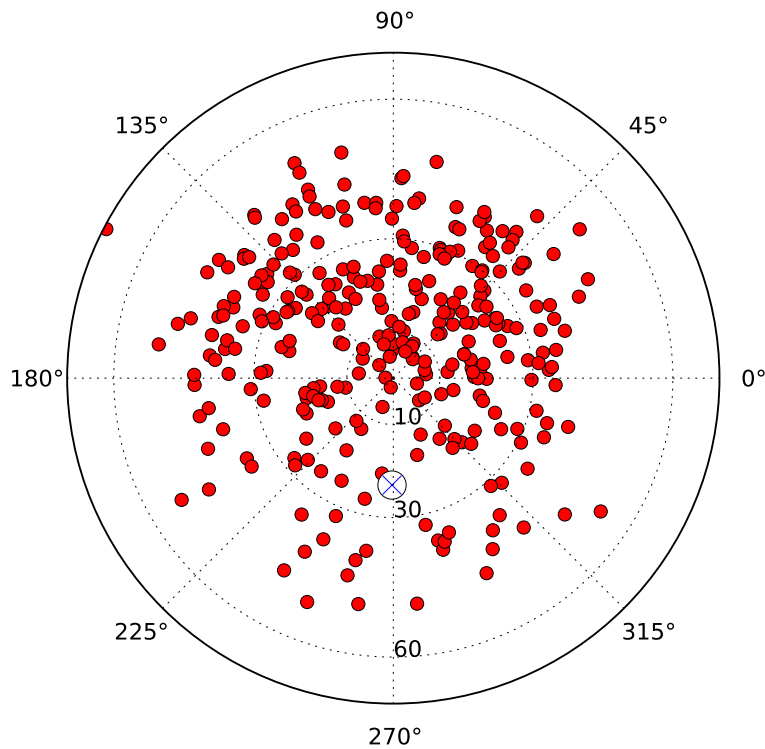
30 - 80 MHz

110 - 190 MHz

A. Nelles et al., *Astroparticle Physics* 65 (2015) 11

Arrival direction of showers with strong radio signals

north-south asymmetry
 $v \times B$ effect

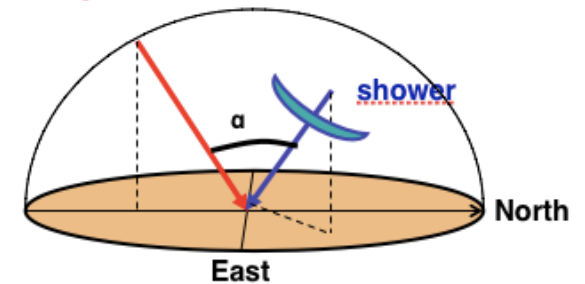


LOFAR

30 - 80 MHz



Geomagnetic field



Geomagnetic effect

T. Huege / Physics Reports 620 (2016) 1–52

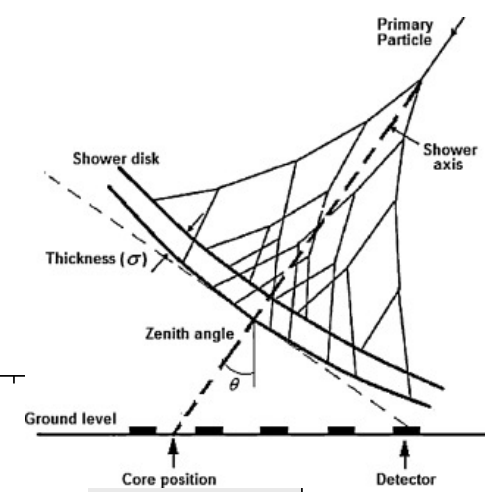
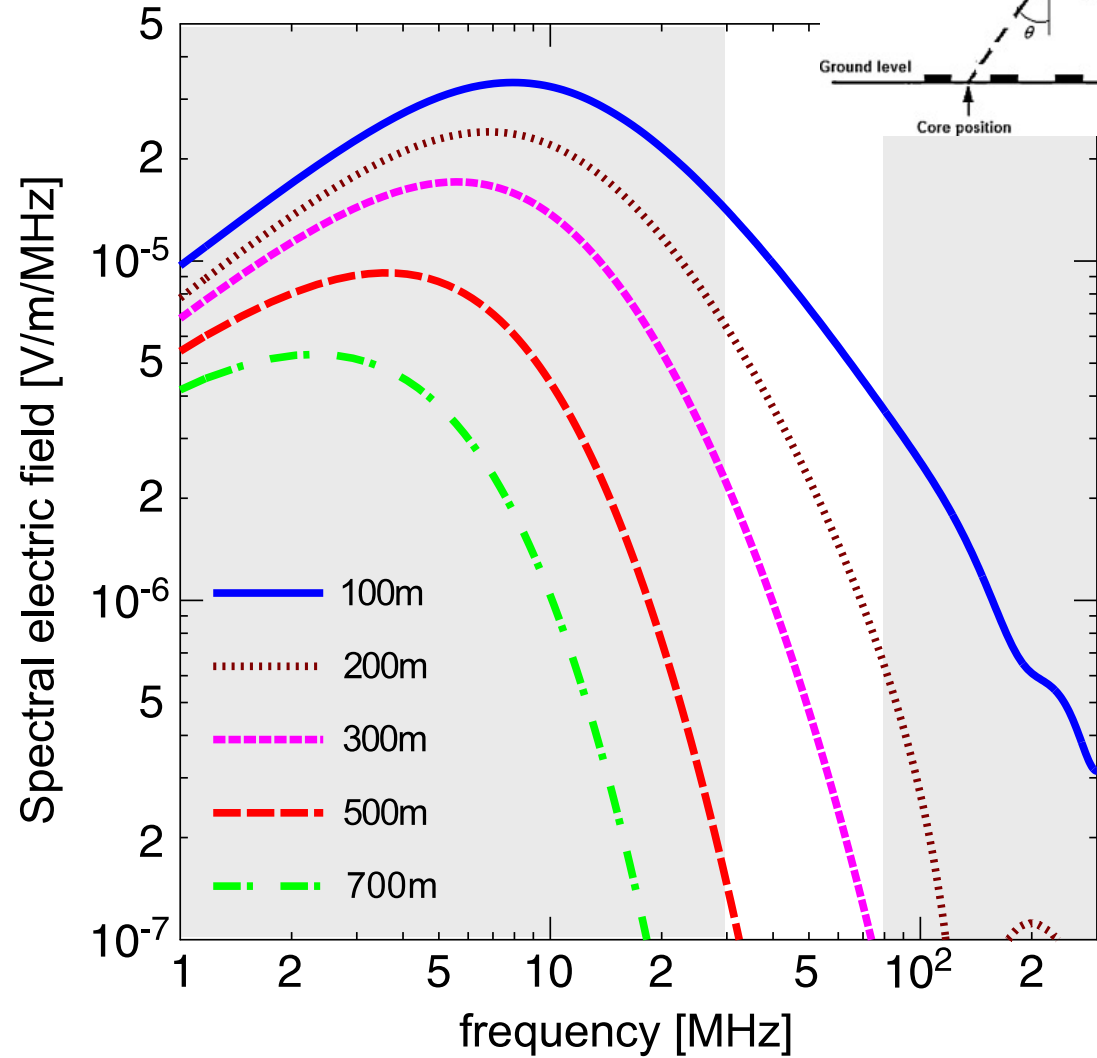
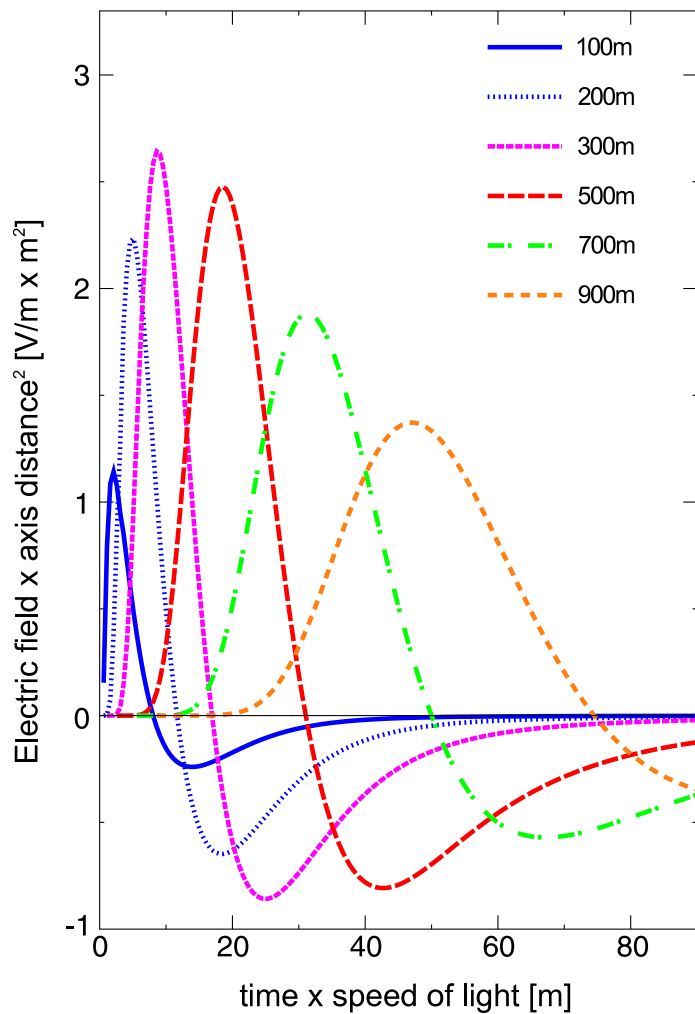


Fig. 4. Radio pulses (top) arising from the time-variation of the geomagnetically induced transverse currents in a 10^{17} eV air shower as observed at various observer distances from the shower axis and their corresponding frequency spectra (bottom). Refractive index effects are not included.

Source: Adapted from [18].

Radio Emission in Air Showers

 **Mainly: Charge separation in geomagnetic field**

$$\vec{E} \propto \vec{v} \times \vec{B}$$

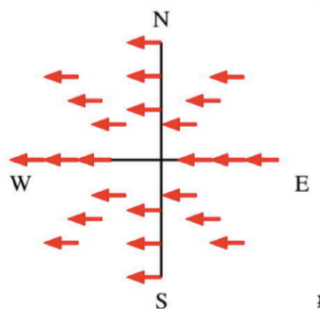
Theory predicts additional mechanisms:

 **excess of electrons in shower: charge excess**

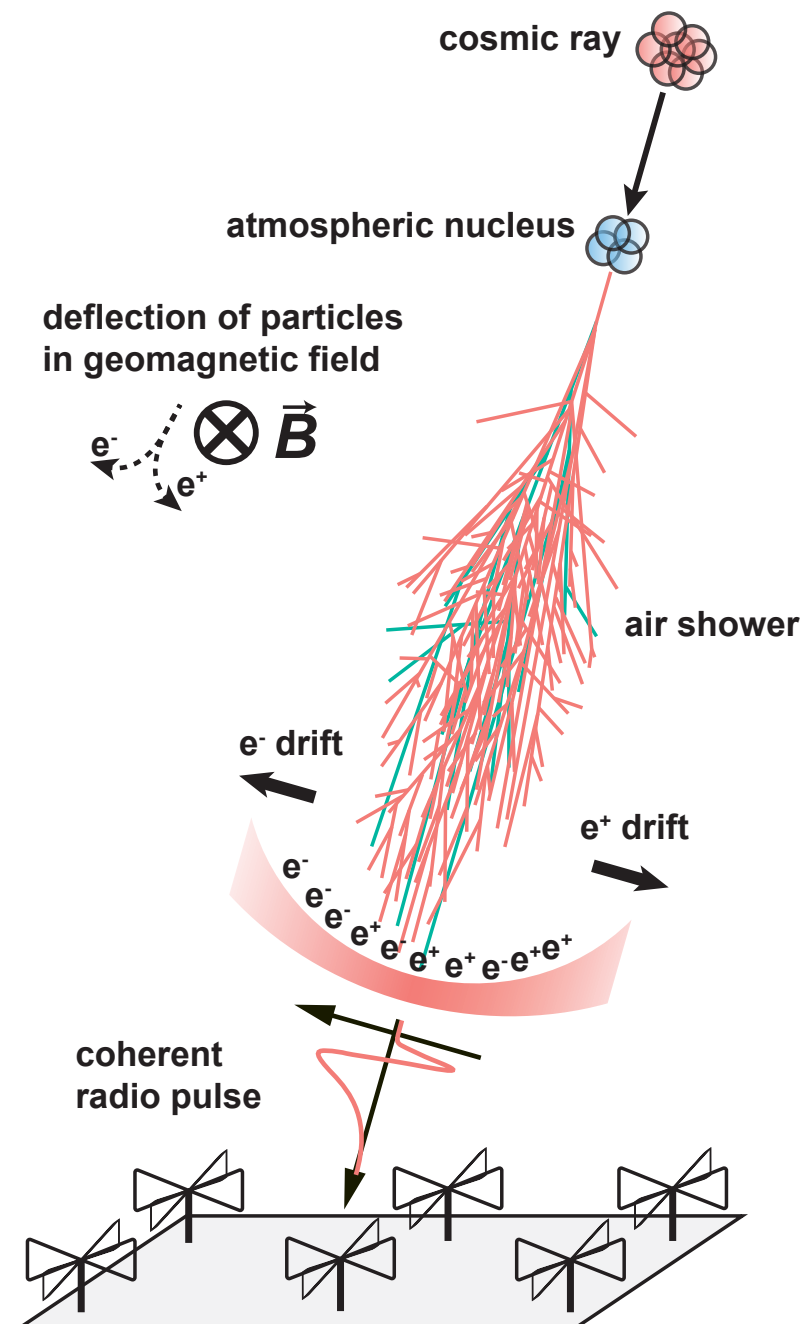
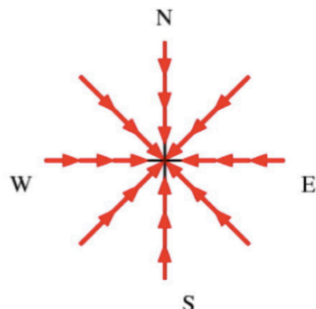
 **superposition of emission due to Cherenkov effects in atmosphere**

polarization of radio signal

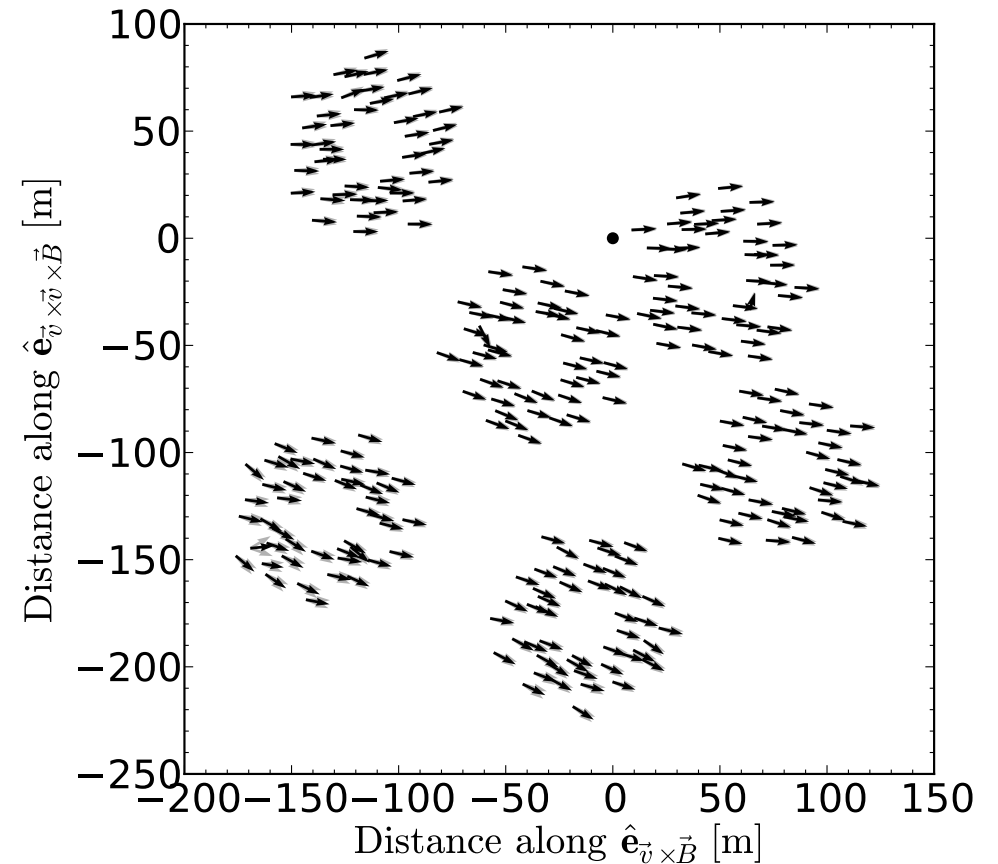
geomagnetic



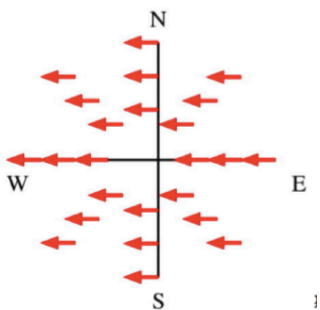
Askaryan



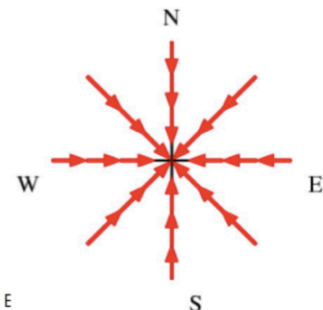
Polarization footprint of an individual air shower



geomagnetic

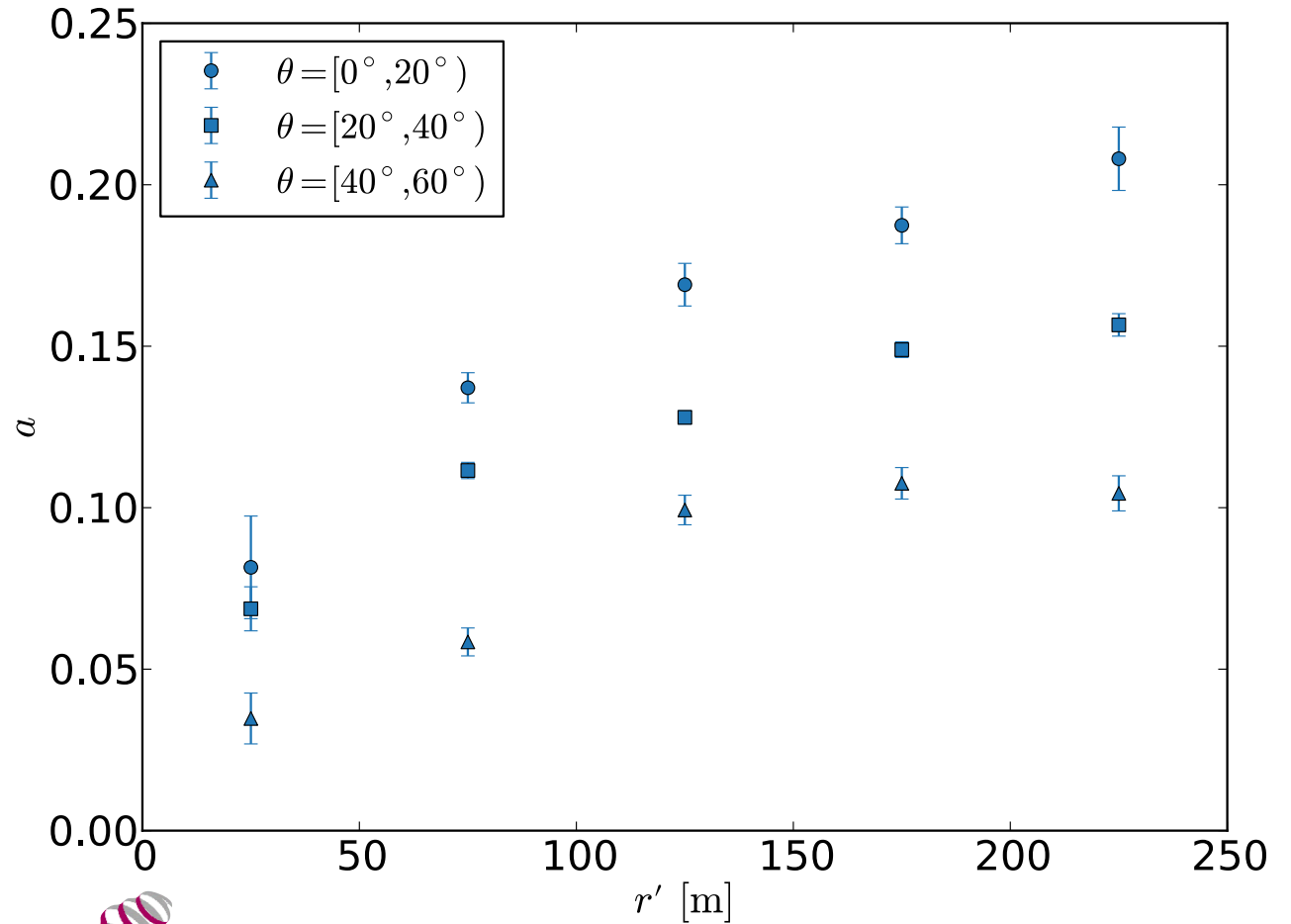
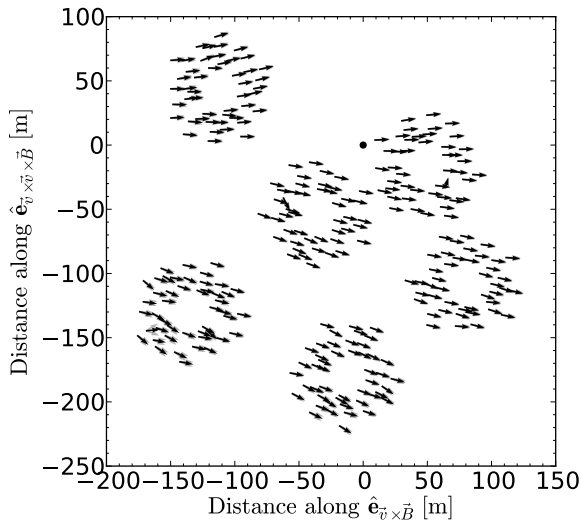


Askaryan



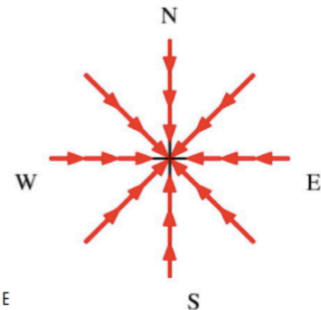
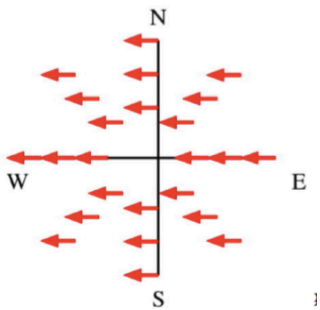
Charge excess fraction

Askaryan geomagnetic

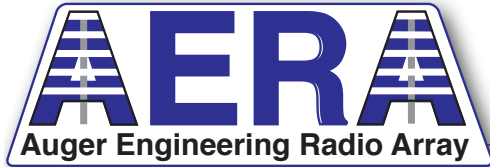


geomagnetic

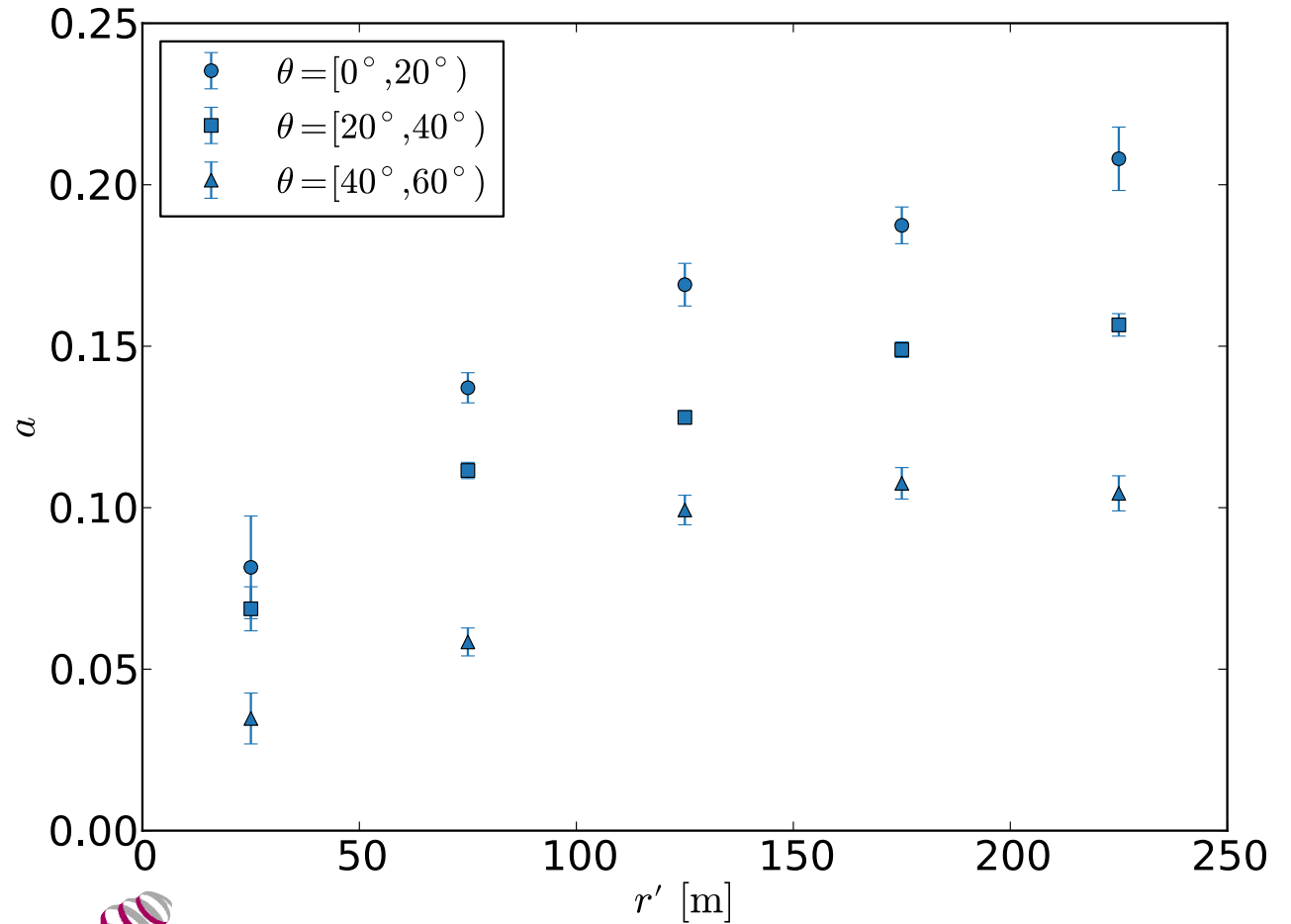
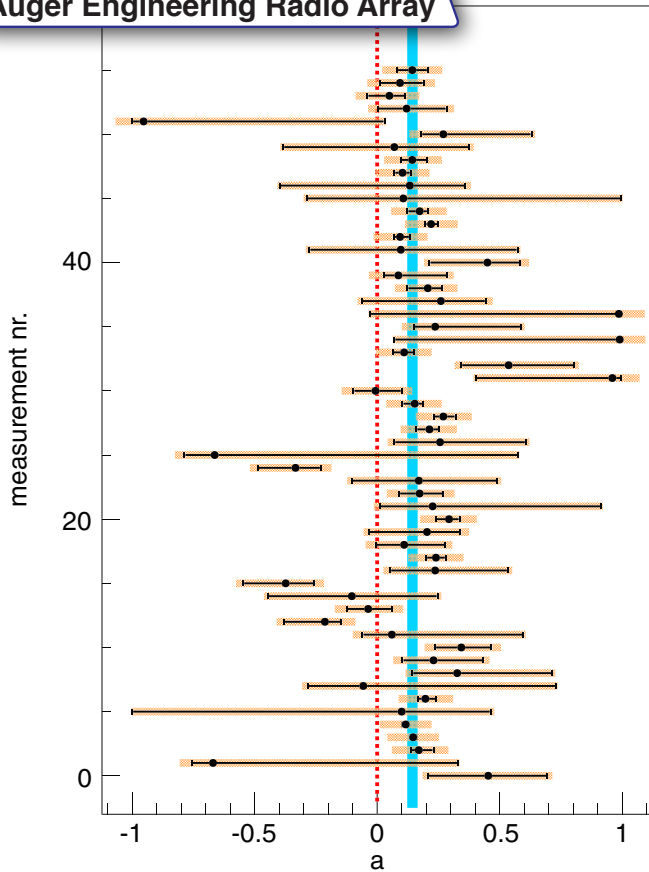
Askaryan



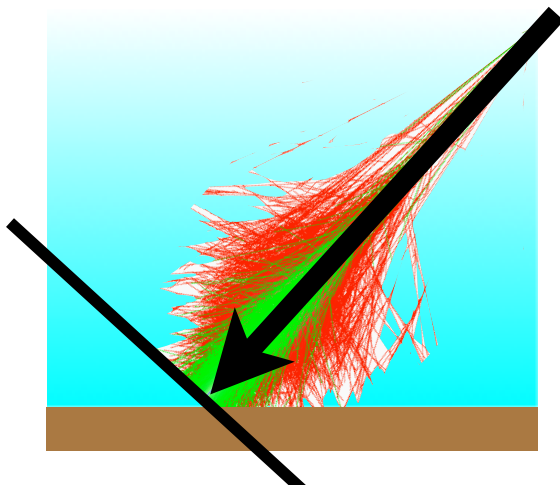
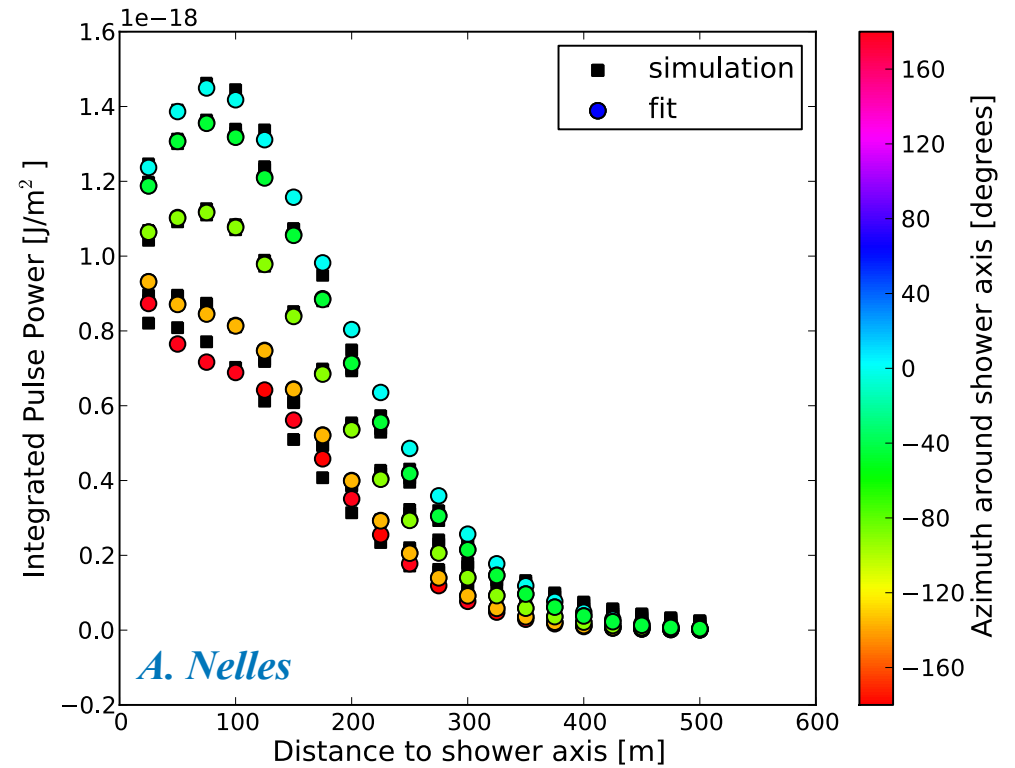
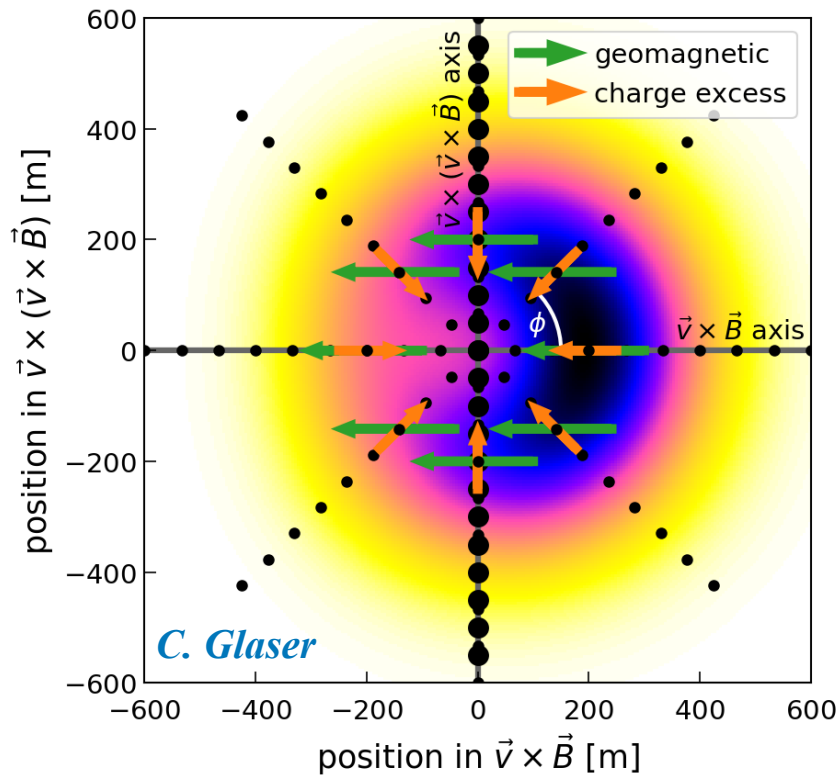
Charge excess fraction



Askaryan
geomagnetic



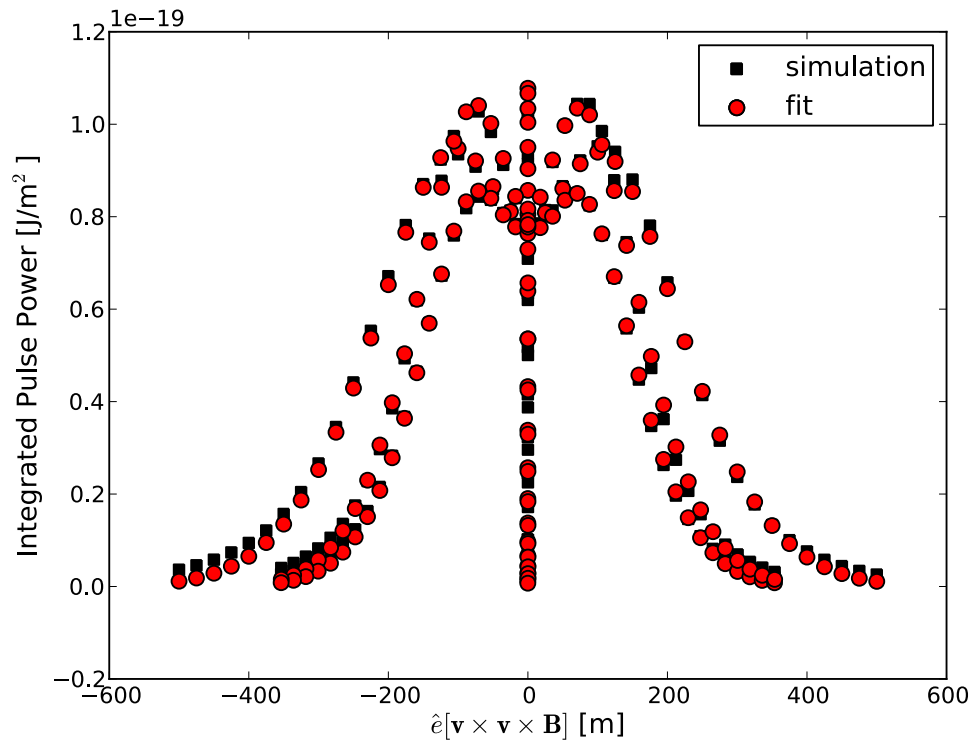
Footprint of radio emission on the ground



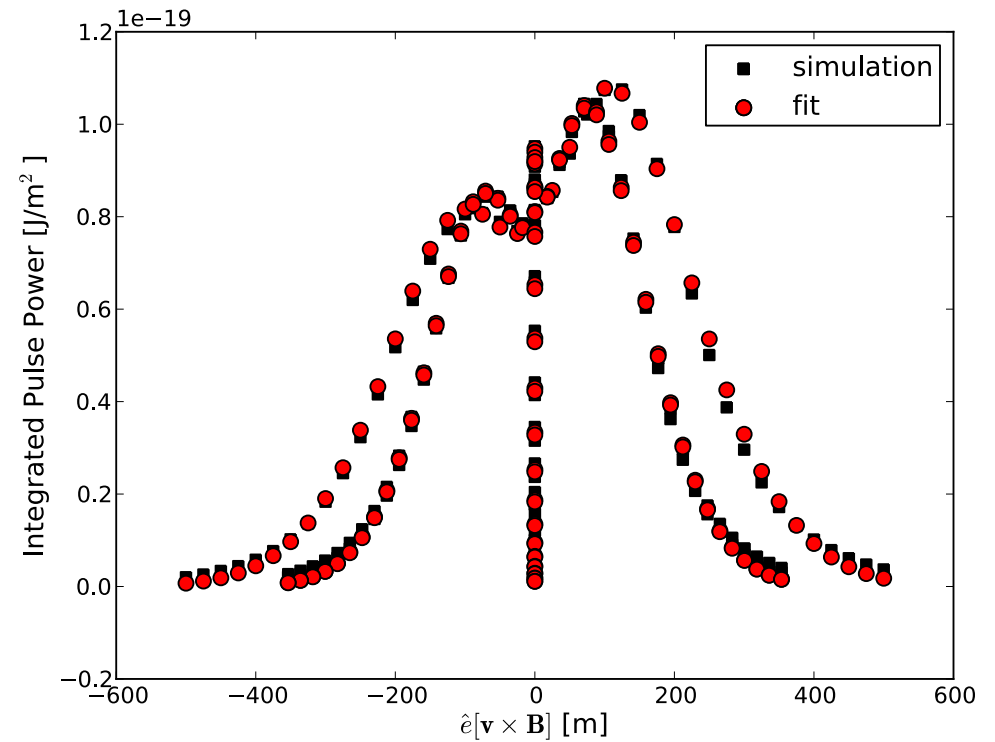
Lateral distribution of radio signals

not rotationally symmetric → fit two Gaussian functions

$\mathbf{v} \times (\mathbf{v} \times \mathbf{B})$



$\mathbf{v} \times \mathbf{B}$



$$P(x', y') = A_+ \cdot \exp\left(\frac{-[(x' - X_+)^2 + (y' - Y_+)^2]}{\sigma_+^2}\right) - A_- \cdot \exp\left(\frac{-[(x' - X_-)^2 + (y' - Y_-)^2]}{\sigma_-^2}\right) + O$$

Properties of incoming cosmic ray

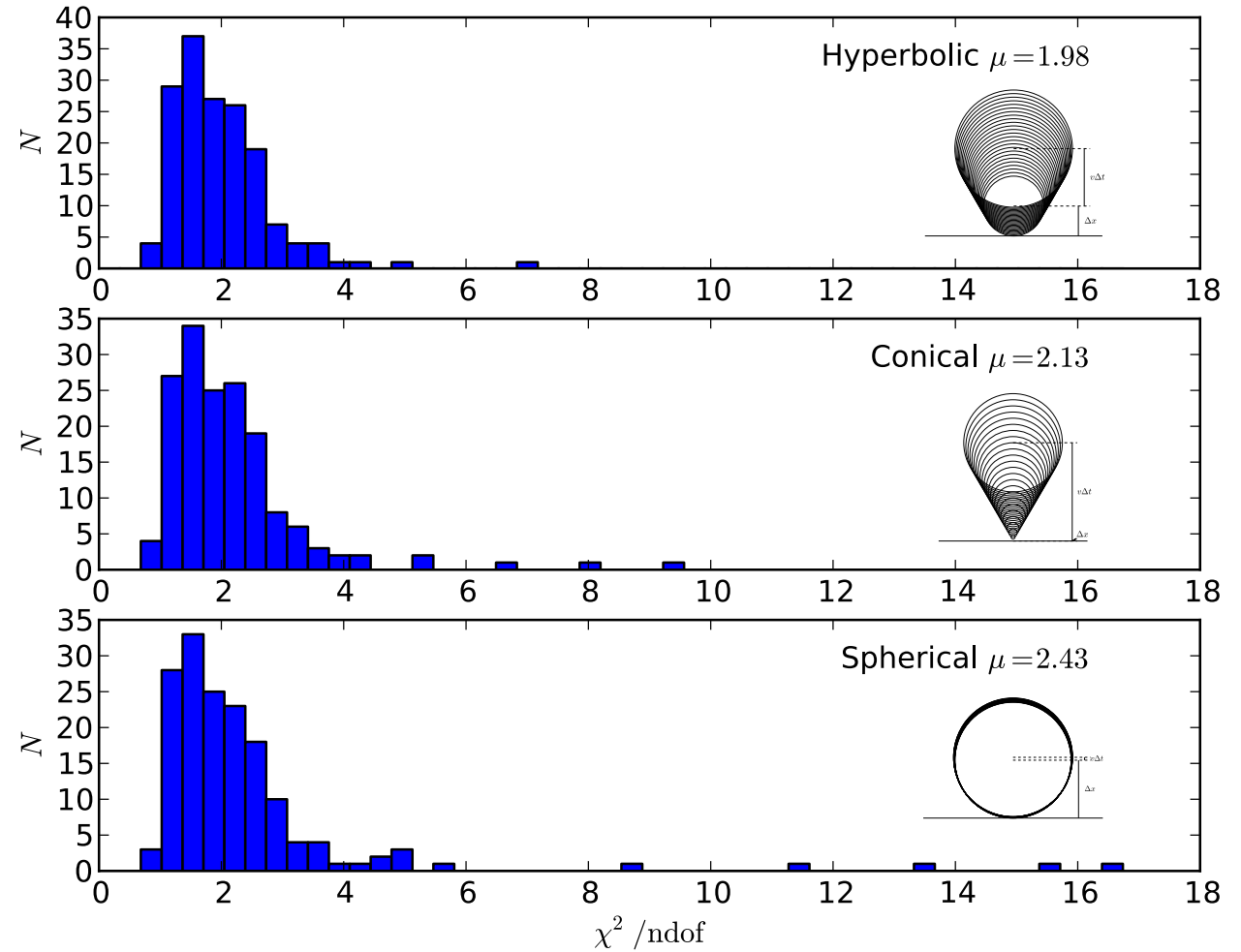
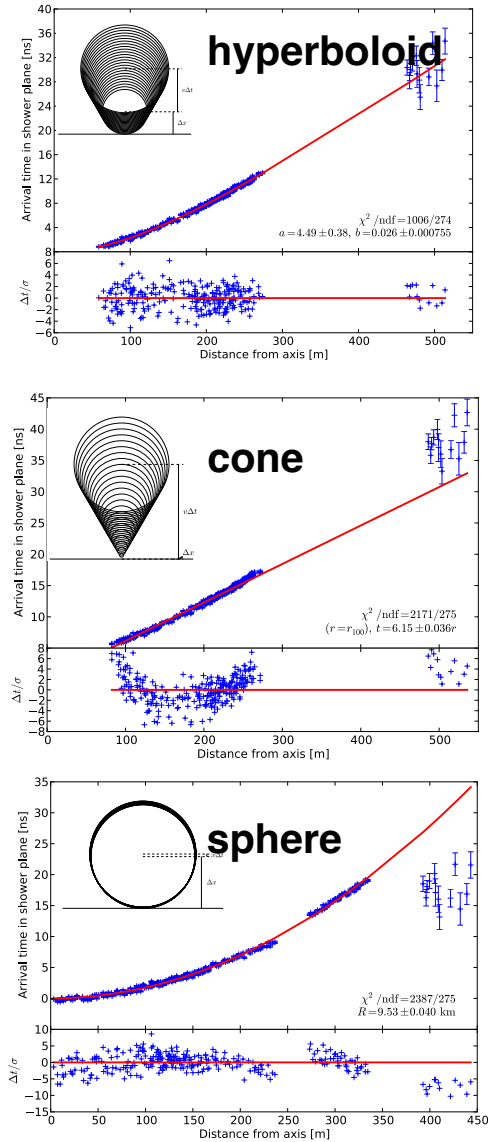
- **direction**
- **energy**
- **type**

Direction



Shape of Shower Front

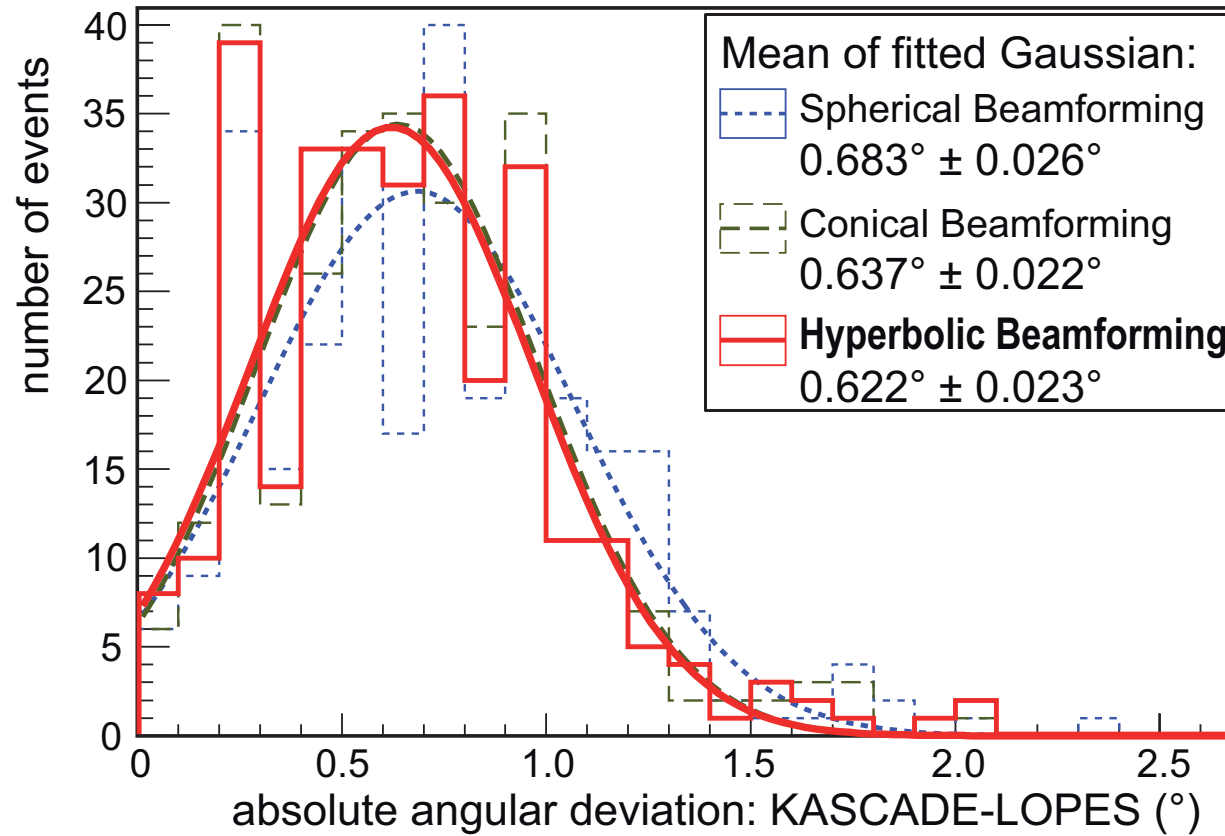
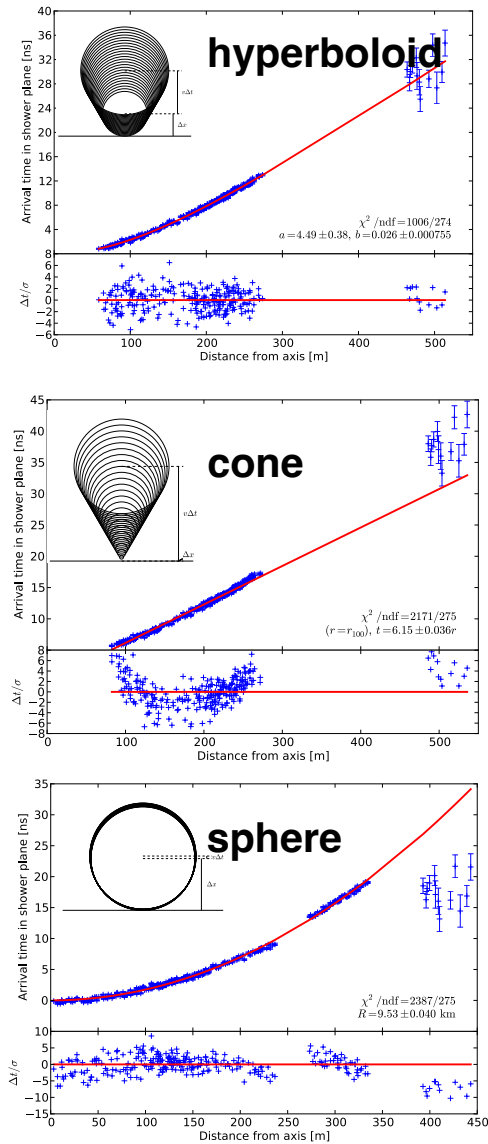
fit quality



Shape of Shower Front



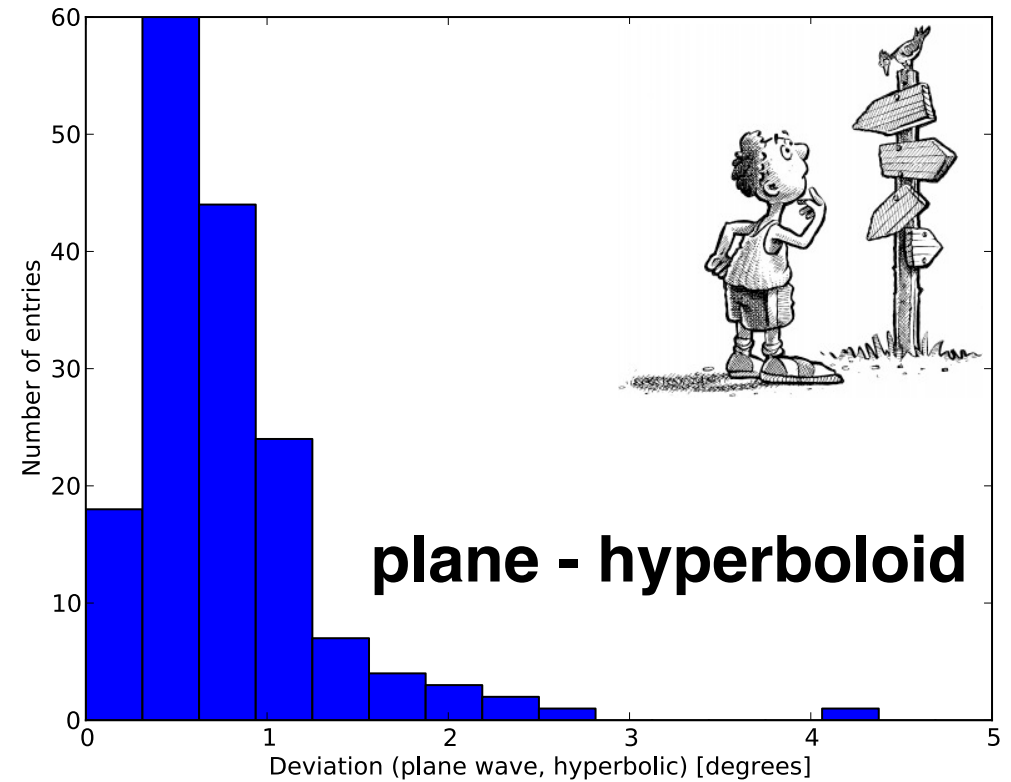
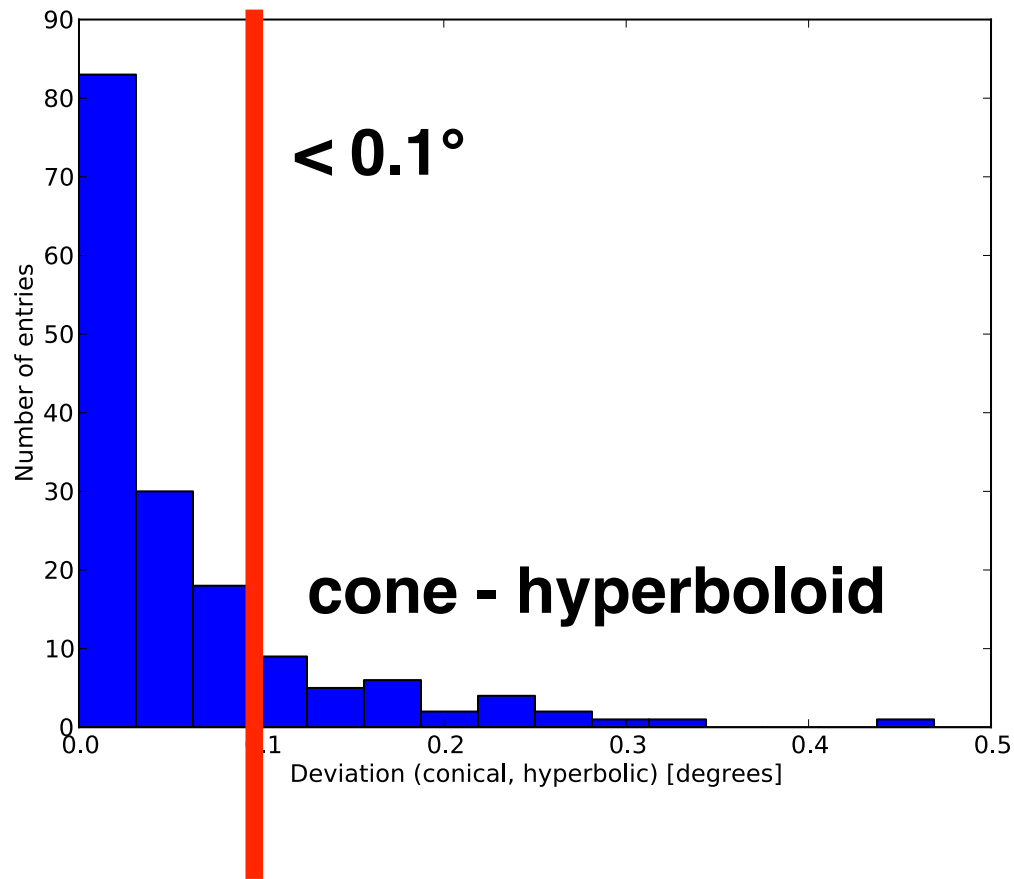
LOFAR



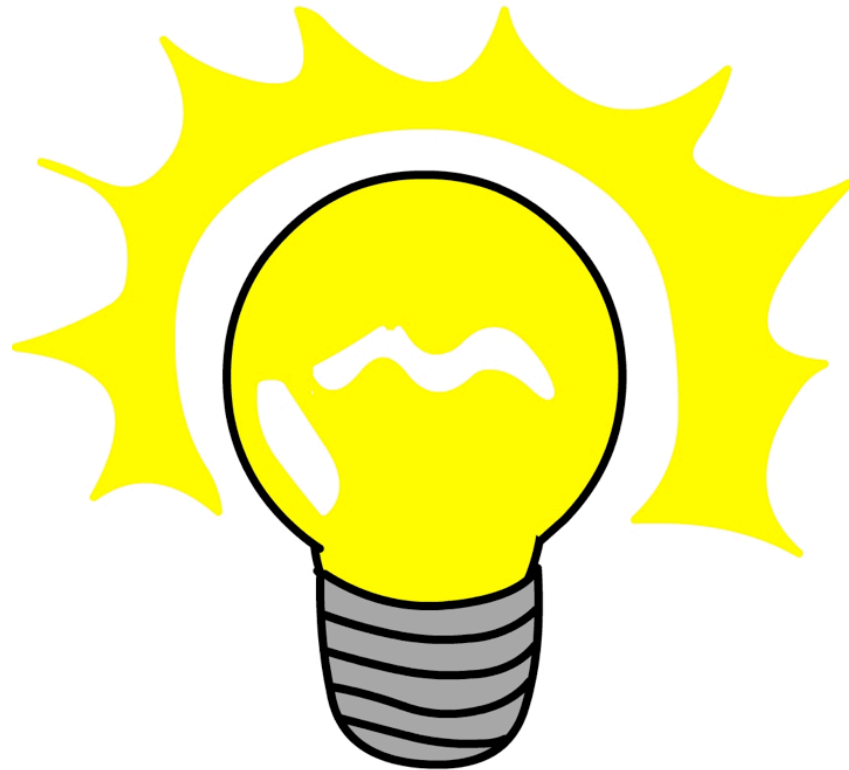
W.D. Apel et al., JCAP 1409 (2014) no.09, 025

Accuracy of Shower Direction

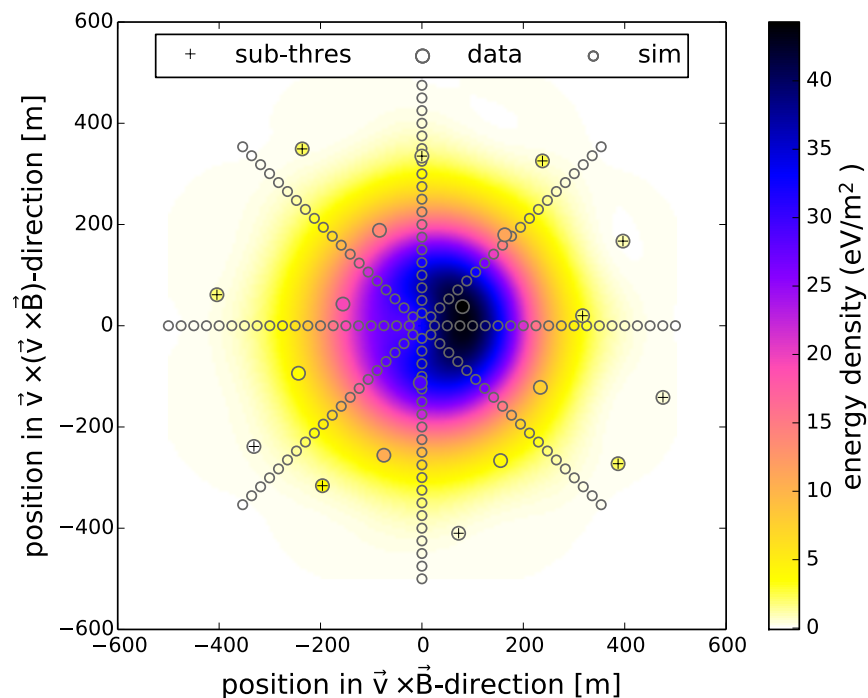
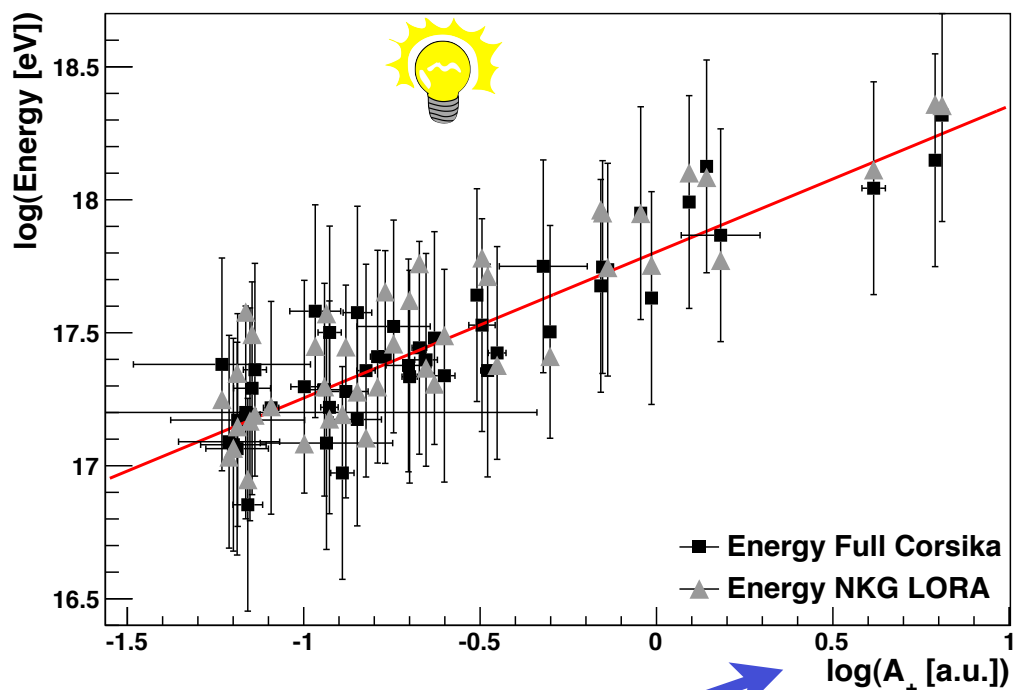
angular difference
between..



Energy

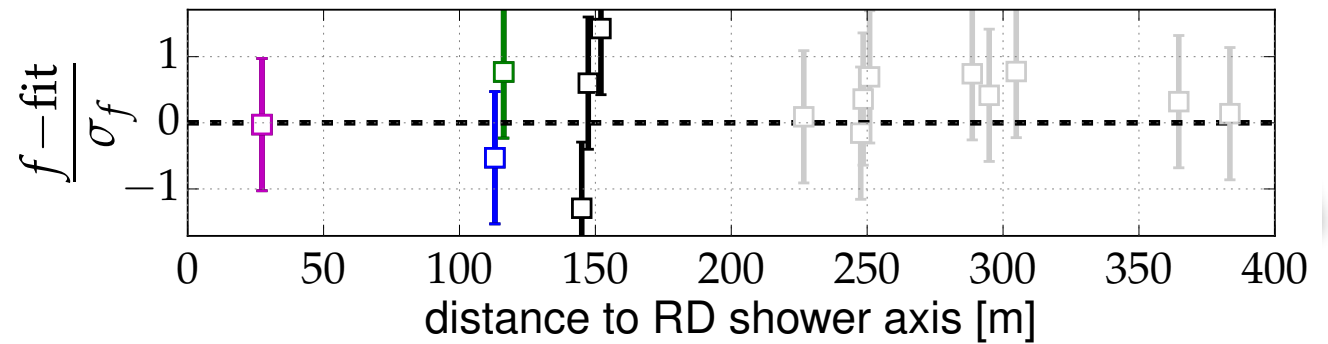
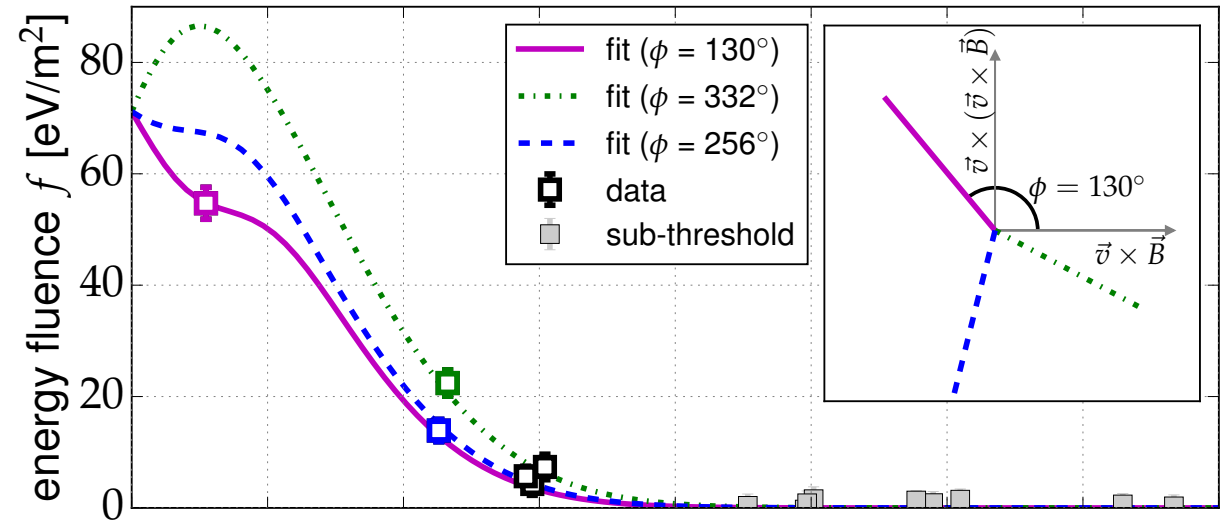
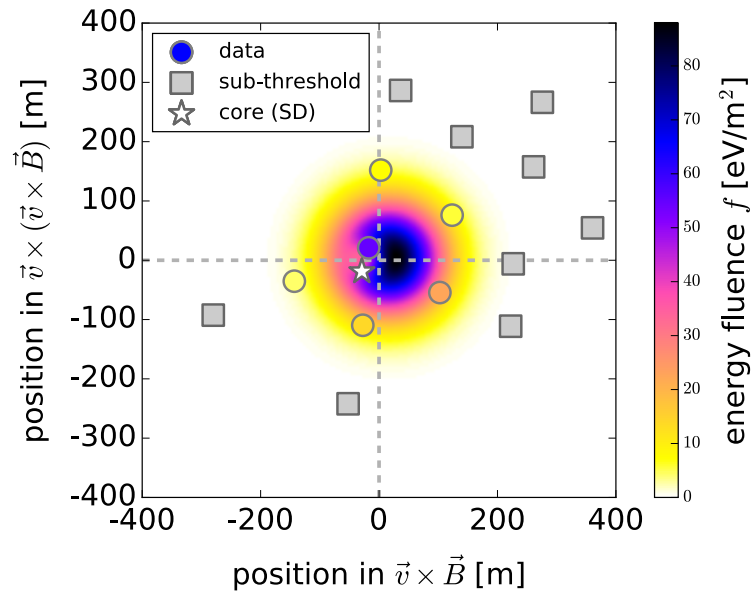


Energy of primary particle

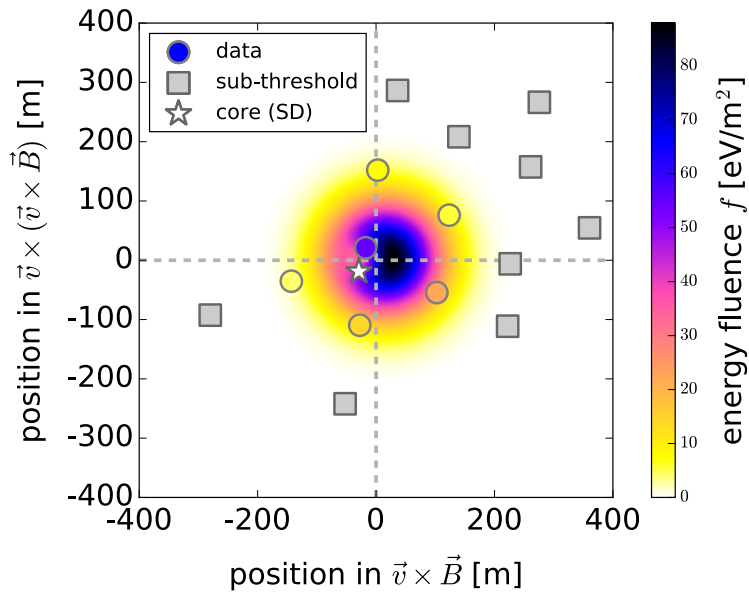


$$P(x', y') = A_+ \cdot \exp\left(\frac{-[(x' - X_+)^2 + (y' - Y_+)^2]}{\sigma_+^2}\right) - A_- \cdot \exp\left(\frac{-[(x' - X_-)^2 + (y' - Y_-)^2]}{\sigma_-^2}\right) + O$$

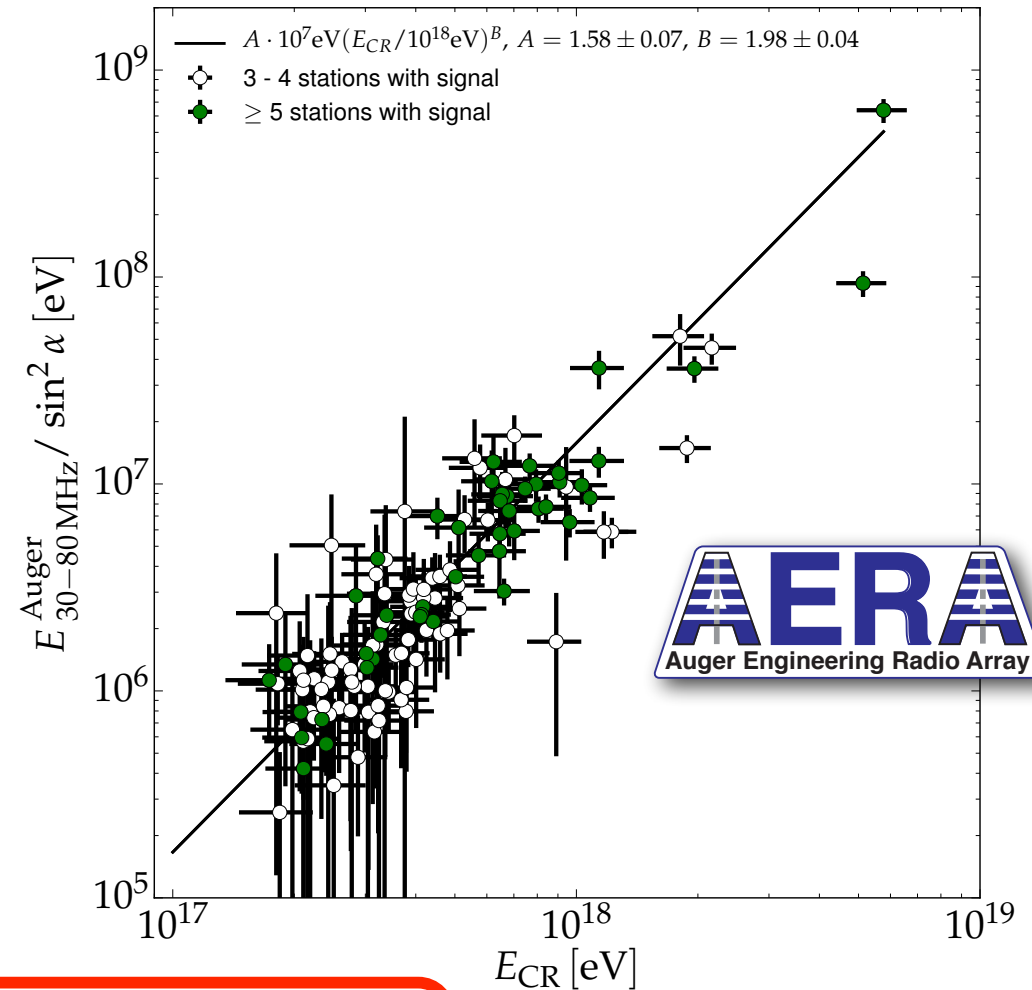
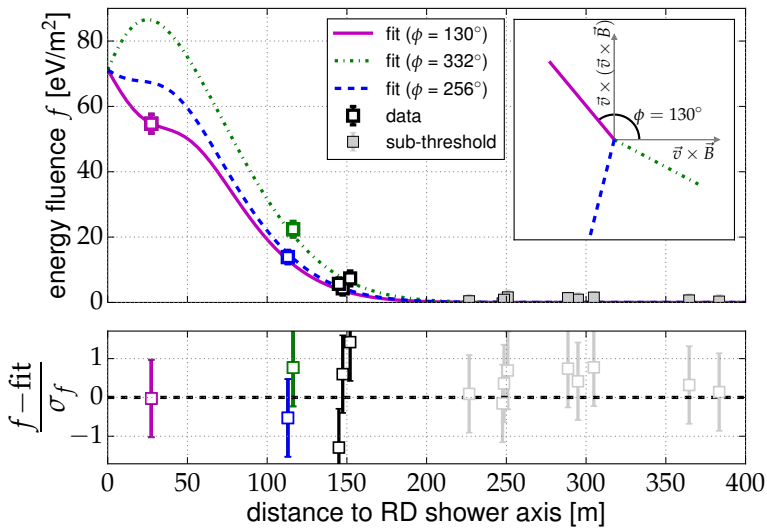
Measurement of the Radiation Energy in the Radio Signal of Extensive Air Showers as a Universal Estimator of Cosmic-Ray Energy



Measurement of the Radiation Energy in the Radio Signal of Extensive Air Showers as a Universal Estimator of Cosmic-Ray Energy



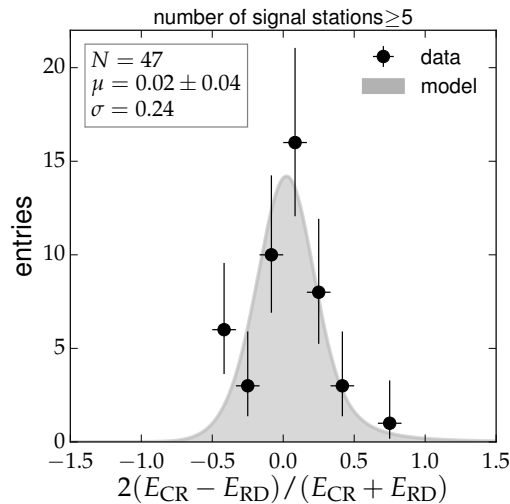
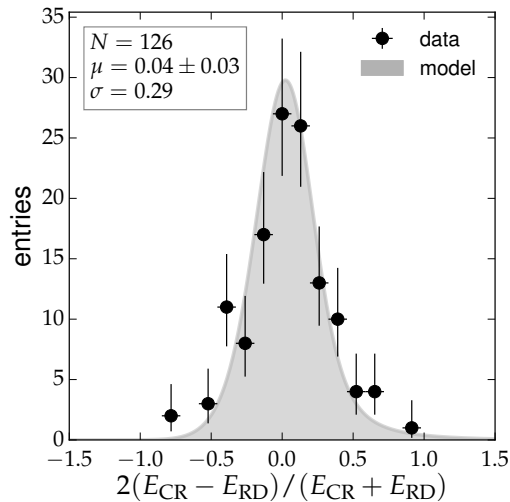
$E_{30-80 \text{ MHz}} = 15.8 \text{ MeV} @ 10^{18} \text{ eV}$



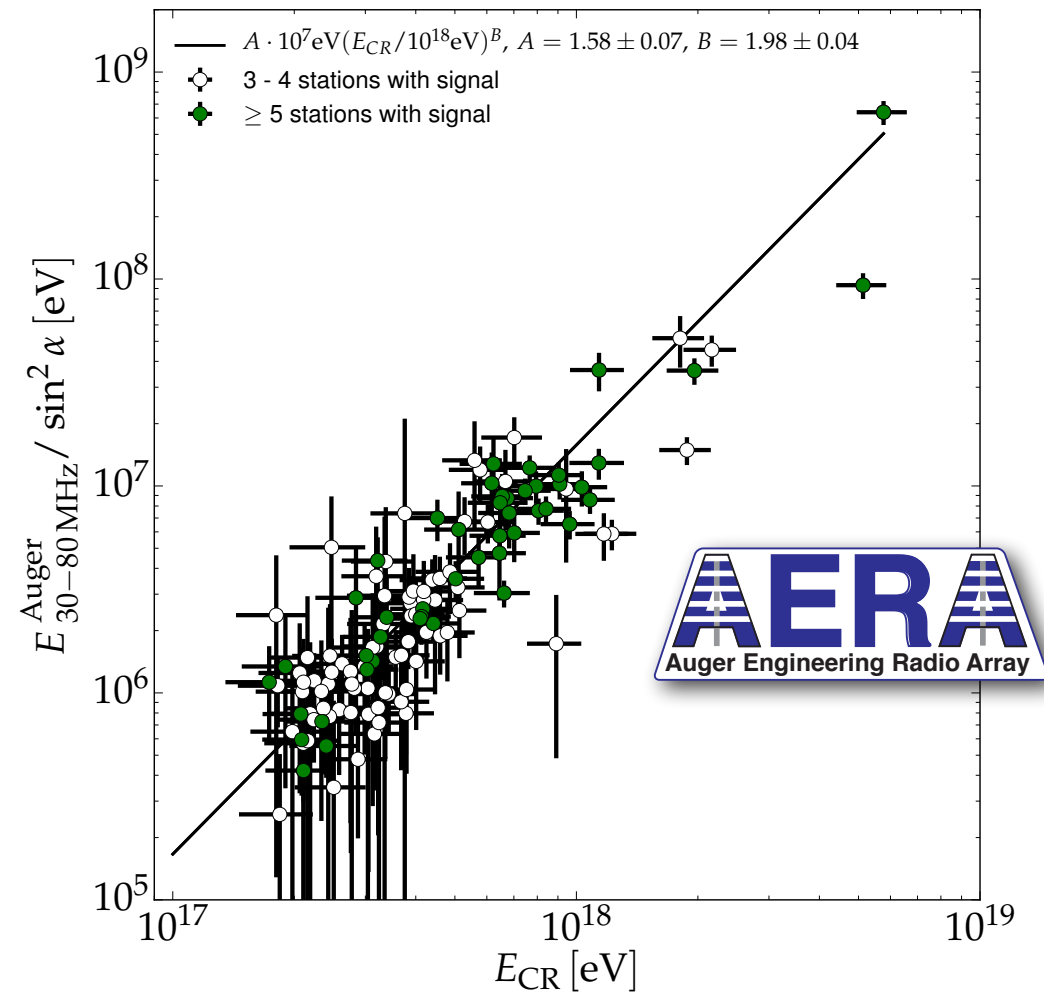
$$E_{30-80 \text{ MHz}} = (15.8 \pm 0.7(\text{stat}) \pm 6.7(\text{syst}) \text{ MeV}) \times \left(\sin \alpha \frac{E_{CR}}{10^{18} \text{ eV}} \frac{B_{Earth}}{0.24 \text{ G}} \right)^2$$

Energy Estimation of Cosmic Rays with the Engineering Radio Array of the Pierre Auger Observatory

E_{30-80} MHz = 15.8 MeV @ 10^{18} eV



$\sigma \approx 24\%$



A. Aab et al., PRD 93 (2016) no.12, 122005

A. Aab et al., PRL 116 (2016) no.24, 241101

Cosmic-ray energy (Cherenkov) vs radio signal

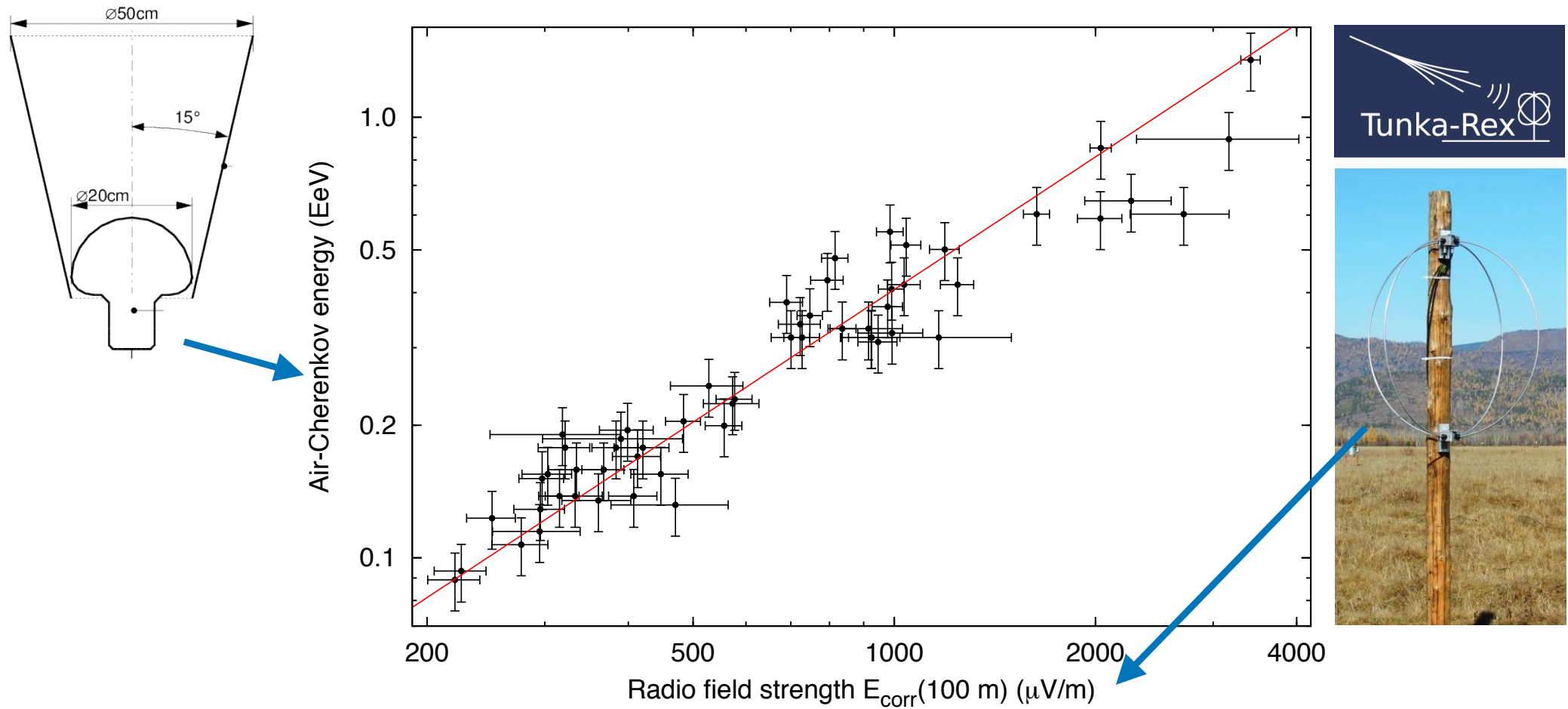


Fig. 3. Correlation of the energy measured with the air-Cherenkov array and an energy estimator based on the radio amplitude at 100 m measured with Tunka-Rex. The line indicates a linear correlation.

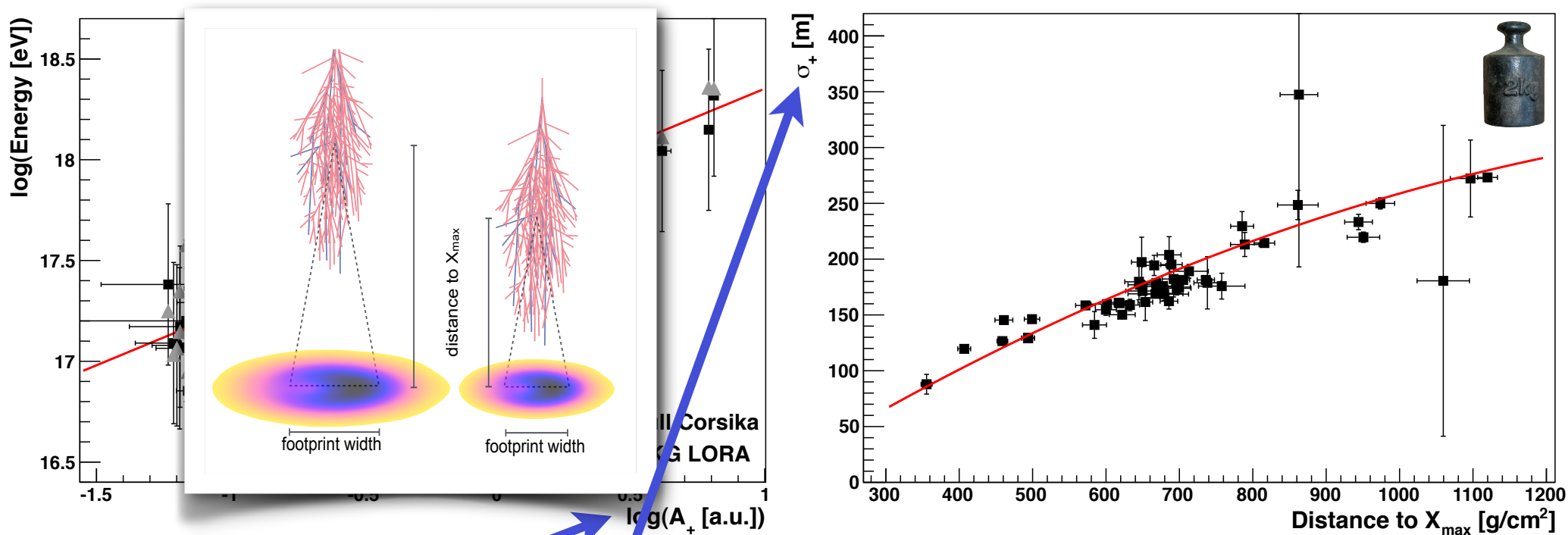
Mass



Properties of primary particle

energy

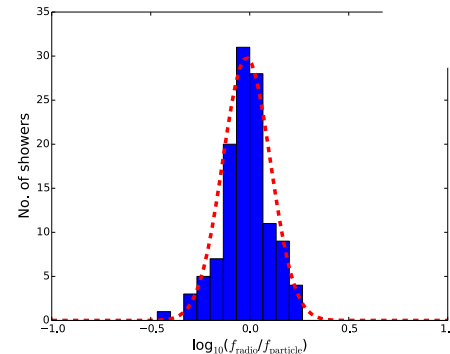
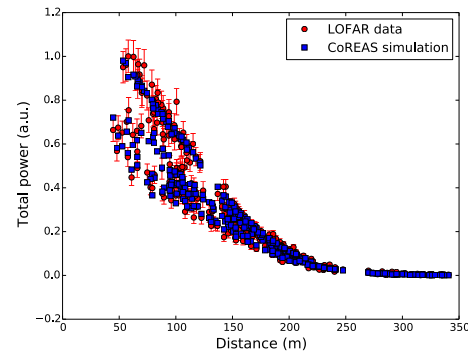
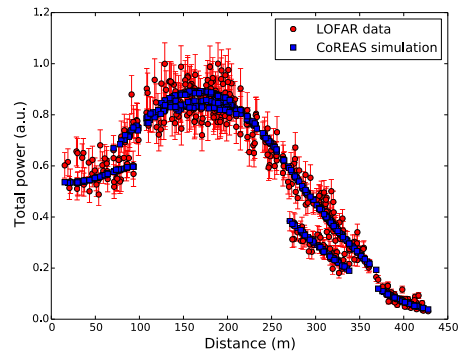
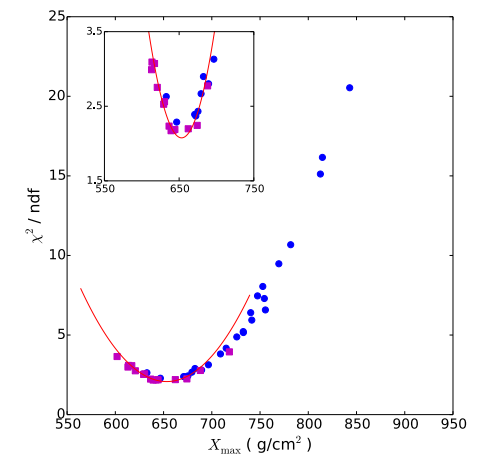
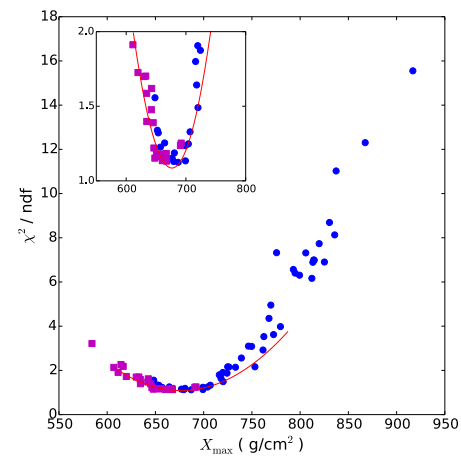
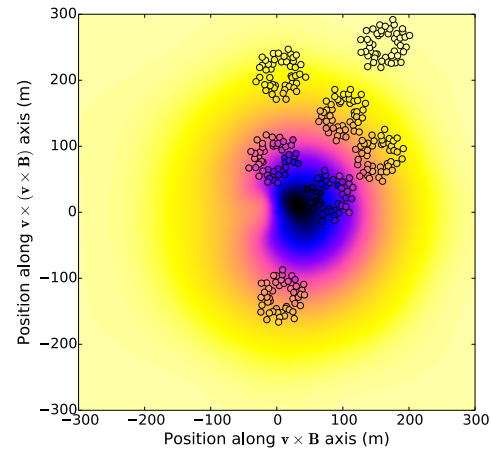
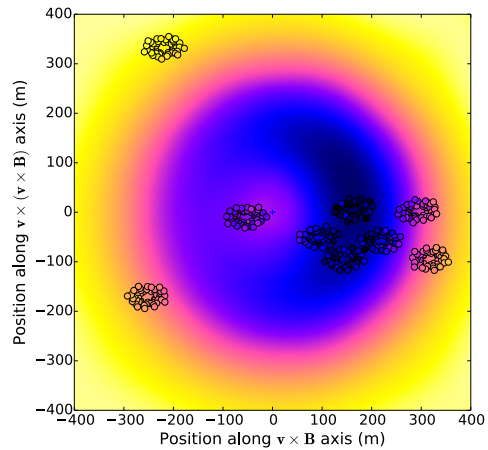
distance to Xmax



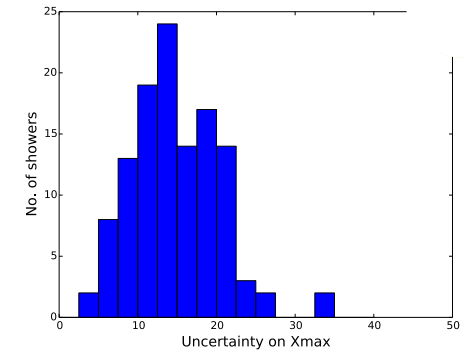
$$P(x', y') = A_+ \cdot \exp\left(\frac{-[(x' - X_+)^2 + (y' - Y_+)^2]}{\sigma_+^2}\right) - A_- \cdot \exp\left(\frac{-[(x' - X_-)^2 + (y' - Y_-)^2]}{\sigma_-^2}\right) + O$$



Measurement of particle mass



$$\sigma_E \approx 32\%$$



$$\sigma_{X_{max}} \approx 17 \text{ g/cm}^2$$

Depth of the shower maximum

LETTER **nature**

doi:10.1038/nature16976

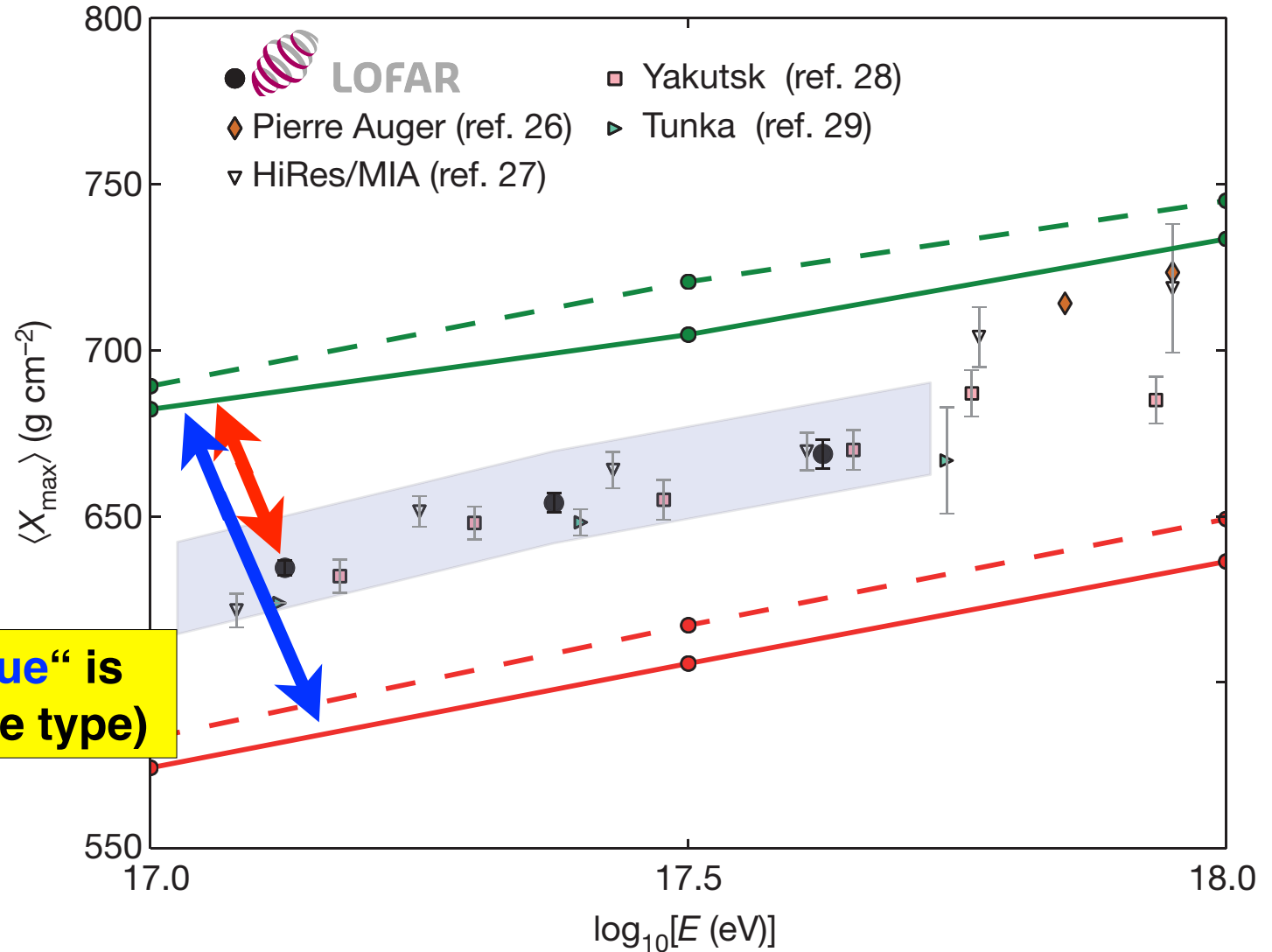
A large light-mass component of cosmic rays at 10^{17} – $10^{17.5}$ electronvolts from radio observations

S. Buitink^{1,2}, A. Corstanje², H. Falcke^{2,3,4,5}, J. R. Hörandel^{6,7}, T. Huege⁸, A. Nelles^{9,7}, J. P. Rachen¹, L. Rossetto², P. Schellart², O. Scholten¹⁰, S. ter Veer¹, S. Thoudam¹, T. N. G. Trinh¹, J. Anderson¹¹, A. Asgekar¹², I. M. Avrukh^{13,14}, M. E. Bell¹⁵, M. J. Bentsun^{1,15}, G. Bernardini¹⁶, P. Best¹⁸, A. Bonafede¹⁹, F. Breitenlohner²⁰, J. W. Broderick²¹, W. N. Brown^{1,15}, M. Brüggen¹⁹, H. R. Butcher²², D. Carbone²³, B. Clardi²⁴, J. E. Conway²⁵, F. de Gasperin¹⁹, E. de Geus^{1,26}, A. Deller¹, R.-J. Dettmar²⁷, G. van Diepen¹, S. Duscha¹, J. Eislöffel²⁸, D. Engels²⁹, J. E. Enriquez³⁰, R. A. Fallows¹, R. Fender³⁰, C. Ferrari³¹, W. Frieswijk³, M. A. Garrett^{1,32}, J. M. Grießmeier^{1,34}, A. W. Gunst¹, M. P. van Haarlem¹, T. E. Hassall³⁵, G. Heald^{1,33}, J. W. T. Hessels^{1,33}, M. Hoefft³⁶, A. Hornberger¹, M. Iacobelli³⁷, H. Intema^{1,38}, E. Juette³⁹, A. Karastergiou⁴⁰, V. I. Kondratiev^{41,42}, M. Kramer^{4,37}, M. Kuniyoshi⁴³, G. Kuper¹, J. van Leeuwen^{1,44}, G. M. Looze¹, P. Maat¹, G. Mann⁴⁵, S. Markoff⁴⁶, R. McFadden¹, D. McKay-Bukowski^{47,48}, I. P. McKean^{1,49}, M. Mevius^{1,50}, D. D. Mulcahy⁵¹, H. Munk¹, M. J. Norden¹, E. Orru¹, H. Paas⁵², M. Pandey-Pommier⁵³, V. N. Pandey¹, M. Pietka³⁰, R. Pizzo¹, A. G. Polatidis¹, W. Reich⁵⁴, H. J. A. Röttgering³², A. M. M. Scaife⁵⁵, D. J. Schwarz⁵⁶, M. Serylak⁵⁷, J. Shuman¹, O. Smirnov^{17,44}, B. W. Stappers³⁷, M. Steinmetz²⁰, A. Stewart³⁰, J. Swinbank^{23,45}, M. Tagger⁵⁸, Y. Tang¹, C. Tasse^{44,46}, M. C. Toribio^{1,52}, R. Vermeulen¹, C. Vocks²⁰, C. Vogt¹, R. J. van Weeren¹⁸, R. A. M. J. Wijers²³, S. J. Wijnholds¹, M. W. Wise^{1,59}, O. Wucknitz¹, S. Yatawatta¹, P. Zarka⁴⁷ & J. A. Zensus¹

Cosmic rays are the highest-energy particles found in nature. Measurements of the mass composition of cosmic rays with energies of 10^{17} – 10^{19} electronvolts are essential to understanding whether they have galactic or extragalactic sources. It has also been proposed that the astrophysical neutrino signal¹ comes from accelerators capable of producing cosmic rays of these energies². Cosmic rays initiate air showers—cascades of secondary particles in the atmosphere—and their masses can be inferred from measurements of the atmospheric depth of the shower maximum (X_{\max}), the depth of the air shower when it contains the most particles³ or of the composition of shower particles reaching the ground⁴. Current measurements⁵ have either high uncertainty, or a low duty cycle and a high energy threshold. Radio detection of cosmic rays^{6–8} is a rapidly developing technique⁹ for determining X_{\max} (refs 10, 11) with a duty cycle of, in principle, nearly 100 per cent. The radiation is generated by the separation of relativistic electrons and positrons in the geomagnetic field and a negative charge excess in the shower front^{6,12}. Here we report radio measurements of X_{\max} with a mean uncertainty of 16 grams per square centimetre for air showers

initiated by cosmic rays with energies of 10^{17} – $10^{17.5}$ electronvolts. This high resolution in X_{\max} enables us to determine the mass spectrum of the cosmic rays: we find a mixed composition, with a light-mass fraction (protons and helium nuclei) of about 80 per cent. Unless, contrary to current expectations, the extragalactic component of cosmic rays contributes substantially to the total flux below $10^{17.5}$ electronvolts, our measurements indicate the existence of an additional galactic component, to account for the light composition that we measured in the 10^{17} – $10^{17.5}$ electronvolt range. Observations were made with the Low-Frequency Array (LOFAR¹³), a radio telescope consisting of thousands of crossed dipoles with built-in air-shower-detection capability¹⁴. LOFAR continuously records the radio signals from air showers, while simultaneously running astronomical observations. It comprises a scintillator array (LORA) that triggers the read-out of buffers, storing the full waveforms received by all antennas.

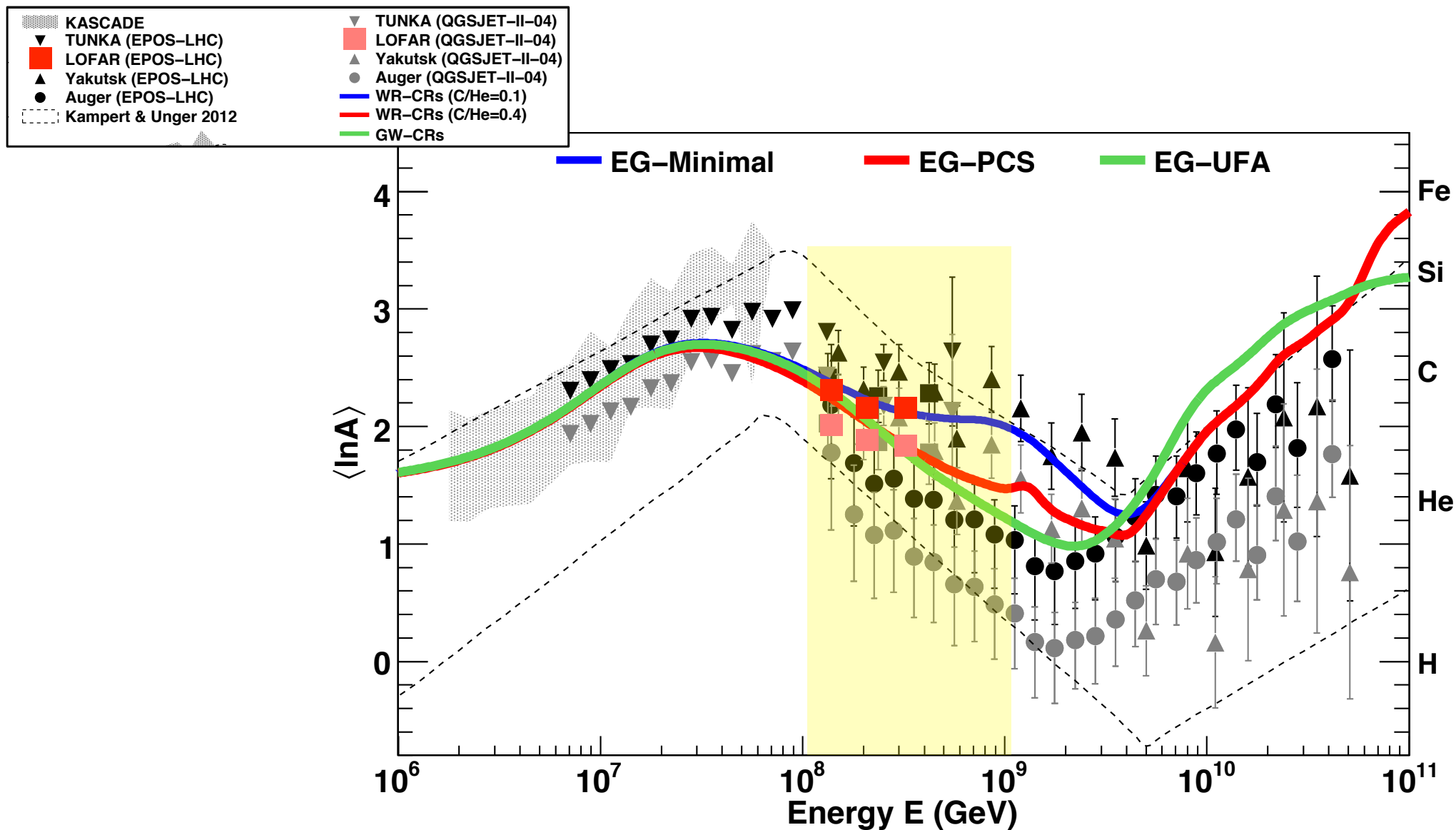
We selected air showers from the period June 2011 to January 2015 with radio pulses detected in at least 192 antennas. The total uptime was about 150 days, limited by construction and commissioning of the



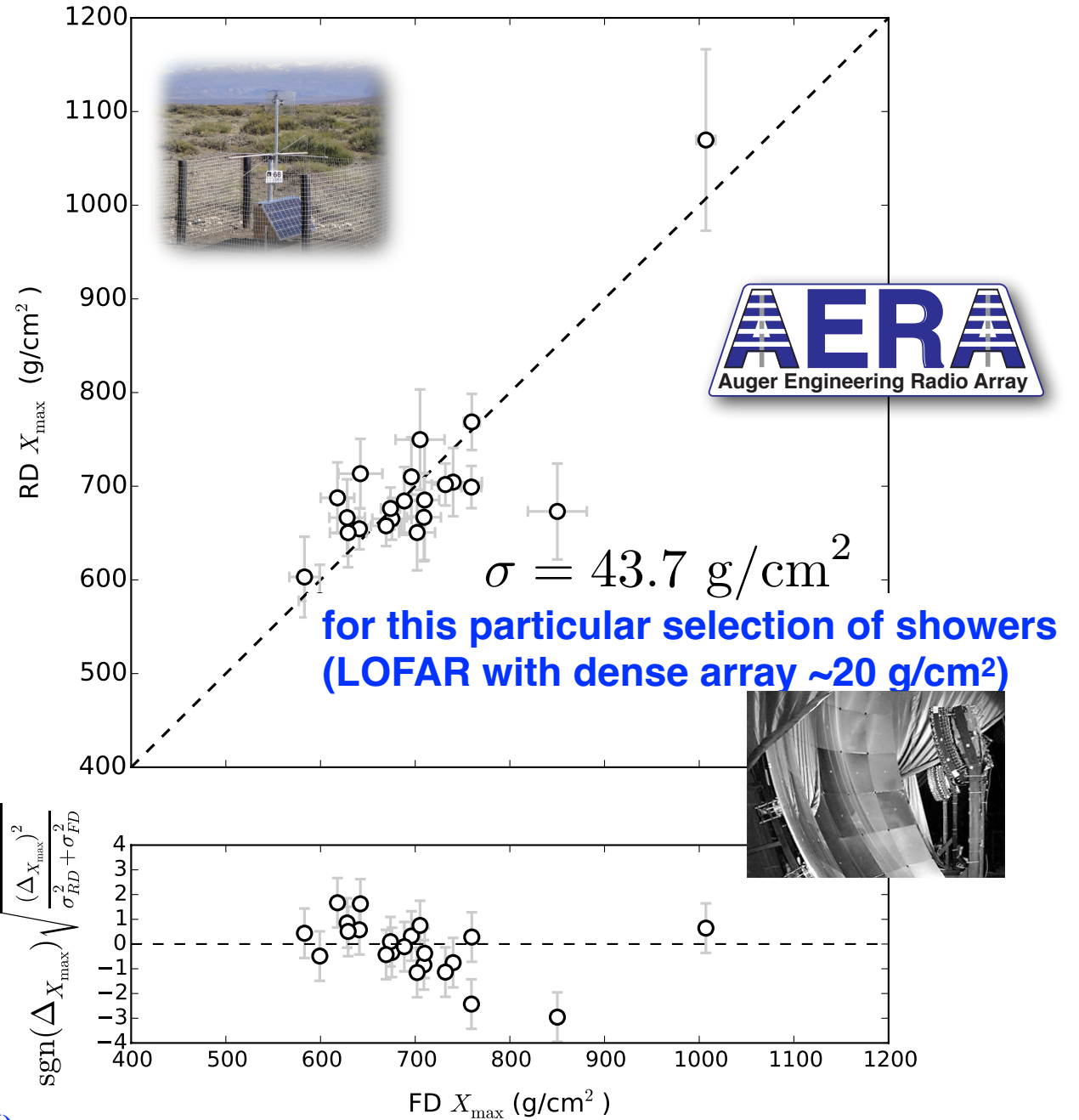
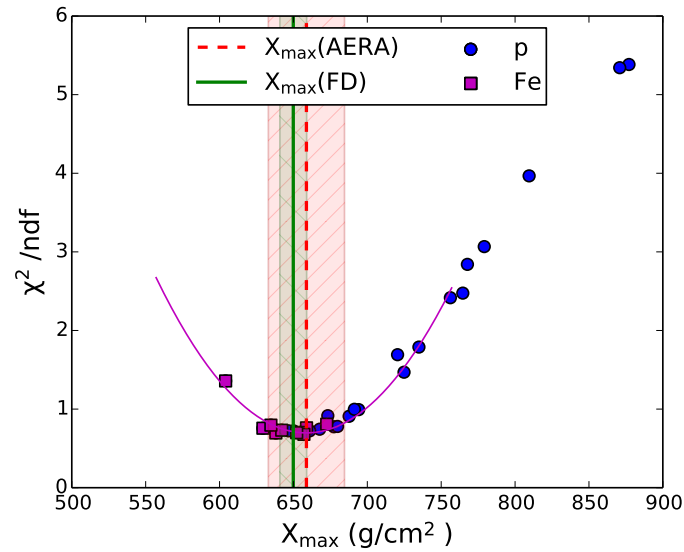
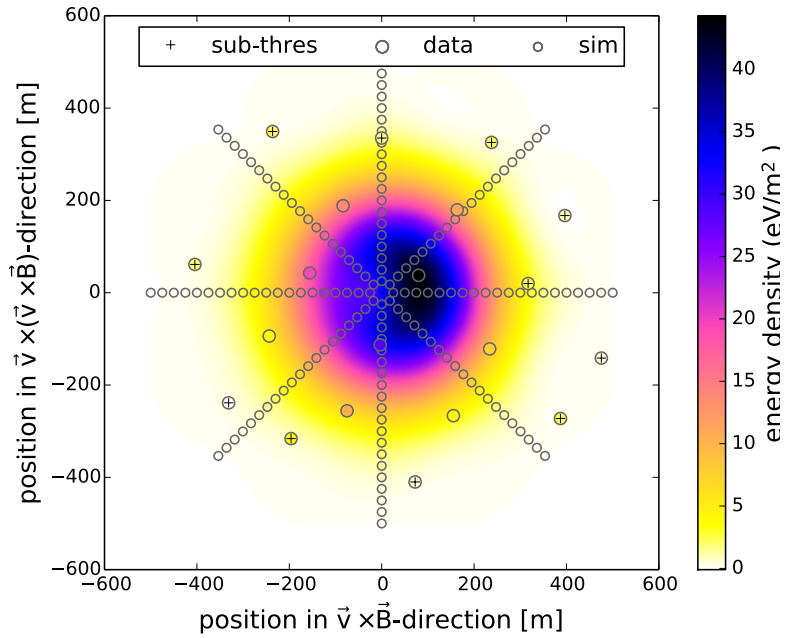
relative distance “red/blue” is measure for $\ln A$ (particle type)

Mean logarithmic mass

$$\ln A = \sum k_i \ln A_i$$

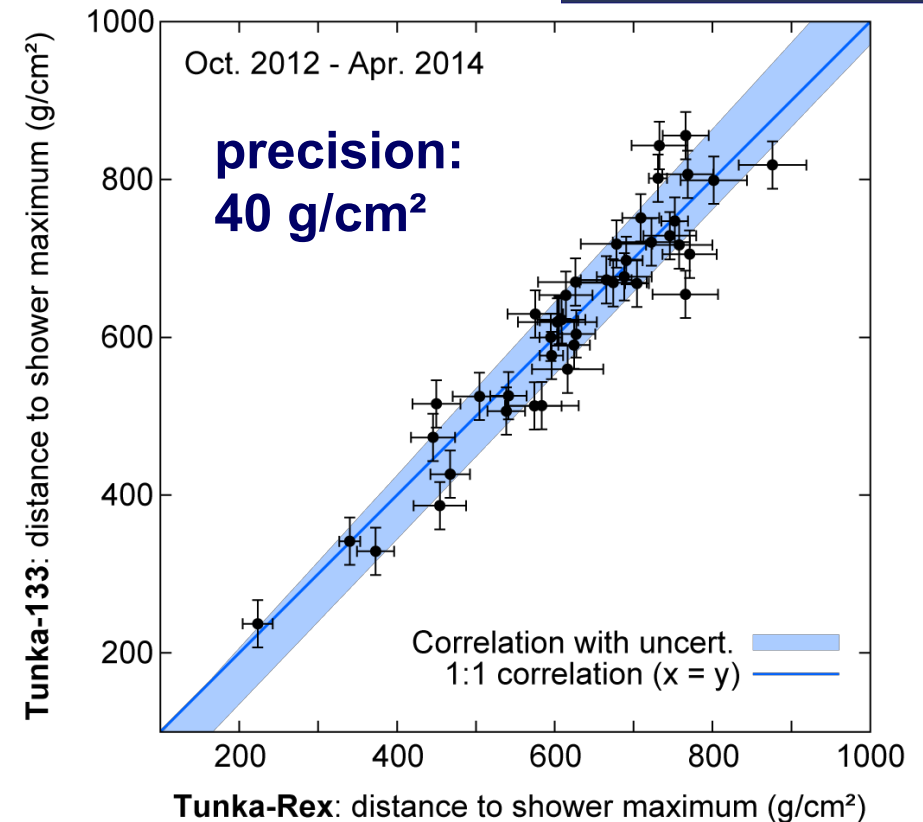
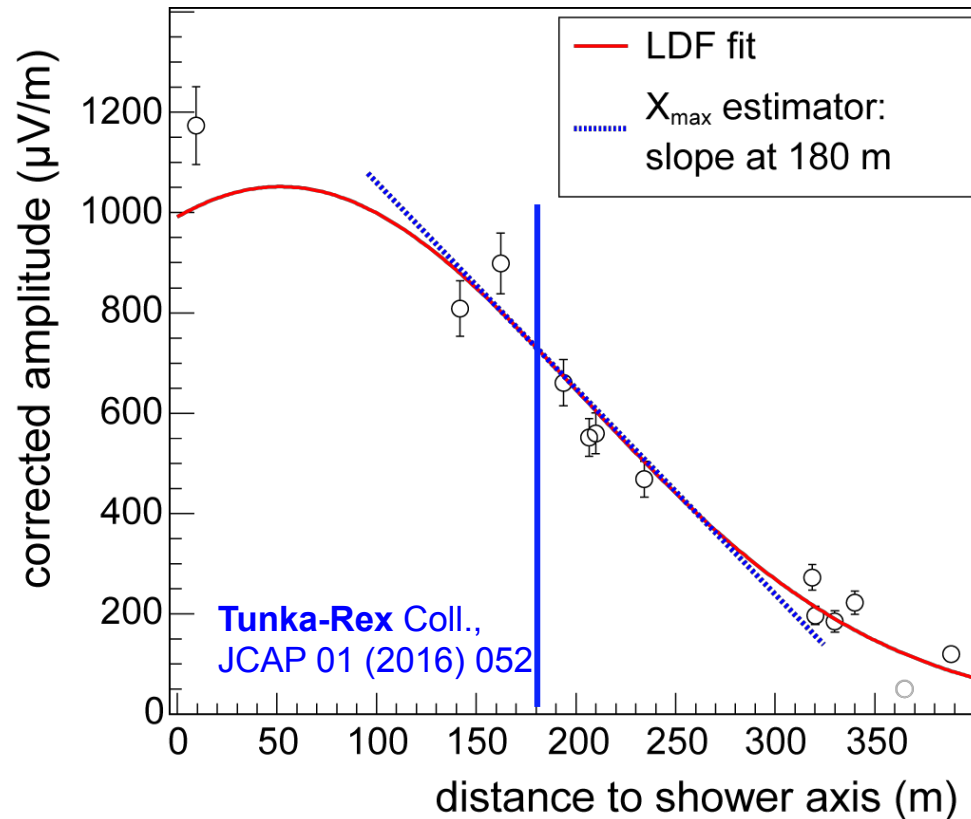


Xmax RD vs FD



Shower maximum: proof by Tunka-Rex

- One of several methods: slope of lateral distribution



Determine the properties of the incoming particle with the radio technique

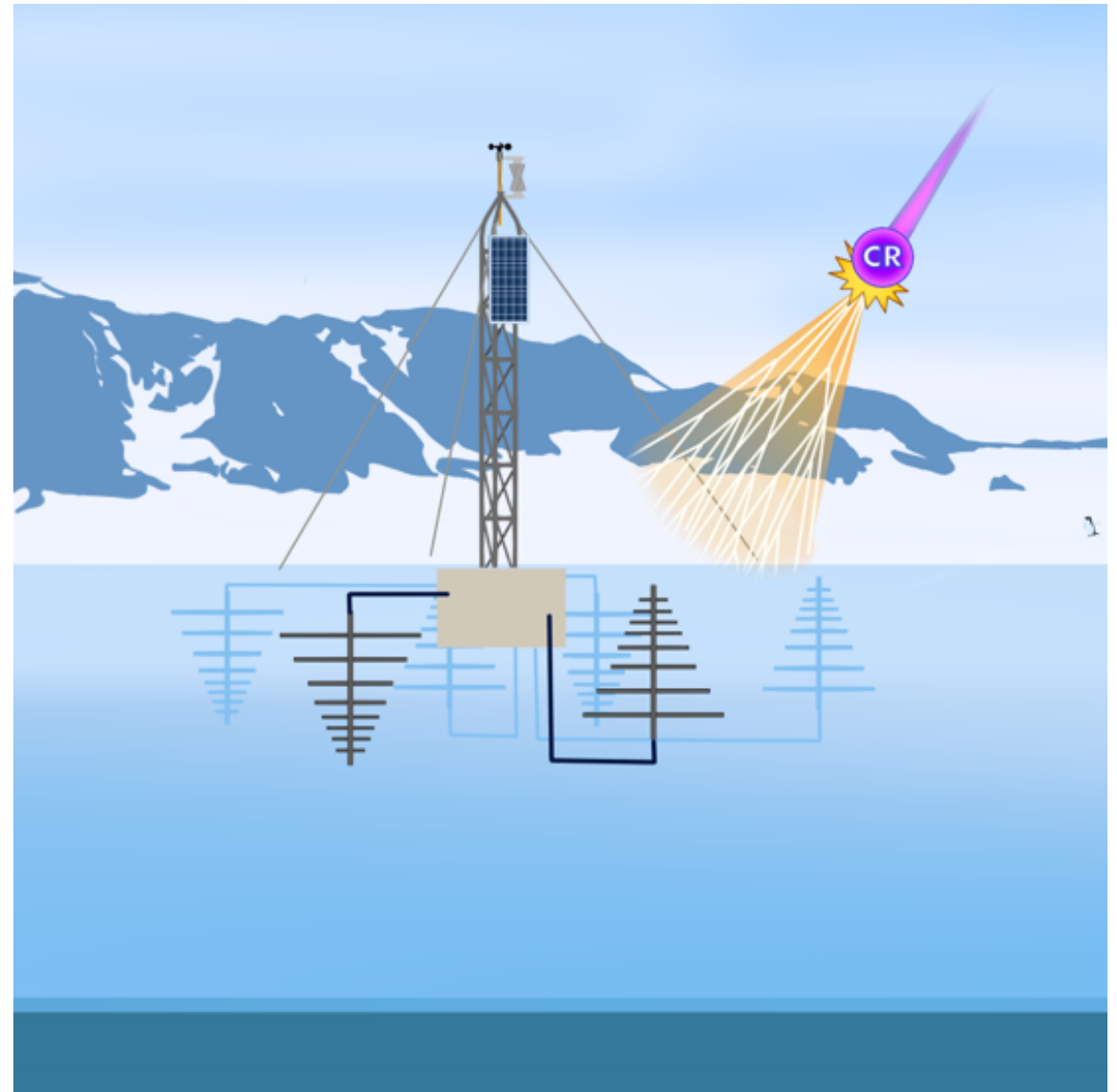
- **direction** ~ 0.1° - 0.5°
- **energy** ~ 20% - 30%
- **type (X_{\max})** ~ 20 - 40 g/cm²
(depending on detector spacing)

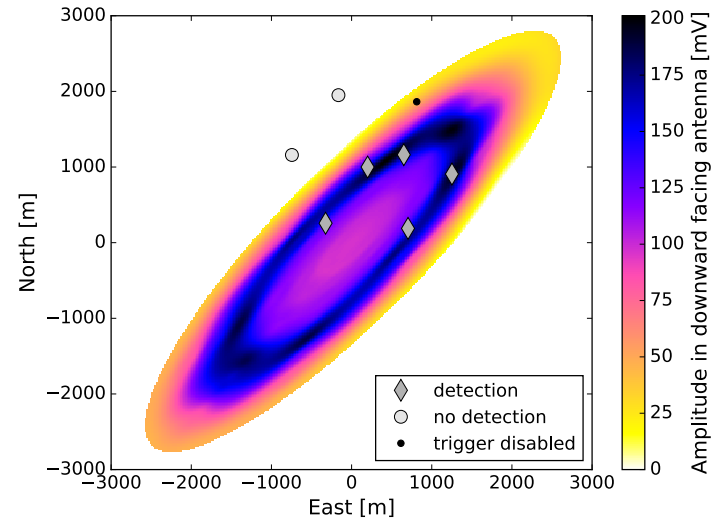
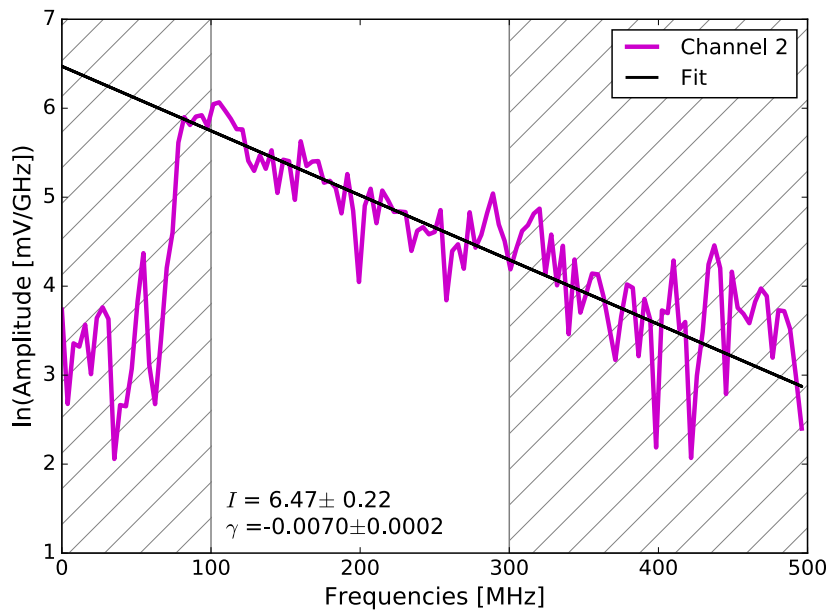
—> **radio technique is routinely used to measure properties of cosmic rays**



Concept of ARIANNA

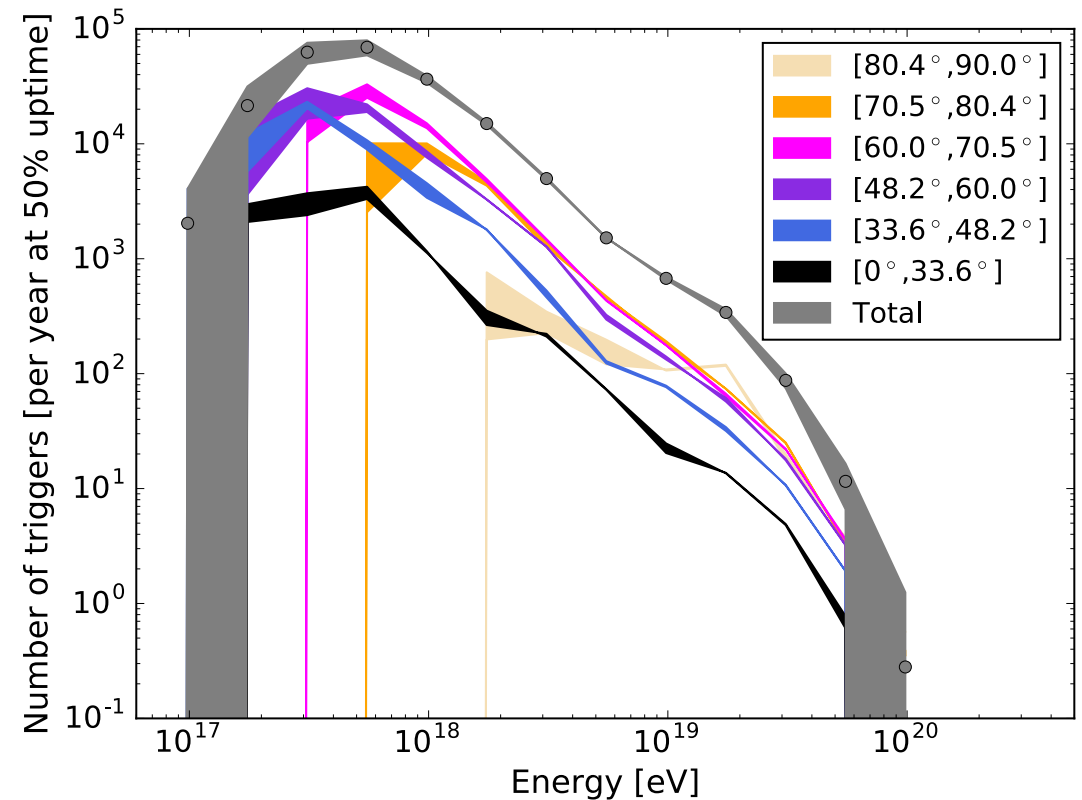
- On ice-shelf: **Ice-water boundary** almost perfect reflector for radio emission
- **Independent antenna stations** can be installed at low costs on the surface
- **Real-time data transfer** via satellite
- Solar and wind power possible
- **High gain antennas** (50 - 1000 MHz) can be used to instrument a large volume
- Array of about 1000 antennas needed





use **slope** of
measured **frequency**
spectrum to derive
energy and other
shower parameters

full ARIANNA
36 km² x 36 km²
1296 km²



Extension of scintillator array (LORA)

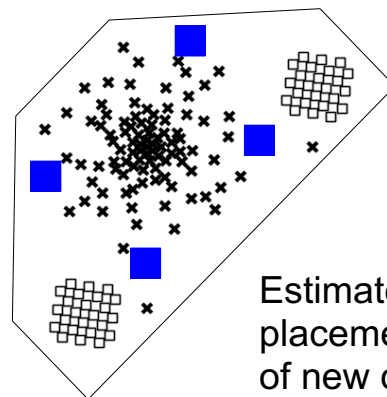


S. Buitink
K. Mulrey

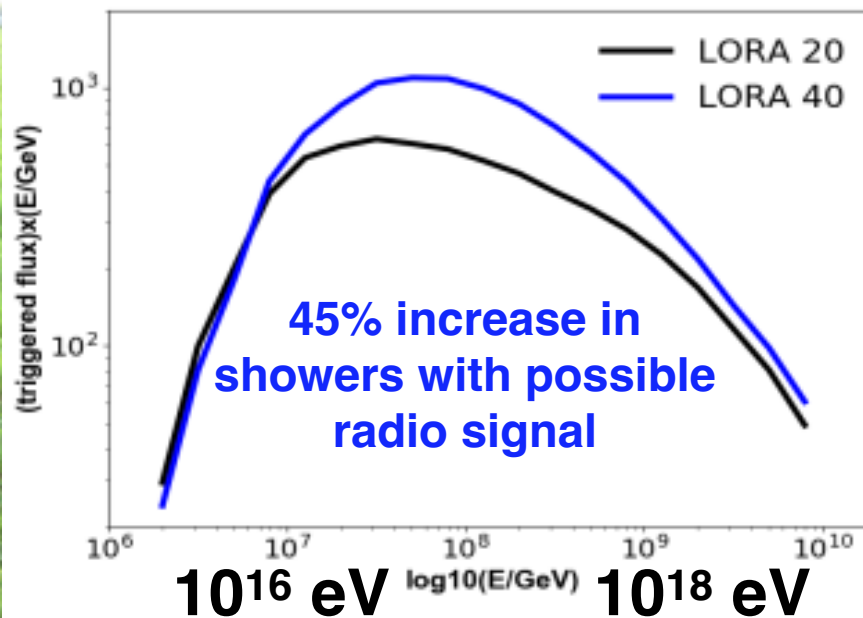


← 2.5 km →

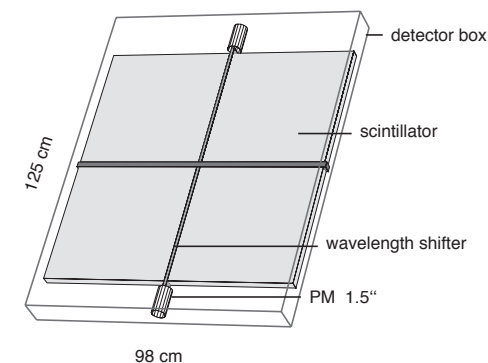
- Existing station
- New station



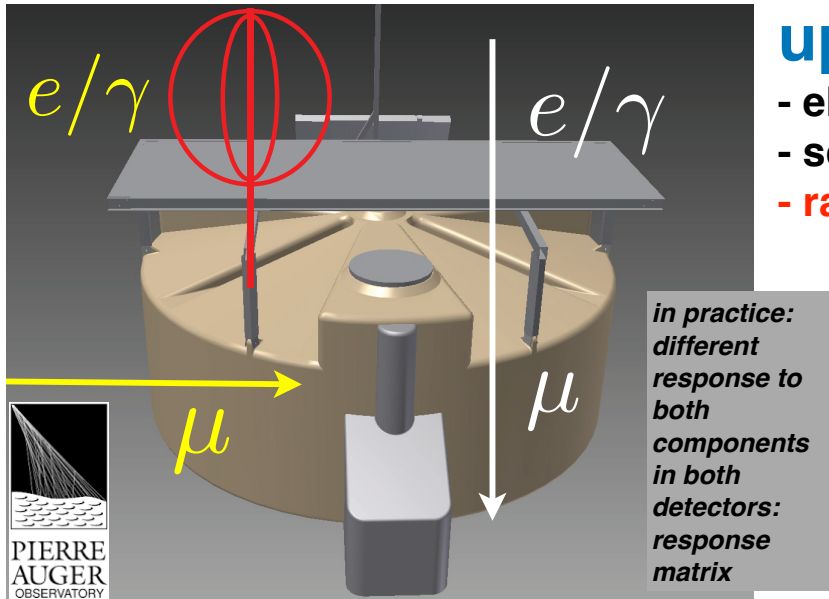
Estimated placement of new detectors



adding 20 scintillator stations in 2018



Upgrade of the Pierre Auger Observatory (astro-)physics of the highest-energy particles in nature

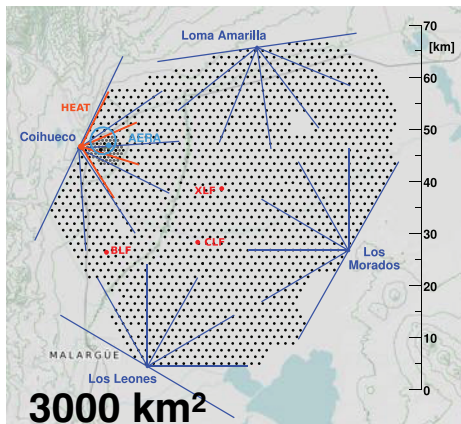
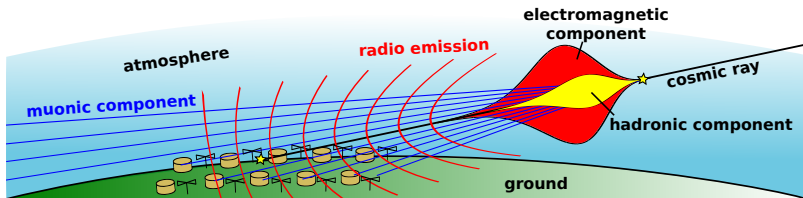


upgrade PAO

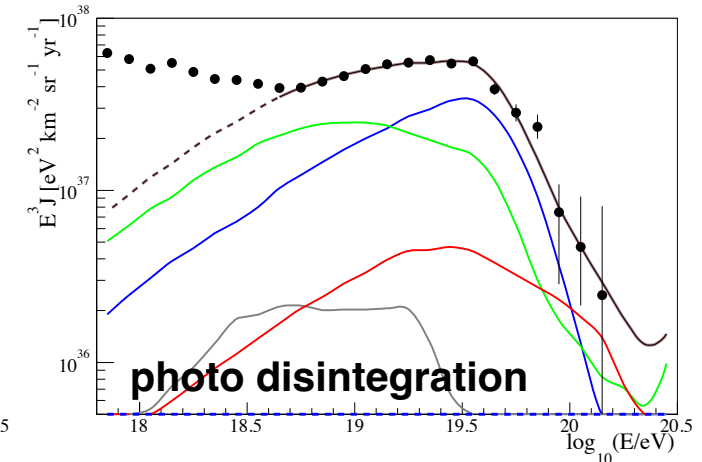
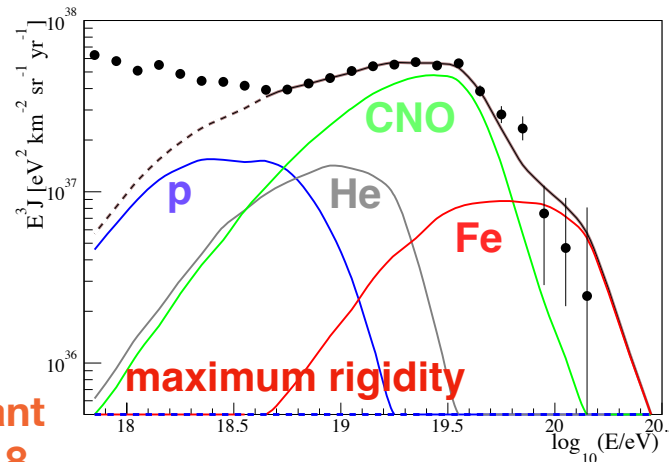
- electronics
- scintillator layer
- radio detector

Key science questions

- What are the **sources** and **acceleration** mechanisms of ultra-high-energy cosmic rays (UHECRs)?
- Do we understand **particle** acceleration and **physics** at energies well beyond the LHC (Large Hadron Collider) scale?
- What is the fraction of **protons**, **photons**, and **neutrinos** in cosmic rays at the highest energies?



Advanced Grant
Hörandel 2018



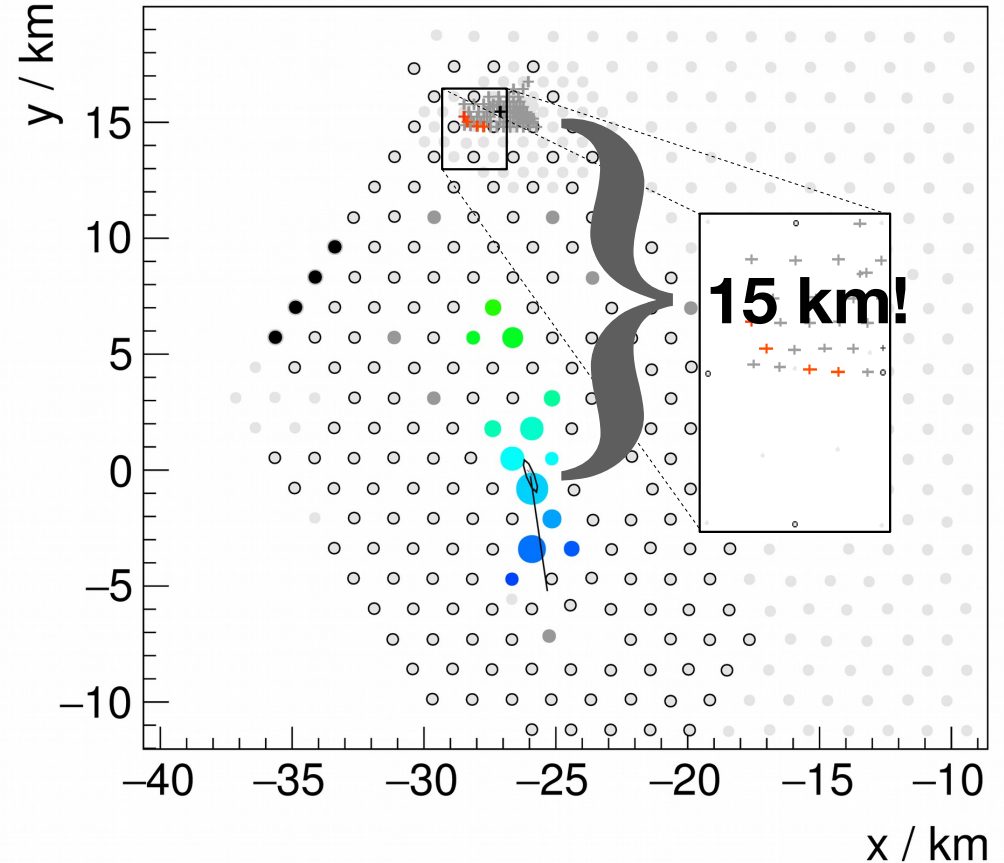
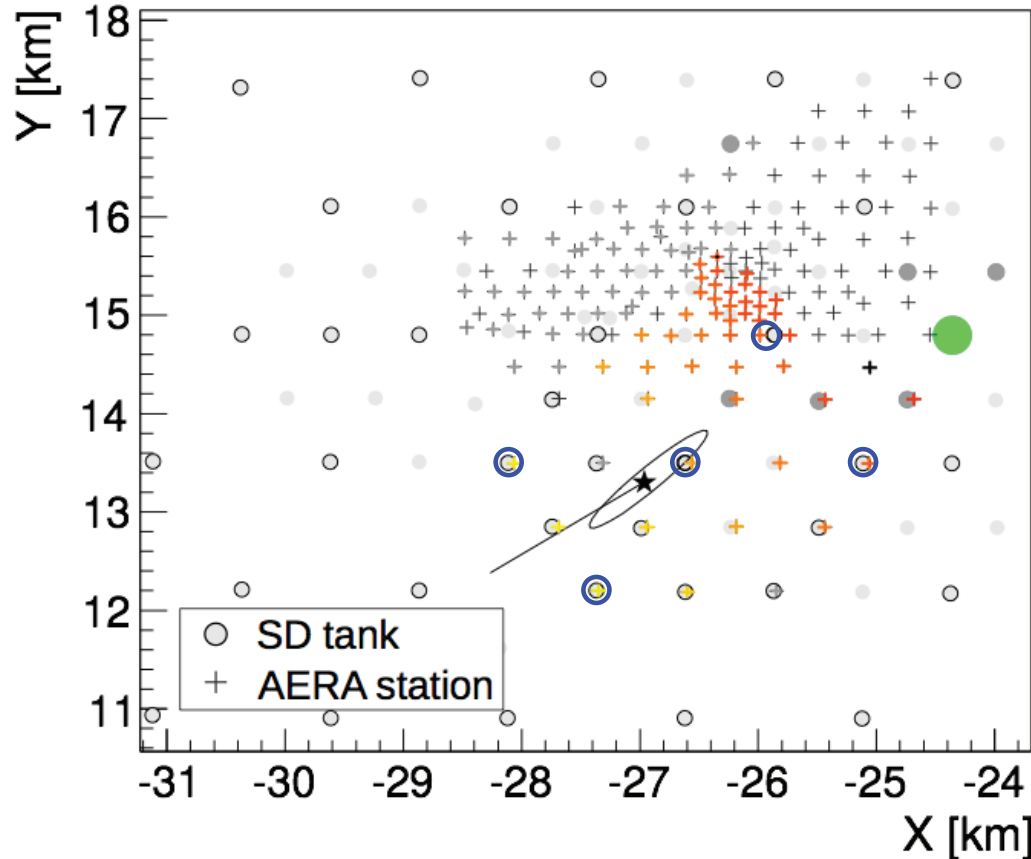


PIERRE
AUGER
OBSERVATORY

A large radio array at the Pierre Auger Observatory

preparatory work & feasibility

AERA 17 km²
--> 3000 km²



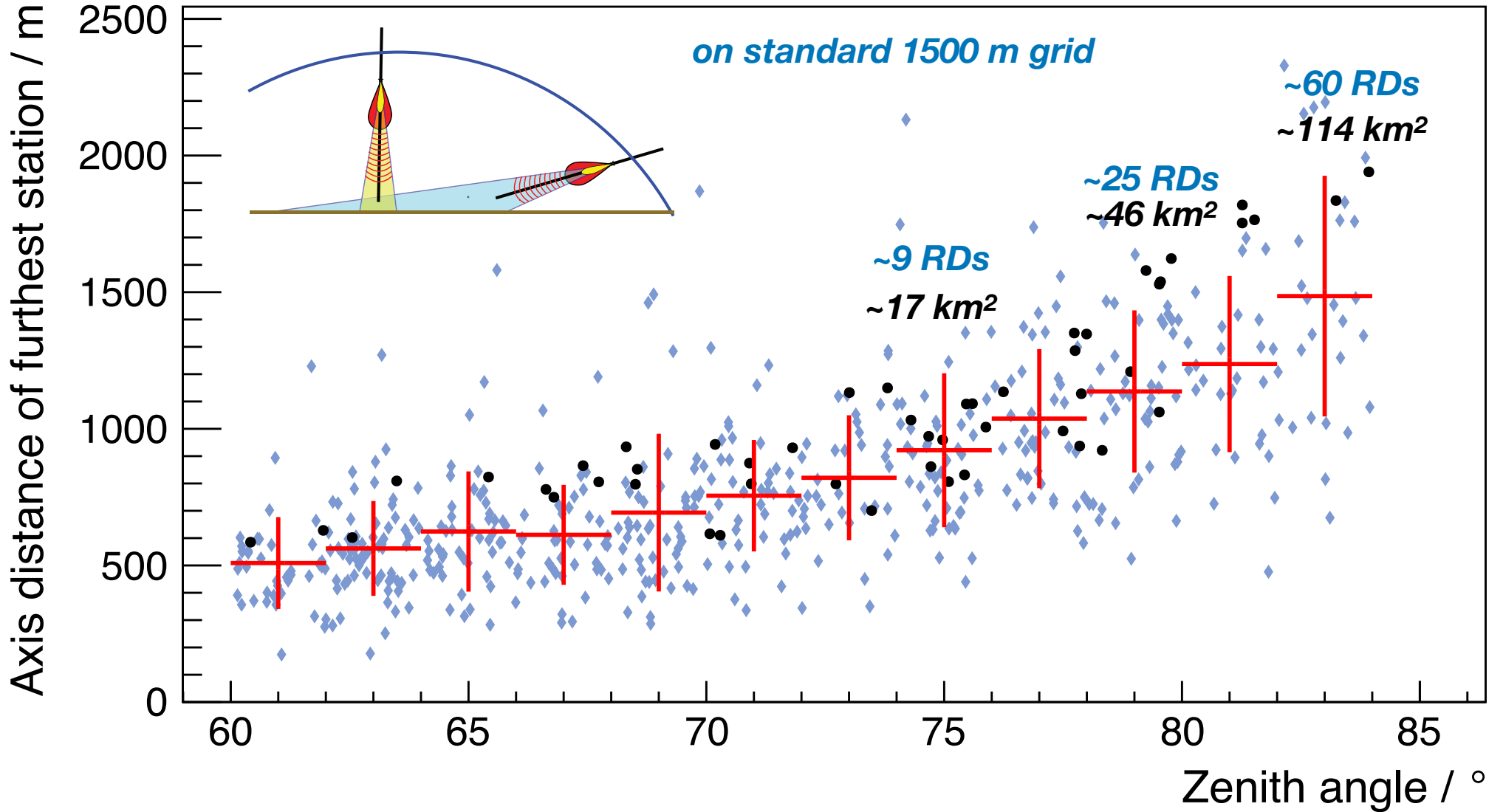
horizontal air showers registered and reconstructed with existing AERA

Horizontal air showers have large footprints in radio emission

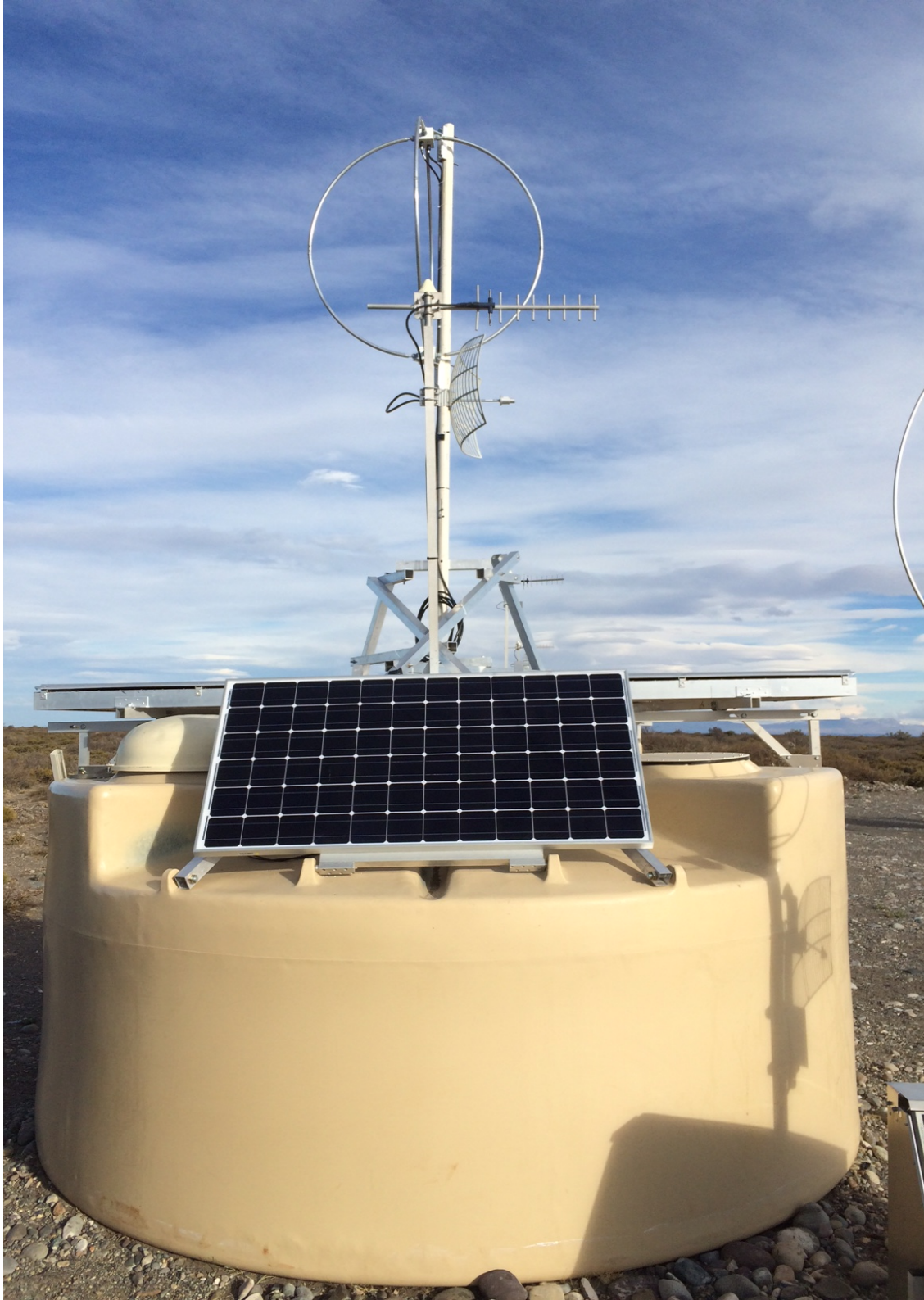


M. Gottowik

AERA 17 km²
--> 3000 km²



this is MEASURED with the *small* 17km² AERA



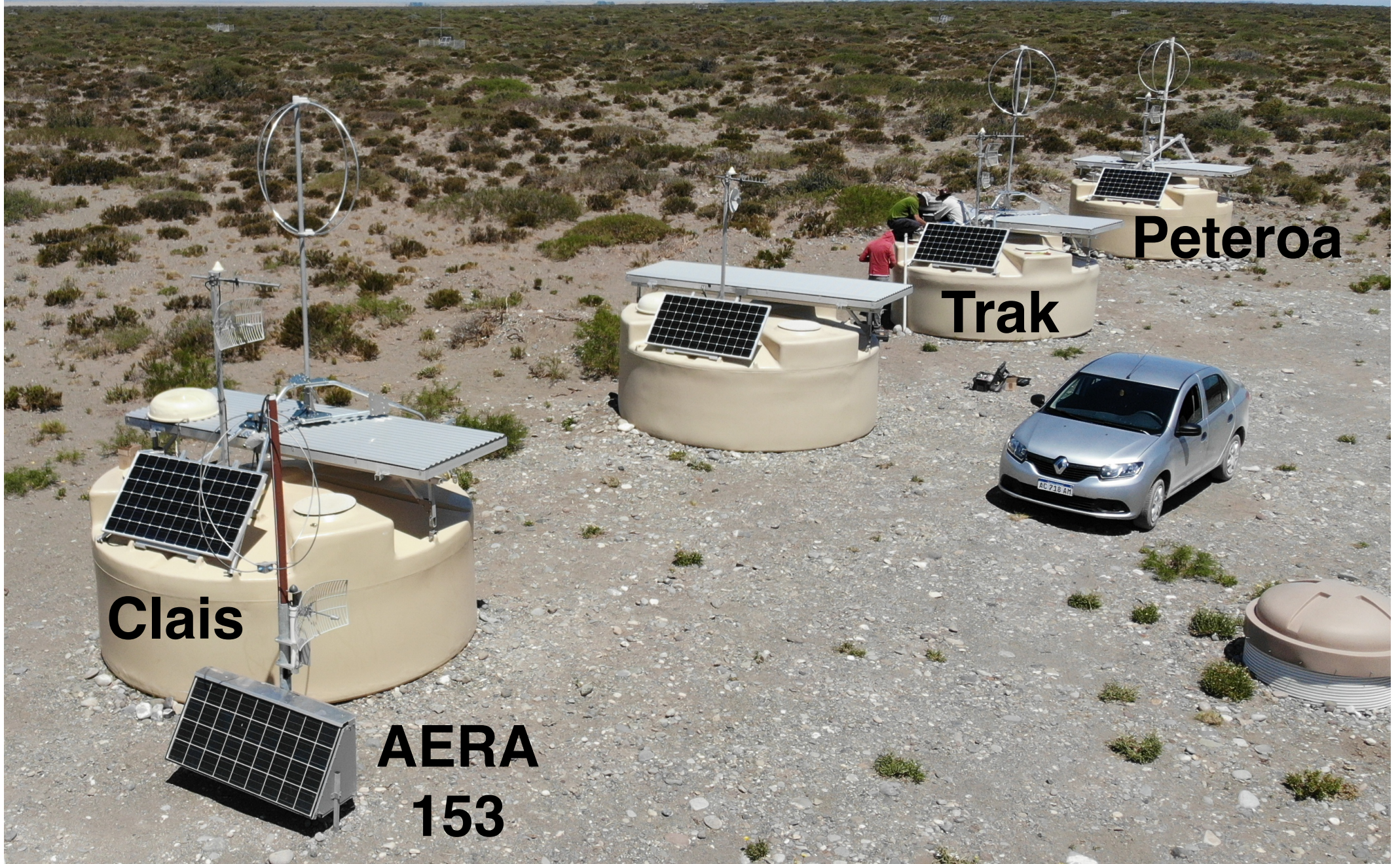
since May 2019 complete prototype at Auger observatory

- new SALLA antenna
- new LNA
- new digitizer/front end coupled to UUB

data are integrated in SD data stream and transported to CDAS

we have now *ONE* system comprising of WCD, SSD, RD

since November 2019
10 prototype stations installed



Clais

**AERA
153**

Trak

Peteroa

First Rd Signal

File FD SD RD MD Atm MC Help

Auger Los Leones Los Morados Loma Amarilla Colihueco Heat HeCo SD RD MD Selection

Event Info MC Info LDF Info HAS LDF Info

Run 101483 Event 116113
 GPS Time 1256640536 s 685102975 ns
 UTC Date: 2019/11/01 10:48:38
 RecStage = LDFFit2dWithCore
 $\theta = 12.19$ deg $\phi = 102.62$
 radiation energy: $7.13e+06 \pm 1.47e+06$ eV
 sigma (2D LDF): 46 ± 0.78 m
 core x, y = 8.8 m, -46 m
 Stations: 9
 radius = $1 \pm$ nan m
 FitStatus = successful
 Chi2/NDF = 4.78 / 6
 x = -26.33 km, y = 15.46 km
 Energy = $1.005e+18$ eV
 $\alpha = 41.58^\circ$

Station List Options

AERA_13	212.1 +/- 11.7 muV/m	8.5 +/- 0.9 eV/m^2	SNR=72.1	d=154.637 m
AERA_16	81 +/- 14.6 muV/m	1 +/- 0.3 eV/m^2	SNR=10.8	d=243.676 m
AERA_23	231.1 +/- 25.7 muV/m	11.1 +/- 2.4 eV/m^2	SNR=93.5	d=209.744 m
AERA_24	169.7 +/- 16.5 muV/m	4.4 +/- 0.8 eV/m^2	SNR=24.3	d=239.23 m
AERA_129	88.7 +/- 16.3 muV/m	2.3 +/- 0.6 eV/m^2	SNR=12.9	d=1937.09 m
AERA_153	285.8 +/- 18.1 muV/m	14.3 +/- 1.8 eV/m^2	SNR=187.2	d=106.215 m
AERA_2	67.5 +/- 38.8 muV/m	0.8 +/- 0.5 eV/m^2	SNR=3.6	d=257.811 m
AERA_5	49.1 +/- 33 muV/m	0.2 +/- 0.2 eV/m^2	SNR=3.2	d=367.637 m
AERA_6	55.8 +/- 58.4 muV/m	-0.1 +/- 0.4 eV/m^2	SNR=2.3	d=275.241 m

AERA_153 $\beta = 45.3 \pm 2$ deg Time Residual = -16.9 ± 13.4 ns
 Rejection Status: not rejected Saturation Status: not saturated
 Signal Peak = 1000 ns Signal Window = [819.8 ns ... 1140.8 ns]
 Time Correction by GPS | Beacon | Calibration: not set | not set | not set
 Polarization | Observ Angle: not calculated | not calculated a: not calculat

Array 2D-LDF LDF HAS-LDF Residuals Lorentz Angle

55903011_1572605320

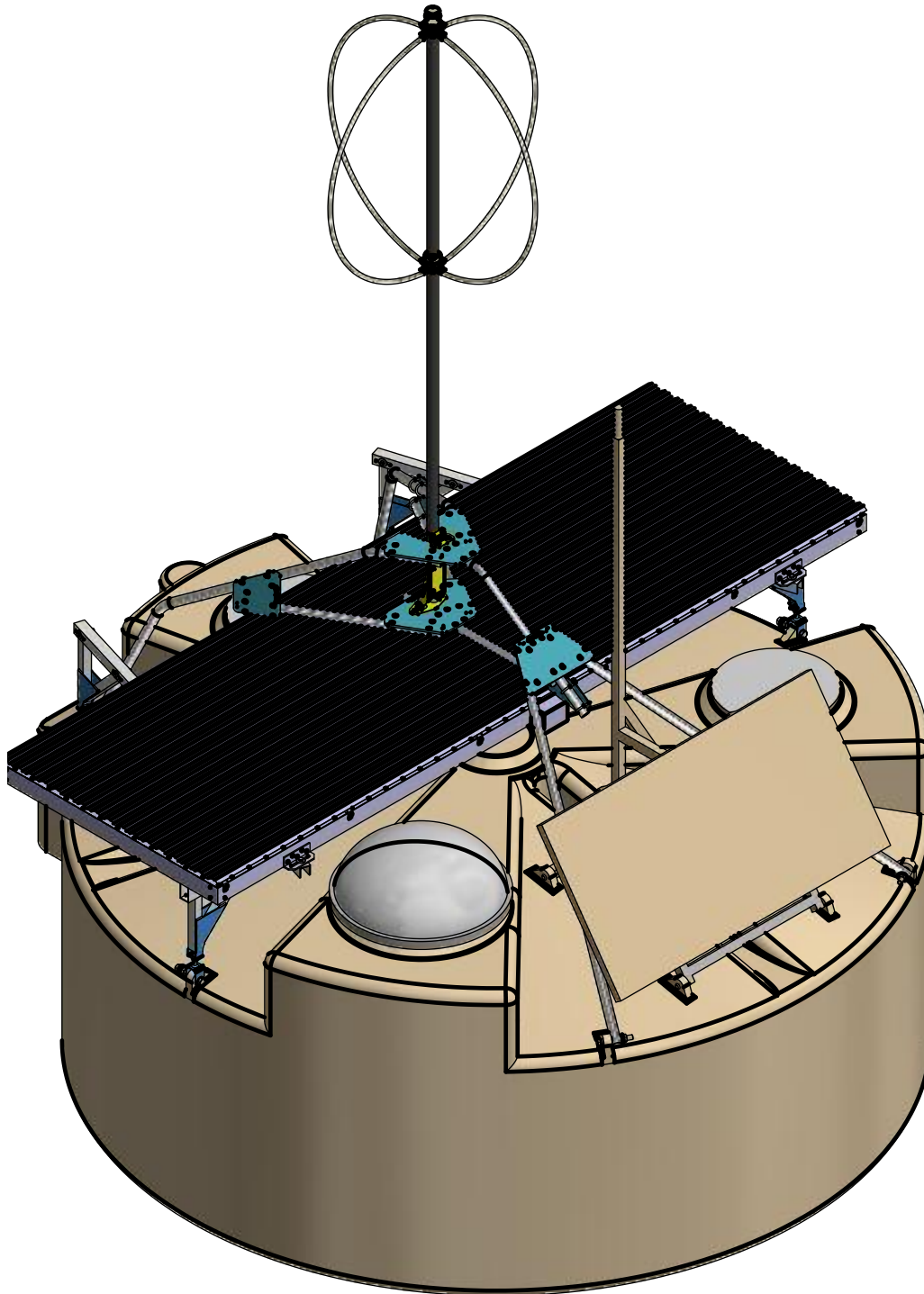
Traces Spectrum 2D-Field Scintillators

2019/11/1 10:48:38 Auger 193048212100 SD 55903011 RD 101483_116113

10

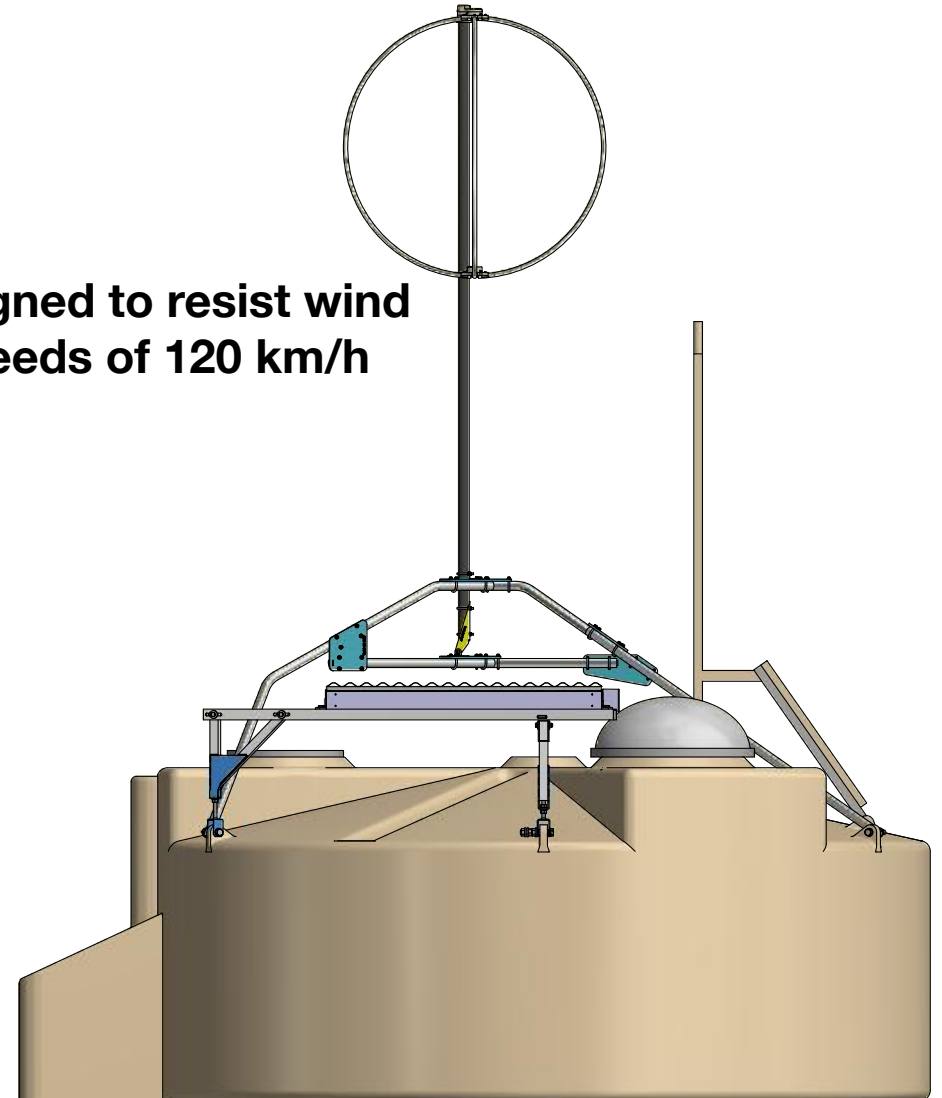
BERGISCHE
UNIVERSITÄT
WUPPERTAL

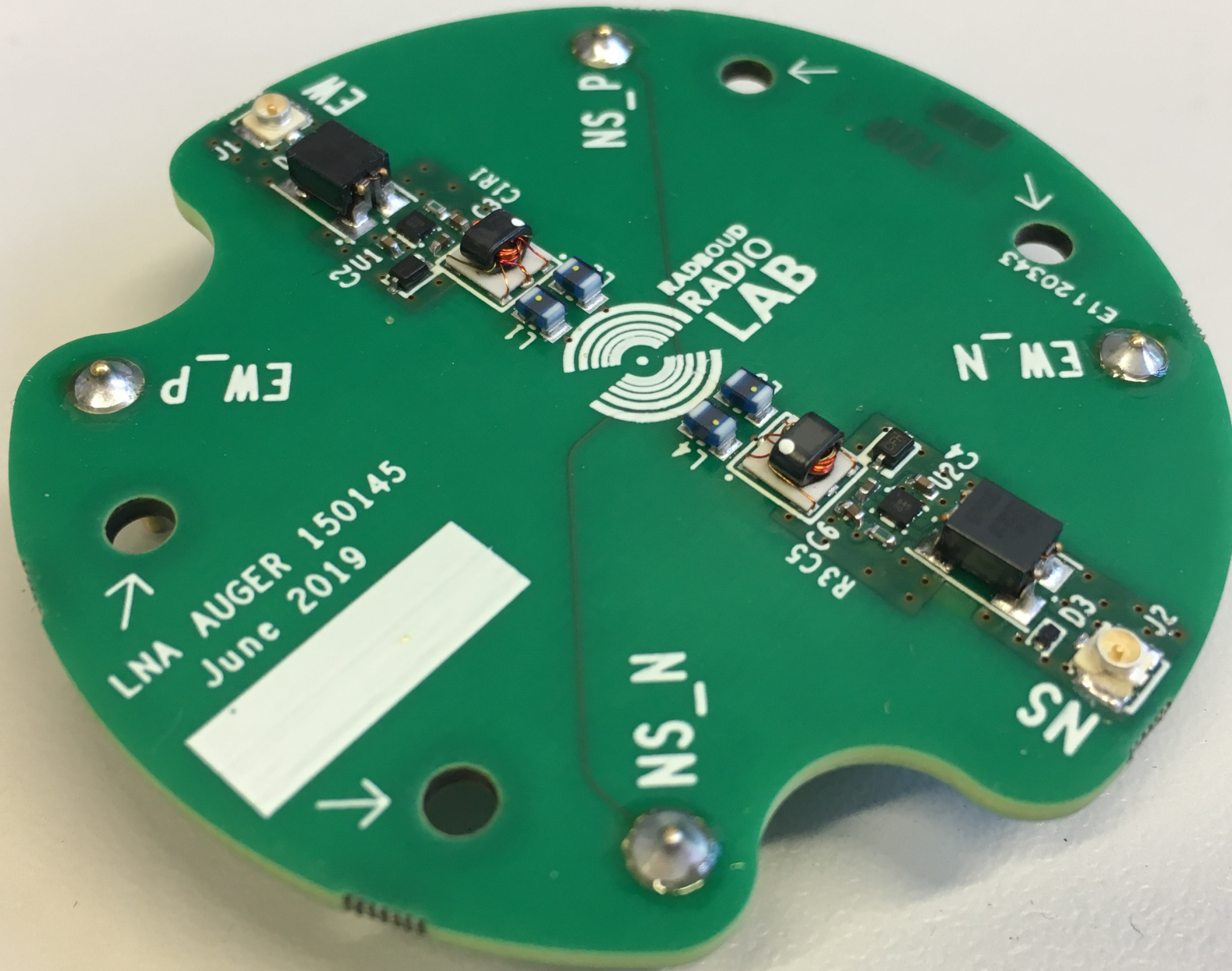
mechanical mounting of RD on wcd



5 m above ground

designed to resist wind
speeds of 120 km/h





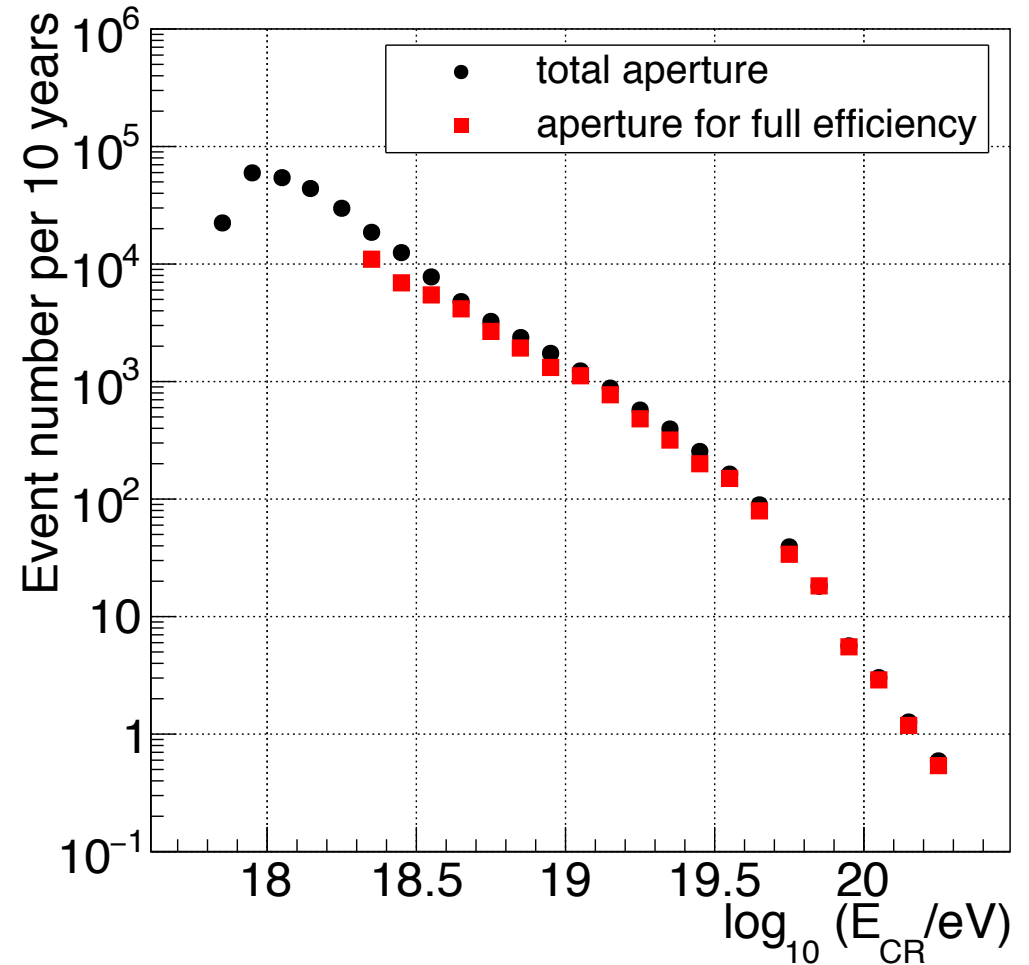
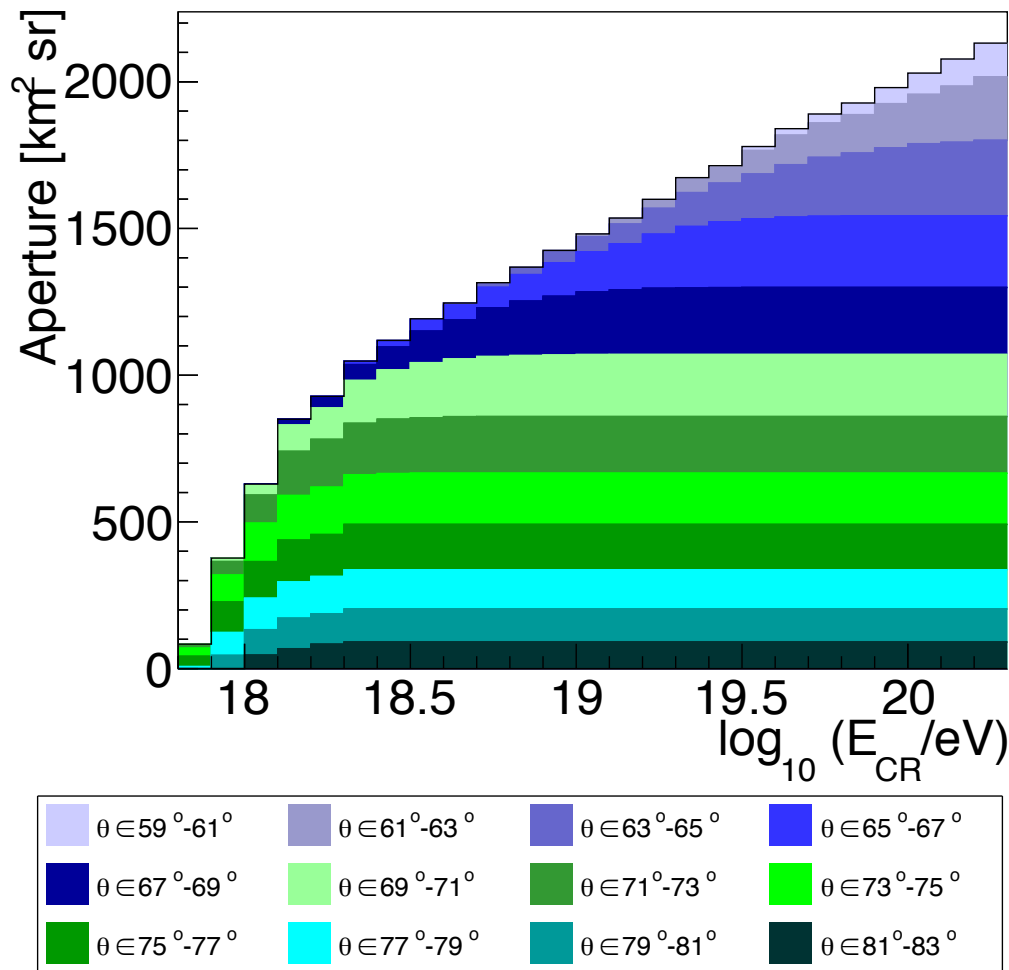
final version of LNA, RU Nijmegen, June 2019

radio digitizer



developed at RU Nijmegen

Detection aperture and event statistics



- High zenith angles become efficient early, contribute smaller apertures
- Lower zenith angles contribute larger apertures, become efficient later
- 3000 fully efficient events above 10^{19} eV in 10 years (300 above $10^{19.5}$ eV)

Measurement of the fluctuations in the number of muons in inclined air showers with the Pierre Auger Observatory

Felix Riehn^{*a} for the Pierre Auger Collaboration^{†b}

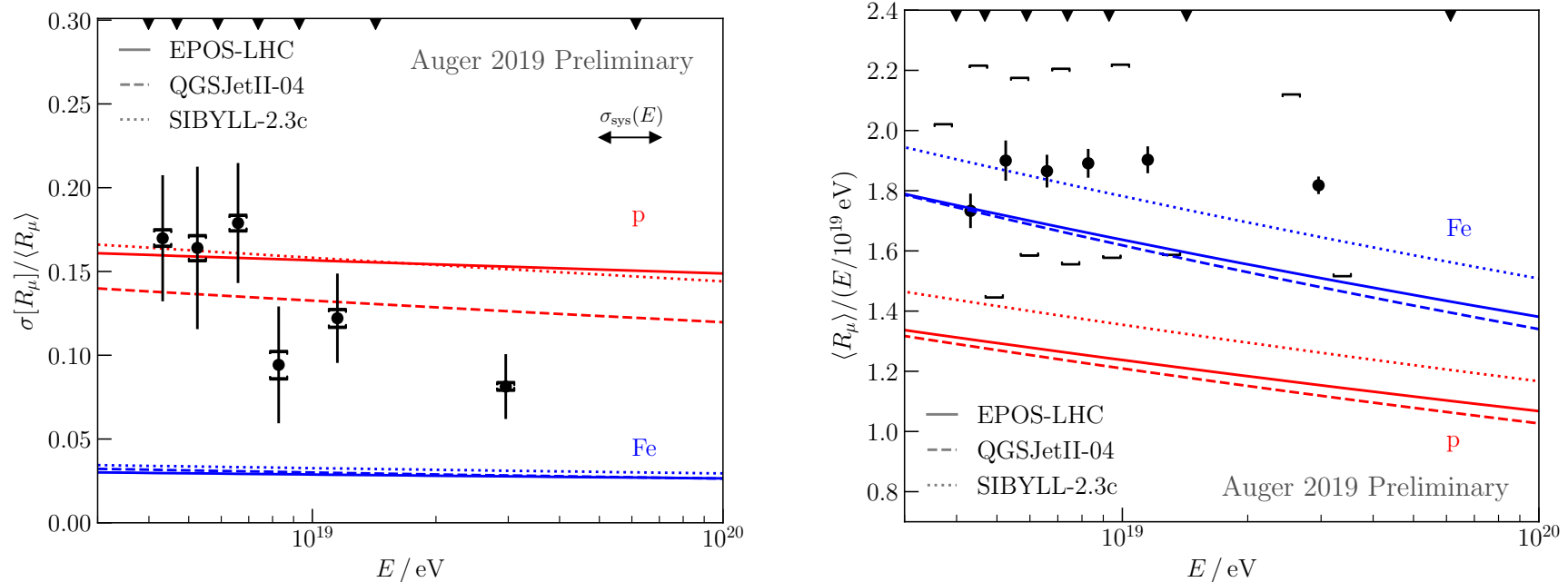
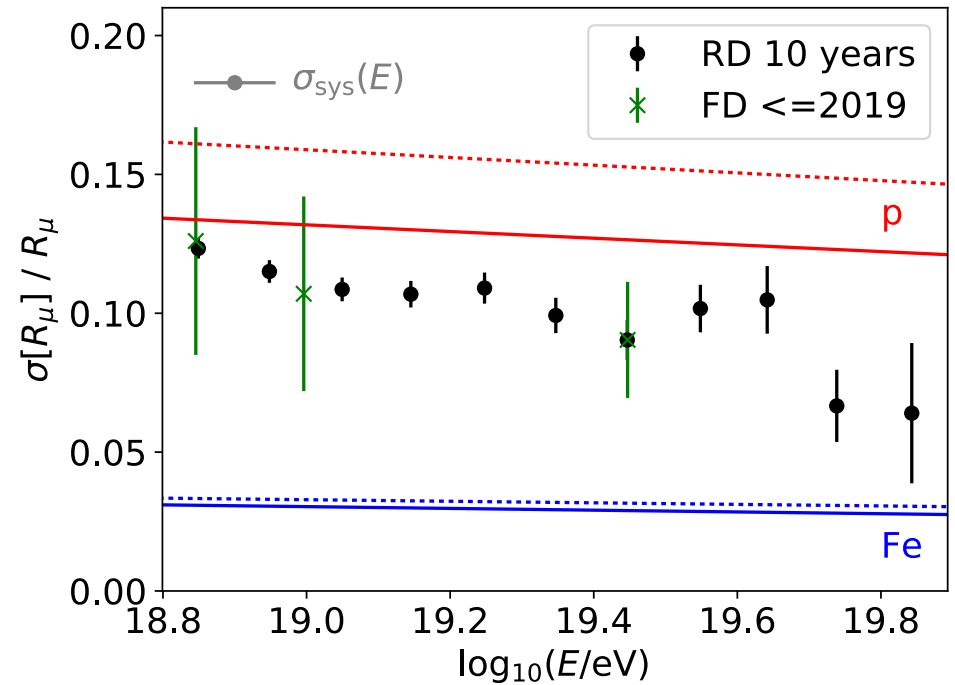
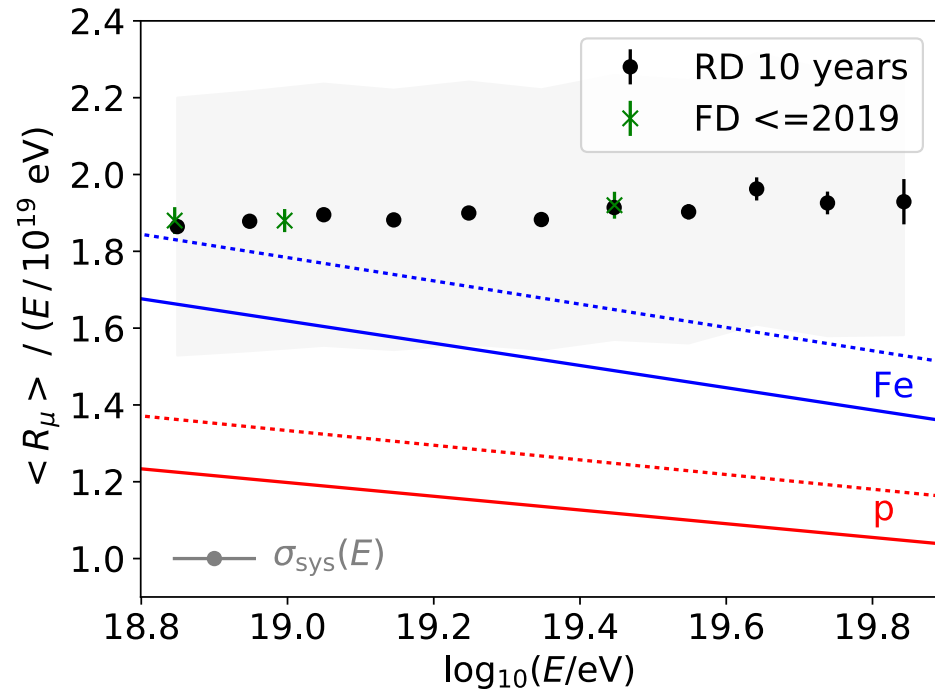


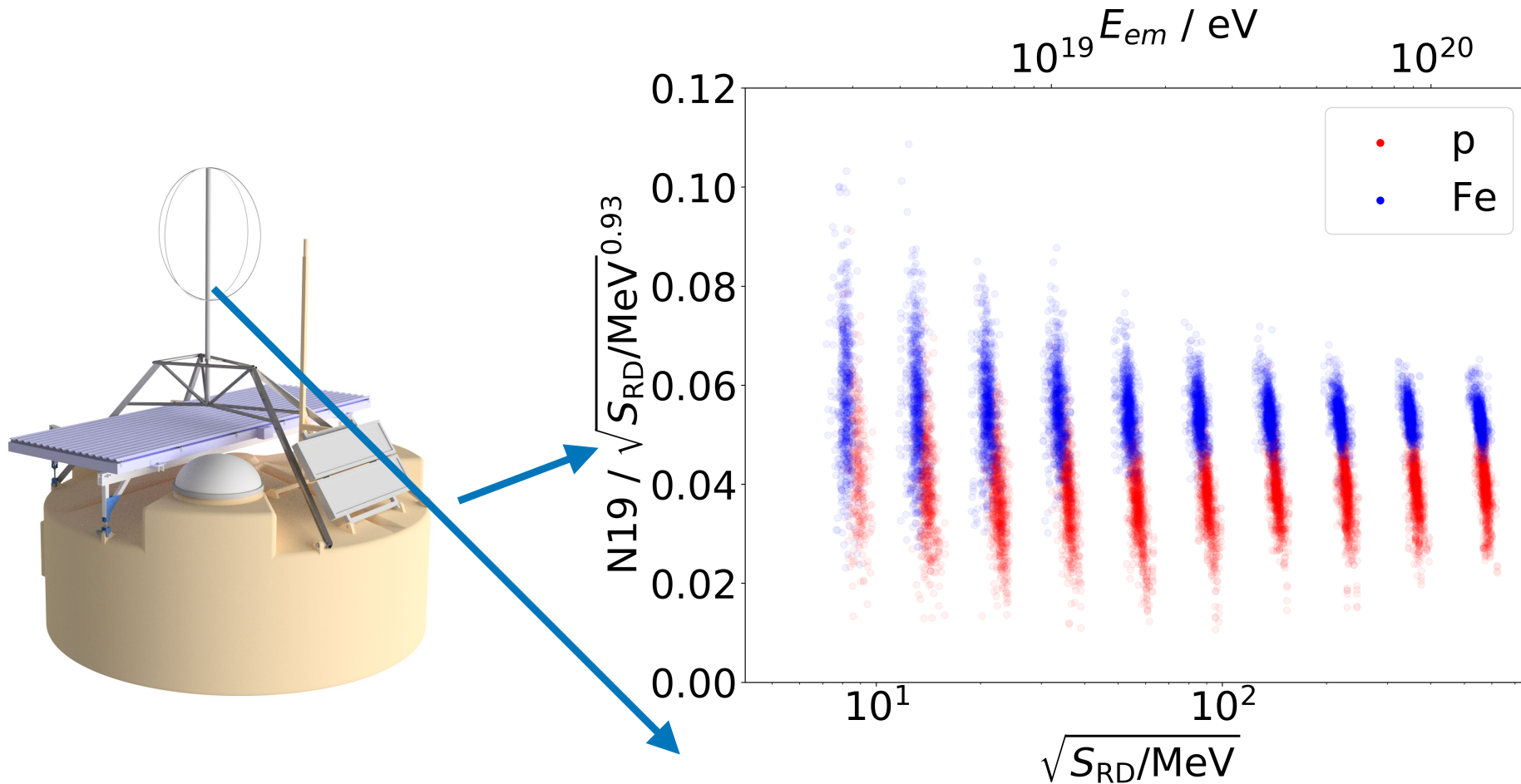
Figure 4: Shower-to-shower fluctuations (left) and the average number of muons (right) in inclined air showers as a function of the primary energy. For the fluctuations, the statistical uncertainty (error bars) is dominant, while for $\langle R_\mu \rangle$ the systematic uncertainty (square brackets) is dominant. The shift in the markers for the systematic uncertainty in the average number of muons represents the uncertainty in the energy scale.

Muon content in horizontal air showers



- More than 6000 showers expected above $10^{18.8} \text{ eV}$ in 10 years
- Energy resolution is not critical (assuming 20% here)
- Can also study zenith angle dependence

Mass composition sensitivity



- Energy from RD
- Muon number from WCD
- Correct for energy dependence of muon number to exploit its mass composition sensitivity

Mass composition sensitivity

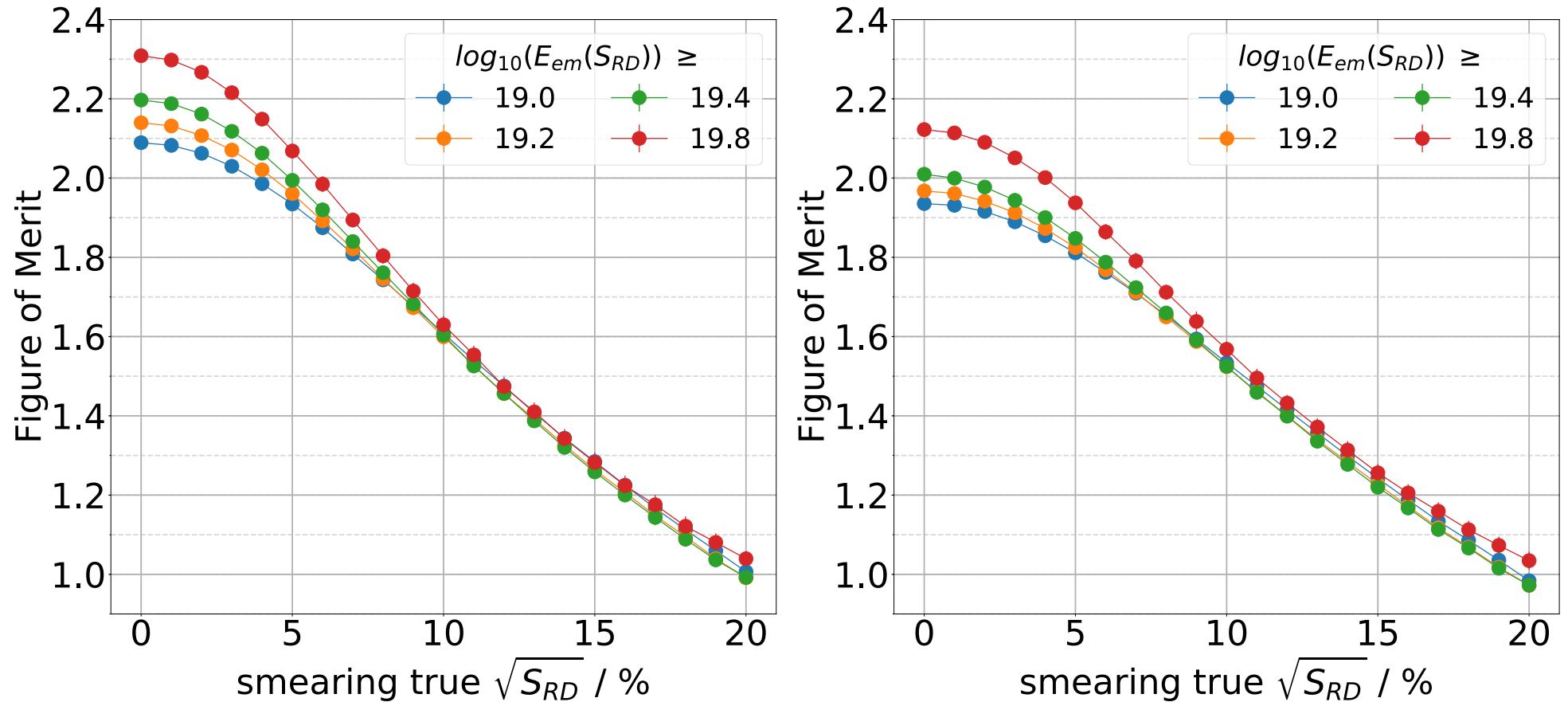
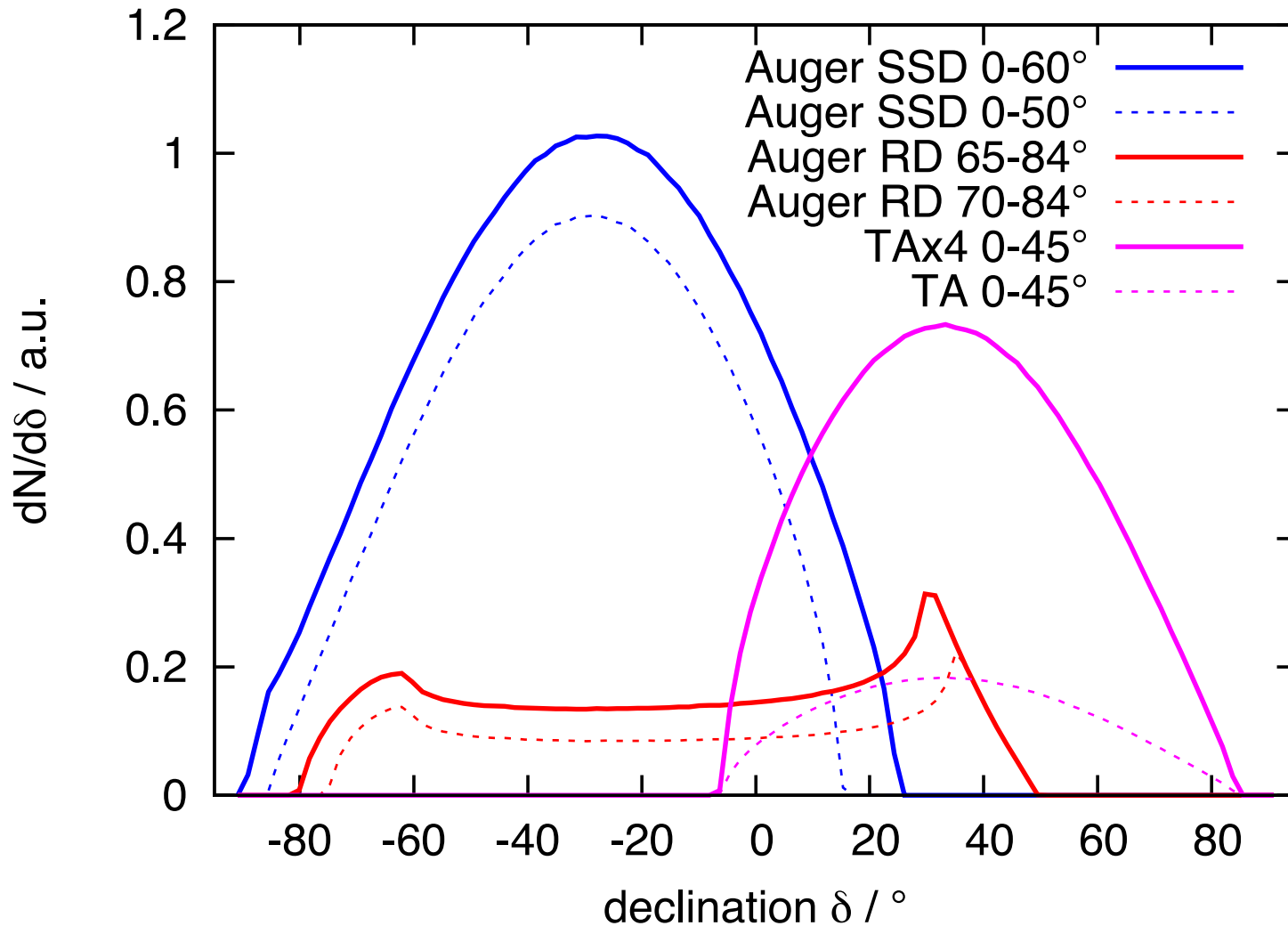


Figure 7: Figure of merit for the separation of proton-induced and iron-induced air showers using the ratio r defined in eqn. (1), various assumed resolutions for the determination of the electromagnetic energy with the Radio Detector, and different cut-offs for the lowest (smeared) electromagnetic energy. Left: using Monte-Carlo true arrival directions and knowledge of X_{\max} for each individual air shower. Right: using arrival directions as reconstructed by the Surface Detector and X_{\max} values known with a resolution of 100 g/cm^2 . [33]

Sky coverage with mass sensitivity



- **Add access at 20° - 45° northern declinations**
- **Shared energy scale**
- **Different systematics than SSD**

Measuring the properties of cosmic rays with the radio technique

The radio technique is now able to characterize cosmic rays:

-direction ✓

-energy ✓

-mass ✓

@100% duty cycle

